GEOCHEMISTRY, PETROGENESIS AND PALAEOMAGNETISM OF THE DYKE SWARMS OF THIRUVANNAMALAI AREA, TAMIL NADU AND THE LITHOSPHERIC PROCESSES IN SOUTH INDIA

Thesis submitted to the

COCHIN UNIVERSITY OF SCIENCE AND TECHNOLOGY

for the degree of

DOCTOR OF PHILOSOPHY

in

GEOLOGY

MATHEW JOSEPH

Geosciences Division
Centre for Earth Science Studies
Thiruvananthapuram-695 031

November 1994

CERTIFICATE

This is to certify that this Thesis is an authentic record of research work carried out by Mr. Mathew Joseph under my supervision and guidance in the Centre for Earth Science Studies for Ph.D. Degree of the Cochin University of Science and Technology and no part of it has previously formed the basis for the award of any other degree in any University.

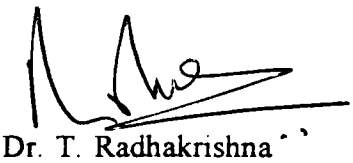

Dr. T. Radhakrishna
(Research Guide)
Centre for Earth Science Studies
Thiruvananthapuram 695 031.

Thiruvananthapuram
November 7, 1994.

CONTENTS

SYNOPSIS

The mafic dykes are the major avenue through which the mantle melts are transferred into the crustal levels. These constitute an important feature, and in some cases the only significant geologic event, of the Proterozoic over the Archaean cratons. The genesis of each swarm indicate clearly a major thermal event affecting the earth's mantle and therefore have important tectonic control for the lithosphere evolution. Numerous and/or large volcanic sequences appear to have occurred during the Archaean and the Phanerozoic period providing valuable information on the lithospheric origin in those periods. It is in this context that mafic dykes of the Proterozoic provide a window to infer mantle evolution, particularly the subcontinental lithosphere, which appear to be the dominant source component for most of the dykes.

One quarter of all Precambrian palaeomagnetic poles worldwide are derived from mafic dykes. In general, palaeomagnetic data from dyke swarms are of high quality and the derived poles are regarded as firm anchor points in the construction of apparent polar wander paths (APWP). Mafic dykes are wide spread over the south Indian shield. In spite of the great potential, detailed geochemical or palaeomagnetic studies of the dykes over the Indian shield are virtually lacking. Our understanding is too little about the Proterozoic Indian lithosphere and the Proterozoic APWP of India is not yet adequately worked out. With the result, we could never probe whether any relative motions took place between/within the crustal blocks of south India in particular and with reference to the Gondwanaland in general. In this context, the dyke intrusions of Tiruvannamalai are quite significant. These dykes intruded the southern granulite terrain during the Proterozoic. A multidisciplinary research of geochemical, palaeomagnetic and

geochronological (K-Ar) study of Tiruvannamalai dykes has been taken up for detailed investigation. The results are integrated to unravel the geodynamics of the Proterozoic south Indian lithosphere.

The thesis is divided into seven chapters. The first chapter introduces the topic of basic magmatism and mafic dykes and its importance. It is followed by a discussion on the distribution of mafic dykes in the Dharwar craton and the Southern Granulite Terrain of south India. Previous work on the dykes of Tiruvannamalai has been summarised and has highlighted the problems which required further geochemical, palaeomagnetic investigations and also the importance to determine their age. The objectives and the approach of the present research work is also discussed.

The second chapter has been devoted to give an over all view of regional geological setting of south India to begin with. Here the concept of different crustal units like Granite-Greenstone Terrain (GGT), Southern Granulite Terrain (SGT) and Eastern Ghat Mobile Belt (EGMB) has been summarised through a review of the vast literature on south India. The geological setting of Tiruvannamalai region is followed by a description of dykes along with their petrographic description.

The isotopic age data is presented in the third chapter. Determination of emplacement age of the Tiruvannamalai dyke swarm is important to provide age constrain to the palaeomagnetic poles and also the timing of thermal activity which generate these mantle melts. The ages were determined using the K-Ar isotope method. The results ascertain an age of about 1650 Ma for the Tiruvannamalai dykes.

The forth chapter deals with geochemical studies of Tiruvannamalai dykes. In this chapter, details of sampling, preparation of samples for geochemical analysis and different instrumental techniques adopted have been described. Subsequent discussion has been focused to provide the distribution of elemental abundances in forty samples,

coming from the entire geographic area of Tiruvannamalai dyke distribution and to classify the magma types. The geochemical results are presented under the broad classification as major element (SiO_2, TiO_2, Al_2O_3, Fe_2O_3, MgO, K_2O, Na_2O, P_2O_5 and MnO) and trace elements (transition elements [Cr, Ni, Co, V and Sc], large ion lithophile elements [Rb, Sr, Ba, Pb, U and Th], high field strength elements [Ta, Nb, Zr, Hf and Y], rare earth elements [La, Ce, Pr, Nd, Sm, Eu, Gd, Tb, Dy, Ho, Er, Tm and Yb] and oxygen isotope). The magma was identified as continental tholeiites in their chemistry.

In the fifth chapter, palaeomagnetic work is detailed. The chapter starts with a general outline on the geomagnetism and its application to construct apparent polar wander paths, palaeomagnetic directions, poles, general problems of secondary magnetisation and possible demagnetisation techniques to overcome from them to derive characteristic magnetisation and the statistical treatment of data to obtain high quality reliable palaeomagnetic record. The details of instruments employed in the study and the measurement procedures are described. Finally the palaeomagnetic results of Tiruvannamalai dykes are described for each site/dyke.

Chapter six is devoted for interpretation of geochemical and palaeomagnetic results of Tiruvannamalai dykes. A geochemical comparison is made between Tiruvannamalai dykes and other major Proterozoic dykes to bring out similarities and differences among the dykes all over the world. It follows an in depth discussion on petrogenetic aspects, which includes crystal fractionation and crustal contamination, which are considered to modify the composition of primary magmas derived from the mantle. The processes of crustal contamination or fractionation do not seem to have produced the relative abundances of incompatible elements and it is argued that the chemistry of the swarm

is controlled by mantle source characteristics. The geochemical data is in agreement with a suggestion of lithospheric mantle component in their chemistry.

Interpretation of the palaeomagnetic data includes presentation of various complex problems to isolate characteristic magnetisation and the derivation of primary palaeomagnetic direction after careful screening of secondary components. The palaeomagnetic study of the Tiruvannamalai dykes was successful in deriving a palaeomagnetic pole of south India at 1650 Ma, for which no palaeomagnetic pole data is available for the Indian shield. Further, the 1650 Ma pole of Tiruvannamalai dykes is compared with other similar poles of adjoining Dharwar craton and with the poles of similar age from Africa, Australia and Antarctica which are thought to be once contiguous parts of the Gondwanaland. The chapter finally discusses how south Indian lithosphere developed and the tectonic implication for the lithospheric plate motion. Based on the geochemical data, it is suggested that the Proterozoic south Indian lithosphere was metasomatised by the fluids derived from subducted oceanic crust, probably ~3.0 Ga, simultaneous to the major crustal building activity. The palaeomagnetic results suggest that there were no major displacements along the Granite-Greenstone Terrain and the Southern Granulite Terrain since at least mid-Proterozoic and the combined data can be used to construct the APWP of Proterozoic south Indian shield.

Chapter seven summarises the important observations and conclusions in the present geochemical and palaeomagnetic investigation of Tiruvannamalai dykes.

INTRODUCTION

1.1 INTRODUCTION

Occurrence of mafic dykes in the Tiruvannamalai area, North Arcot district, Tamil nadu is well known (Pascoe, 1950). They represent a significant phase of basic magmatism in the south Indian shield. The dyke intrusions in the south Indian shield are related to the tectonic development of continental margin or to the lithospheric processes in Granite-Greenstone Terrain (Dharwar nucleus)/Southern Granulite Terrain (figure 1.1). The dykes of Tiruvannamalai are responses to thermal disturbances in the lithosphere closely related to the geodynamics in these terrains. But the implications of these dykes are not yet known. The present study is focused to unravel the significance of these dykes in relation to the south Indian lithosphere, particularly in terms of petrogenesis and lithospheric plate motions. This chapter briefly summarises the concepts of basic magmatism, mafic dykes and their relation to tectonics and the present knowledge on the distribution of mafic dykes within the tectonic frame work of south India. Previous work on Tiruvannamalai dykes, the scope and importance of further study and specific objectives of the present investigation are also presented.

1.2 MAGMATISM, MAFIC DYKES AND TECTONICS

Mafic magmatism is a common manifestation of tectonic activity both in oceanic and continental environments. The inter-plate magmatism is associated with mid ocean ridges and subduction zones, while the within-plate magmatism is commonly associated with

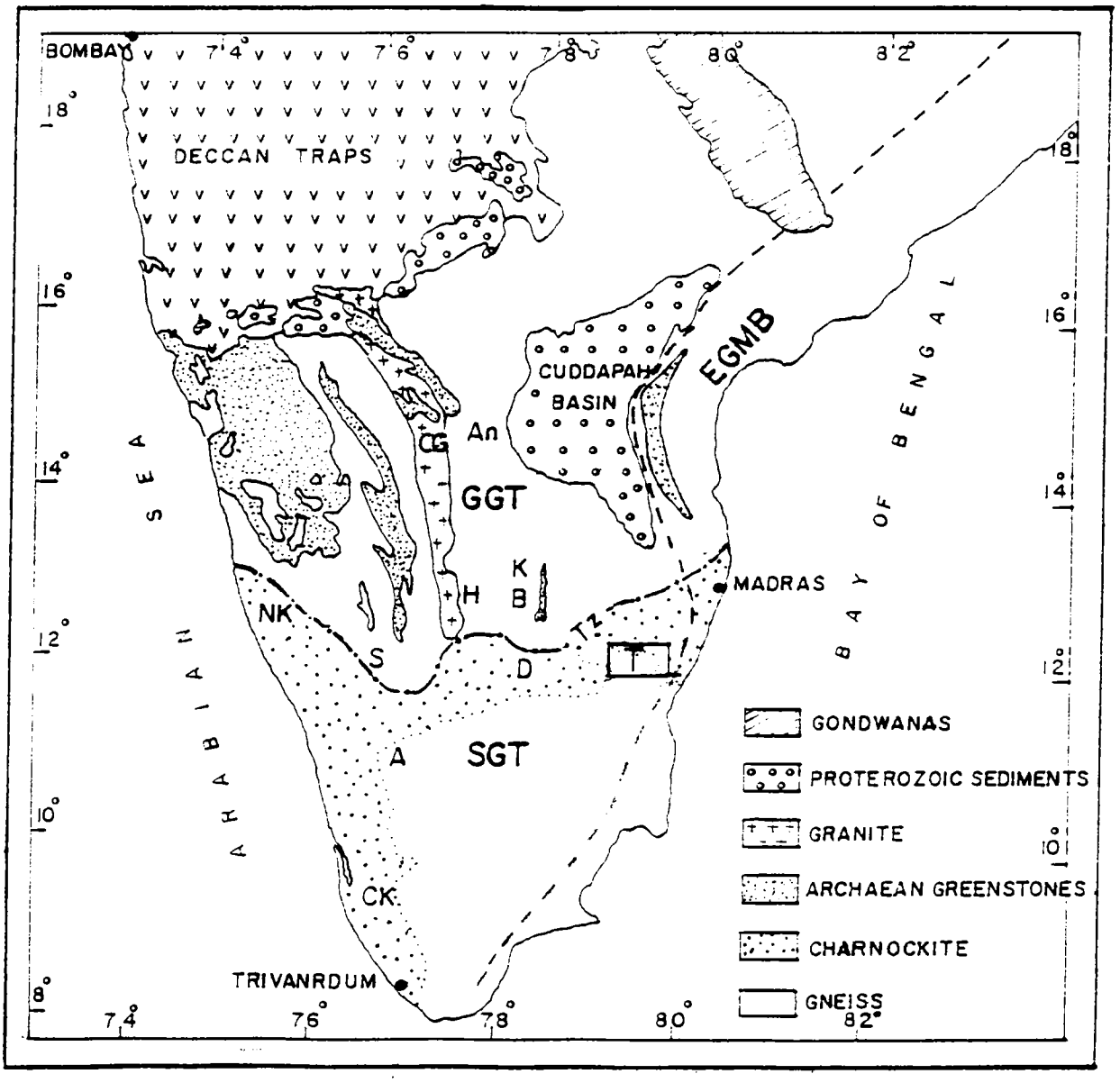

Figure 1.1: Geological sketch of south Indian shield with major lithological units. SGT = Southern Granulite terrain: GGT = Granite Greenstone Terrrain: EGMB = Eastern Ghat Mobile belt: TZ = Transition zone: CG = Closepet Granite: CK = Central Kerala: NK = North Kerala: A = Agali: D = Dharmapuri: T = Tiruvannamalai: B = Bangarpet: K = Kolar: H = Harohalli: S = Sargur: An = Ananthapur.

hotspots/mantle plumes. Seismic, heat flow and experimental petrological data indicate that basaltic and ultramafic magmas are generated in the upper mantle. The composition of the magma produced in the mantle is dependent on the composition of the source rock and degree of melting.

The mafic magmas provide information on the chemistry and mineralogy of mantle source rocks. Significant variation in the incompatible elemental distribution and isotope ratios in basic rocks in similar tectonic setting have indicated that the upper mantle is chemically heterogeneous. The distinct chemical characteristics in different mantle regions have facilitated the identification of geochemical mantle reservoirs. Primordial mantle (PM), Depleted mantle (DM), High U/Pb mantle (HIMU), Enriched mantle (I, II) are some possible mantle end members identified (Zindler and Hart, 1986).

Melting in the mantle source region requires thermal energy. This energy may be supplied directly from local concentrations of radioactive elements in the mantle. In the low velocity zone, magma can be generated by the addition of heat at constant pressure, lowering the pressure at constant temperature or by lowering the initial melting temperature of the mantle rock by hydration (Gallagher and Hawkesworth, 1992).

There is a general consensus that the mid ocean ridge basalts (MORB) are produced by 15-30% partial melting of the upper mantle peridotite at depths of 50-85 km. Melting at these depths produces olivine tholeiite magma. This is collected in shallow magma chambers where it undergoes fractional crystallisation to produce tholeiites and quartz tholeiites. The composition of the ocean ridge magmas are derived from a source which is relatively

homogeneous and poor in incompatible elements. The greater incompatible element contents of Transitional-MORB (TMORB) and Enriched-MORB (EMORB) require source heterogeneity.

In the case of within plate magmatism, parental magmas appear to be picrites or olivine tholeiites produced either in rising mantle plumes or in the mantle lithosphere. The melts from the upper mantle rise upwards through weak zones and fractures within the upper crust. These magmas are usually enriched in large ion lithophile elements (LILE) and rare earth elements (REE). The enriched characteristics are regarded as due to the magmas being contaminated as they pass through the crustal column. However, there are equivocal arguments that their characteristics were developed within the lithospheric mantle. Thus dyke geochemistry has a great potential to explain the petrogenetic problems of continental magmatism and to imply the development of lithosphere.

The dyke intrusions within the continental regions are associated with the rift zones. These dykes occupy the failed arms of the rift environments and also lie parallel to the continental spreading margin and the passive margin (Fahrig, 1987). The dykes also act as feeders to large continental flood basalts which may not have led to the ocean formation. Therefore, the mafic dykes provide useful clues on the past lithospheric plate motions. The hypothesis of continental drift, after many years in the wilderness, evolved into the theory of Plate Tectonics through the basic confirmations provided by palaeomagnetism. To estimate and compare the movement of the plates, construction of apparent polar wander path (APWP) is one of the most useful techniques. The magnetic mineral content, the *in situ* nature of exposures and the unmetamorphosed nature even in the Precambrian dykes and their episodic

nature in the continental regions make the dyke ideal for palaeomagnetic study. As the dykes are emplaced, it will acquire magnetism parallel to the earth's ambient magnetic field. The palaeomagnetic poles and palaeolatitudinal positions are calculated from the measured magnetic vectors. The isotope dating of the dykes will provide age constraints to the palaeopole position and help in establishing lithospheric plate motions in the past.

1.3 BASIC MAGMATISM AND MAFIC DYKES IN THE SOUTH INDIAN SHIELD

The Indian shield has experienced several episodes of basic magmatism. Pascoe (1950) provided an overall view of the distribution of the magmatic rocks in the Indian shield.

The amphibolites and metavolcanics in the greenstone belts with relict pillow structures and variolitic and spinifex textures form the earliest mafic magmatic units in the Granite-Greenstone Terrain. The amphibolites in Kolar and metavolcanics of the schist belts of Chitradurga, Bababudan etc. are typical examples. Gabbro-anorthositic complexes in the granulite facies terrain of the south Indian shield are variably deformed and metamorphosed (for example, Sittampundi complex). The emplacement of these are interpreted to have taken place much earlier to the final phase of metamorphism. It is now known that the final phase of metamorphism in the south Indian shield occurred ~2.6-2.5 Ga. Therefore, the metavolcanics in the greenstone belt and the metamorphosed gabbro-anorthosite bodies in the granulite belts are of Archaean age.

In the post-Archaean period, Deccan traps represent the wide spread basic magmatism in the peninsular India. Although, the origin and precise age of the Deccan traps have been

a subject of debate for long, it is considered to represent one of the largest late Phanerozoic flood basalt provinces of the world. The K-Ar ages show a great spread between 100 Ma and 30 Ma but the recent Ar-Ar ages place the event in a restricted period of less than five million years ~65-70 Ma closely matching with the K-T boundary (cf: Vandamme et al., 1991). Some of the mafic dykes in the south Indian shield are considered to be coeval and genetically related to the Deccan volcanism.

In the Proterozoic Eon too, the Indian shield experienced a great deal of basic magmatism. However, the volcanic exposures are very much limited. The Cuddapah traps in the lower stratigraphic sequences of Cuddapah Basin on the western boundary of the Basin is the only extrusive sequence of this age. Apart from Cuddapah traps, the basic magmatism is manifested in the form of small plutonic bodies as in Sivamalai, Ezhimalai etc., as kimberlites, and as dyke intrusions in a variety of strike directions.

Considerable work has been done on the Archaean metavolcanics of the Dharwar and the Phanerozoic Deccan flood basalts (cf: Naqvi and Rogers, 1983, 1987; Subbarao, 1988; Mahoney, 1988; Vandamme et al., 1991) in the recent past. When compared to these two periods, vital information regarding the Proterozoic interval is negligible. Dykes which occur episodically are the potential sources of information on Proterozoic magmatism in India and the development of subcontinental lithosphere.

The dykes of south Indian shield are described below under three broad groups in terms of the geotectonic frame work. They are the late Phanerozoic dykes associated with

the development of western continental margin, the Proterozoic dykes in the Dharwar craton (Granite Creenstone Terrain) and the Proterozoic dykes in the southern granulite terrain.

1.3.1 PHANEROZOIC DYKES ALONG THE WESTERN CONTINENTAL MARGIN

Numerous dykes occur parallel/sub-parallel to the west coast of India in Kerala and Karnataka. Varadarajan and Nair (1978) observed that the dykes in coastal Kerala are oriented parallel to the major lineaments which trend NW-SE, NNW-SSE, NE-SW and WNW-ESE. Even though no age data were available to establish their exact ages of emplacement, Mahadevan (1964) suggested that these dykes were probably of Cretaceous to Eocene age and related them with the Deccan activity.

The K-Ar isotope ages were first reported from the sporadic occurrence near Trivandrum. In conjunction with the oldest K-Ar ages on Deccan basalts, the mafic dykes all along the west coast are regarded as coeval and genetically related to Deccan traps (Sinha-Roy, 1983; Furnes et al., 1983). Radhakrishna et al. (1990, 1994 a,b,c) have determined a series of K-Ar and ^{40}Ar-^{39}Ar isotope ages on several dykes including the Trivandrum dykes. Based on K-Ar isotope ages on three whole-rock and a mineral separate, the Trivandrum dykes were assigned a 144±6 Ma age, indicating that these dykes are much older than the Deccan Traps. Further, these dykes were correlated with the 145 Ma dykes in Sri Lanka (Yoshida et al., 1989) and related them with the rifting of India from Antarctica-Australia.

In central and north Kerala, the dolerite dykes are prominent in a NW-SE to NNW-SSE direction while a gabbro trends in the NNW-SSE in central Kerala. Geochemically, the

dolerites of central and north Kerala are olivine or quartz tholeiites with affinity towards Mid Oceanic Ridge Basalts (MORB) while the gabbros show a Transitional-Oceanic Island Basalt (TOIB) characteristics (Radhakrishna et al., 1990, 1993). The K-Ar and ^{40}Ar-^{39}Ar isotope methods (Radhakrishna et al., 1990, 1994a) placed the age of dolerites at about 69±1 Ma while the gabbros are dated at 81±2 Ma. In the Agali-Coimbatore area isolated ENE-WSW trending basaltic dykes possess T-OIB chemistry and yielded a K-Ar isotope age of 105±2 Ma (Radhakrishna et al., 1994b). In terms of palaeomagnetism, the dolerite dykes have been related to Deccan traps (Radhakrishna et al., 1994a). An intraplate thermal plume setting developed ~80 Ma was suggested to have gradually changed over to a late asthenosphere decompressional setting leading to the eruption of large volumes of Deccan magmatism and rifting of India from Mascarene-Seychelles.

In Karnataka, the occurrence of Phanerozoic dykes have been indicated based on palaeomagnetic direction (Hasnain and Qureshy, 1971). Anil Kumar et al. (1988) reported Deccan equivalent palaeomagnetic direction along with K-Ar ages (84-69 Ma) for dykes near Huliyurdurga area.

It can be seen that the dykes of southwestern Indian coast have invaded the terrain episodically and are closely linked with various stages of rifting, drifting and the development of the western continental margin.

1.3.2 PROTEROZOIC DYKES IN THE GRANITE GREENSTONE TERRAIN

Significant amount of Proterozoic basic magmatism is manifested as mafic dykes in the Dharwar craton (Geological Survey of India, 1975). Pichamuthu (1959) and Radhakrishna (1967) have provided petrographic classification and linked some of the dyke emplacements with the Deccan volcanism. Hasnain and Qureshy (1971) provided preliminary major element geochemistry and palaeomagnetism on ten isolated dykes which are spaced at large distances. They considered that the dykes, which are mildly enriched in alkalies are Proterozoic. Singh and Bhalla (1972) suggested a Precambrian age for a dyke in Hariyur based on palaeomagnetic studies. Satyanarayana et al (1973) reported quartz normative and olivine normative dykes in the Nuggihalli area.

The dykes occurring in the Bidadi-Harohalli area constitute the best studied dykes in the Dharwar craton. The dykes of this area include the NW-SE metadolerite, N-S to NW-SE fresh dolerites and the alkaline dykes. Ikramuddin and Stueber (1976) reported a Rb-Sr whole rock age of 2420±246 Ma for the dolerite dykes. The alkaline dykes were dated as 850 Ma by K-Ar method and at 832±40 Ma based on Rb-Sr whole rock isochron. Sadashivaiah and Devaraju (1963), Devaraju and Sadashivaiah (1965 and 1966) and Ikramuddin (1978) classified the dykes into different petrological types.

In the eastern Dharwar craton, the dykes are more conspicuous and abundant with different trends (N-S, E-W, WNW to NW, NNE to ENE) to the west of the Proterozoic Cuddapah Basin. Palaeomagnetic results were reported for five dykes in Ananthapur area (Anil Kumar and Bhalla, 1983), four phases of dyke intrusion around Tirupati (Anjanappa,

1975), Hyderabad dyke (Verma et al., 1968; Anil Kumar and Prasada Rao, 1979), Karimnagar dykes (Rao et al., 1990) and for a few dykes in the Kolar area (Damodara Reddy and Prasad, 1979). The geochemical results are available for the dykes of Kolar (Sahoo and Balakrishnan, 1994) and Karimnagar (Rao et al., 1990). The close spacing of the dykes was explained as due to a northerly crustal extension (Drury and Holt, 1980) or due to arching about an easterly axis and northerly compression (Drury, 1984).

Among the dykes in this terrain only a few have been isotopically dated. Other than the Bidadi-Harohalli dykes, the isotope data is available for a dyke in south Kanara (K-Ar age of 2193±45 Ma; Balasubrahmanyian, 1975) and a NNW-SSE dyke of Kunigal (Rb-Sr age of 1915±28 Ma; Anil Kumar et al., 1989). The K-Ar ages on the dykes of Cuddapah region span between 2100 Ma and 600 Ma (cf. Murty et al., 1987; Padmakumari and Dayal, 1987) making it difficult to assign any definite age for the dyke emplacement.

1.3.3 DYKES OF THE SOUTHERN GRANULITE TERRAIN

Prominent dyke clusters, which can be regarded unrelated to Phanerozoic west coast tectonics, are seen to occur in Tiruvannamalai, Dharmapuri, Salem, Agali-Coimbatore and in north Kerala. Except for the report 1680 Ma K-Ar age for a dyke near Madras (Afnasseyev et al., 1964), none of the dykes in this terrain were isotopically dated. Sugavanam et al. (1978) provided field descriptions of the Tiruvannamalai dykes. Venkatesh et al. (1987) reported preliminary palaeomagnetism along with major and few trace elements for the Tiruvannamalai dykes and a few dykes occurring around Attur. In Dharmapuri area, to the west of Tiruvannamalai, dolerites occur with a NW-SE strike trend. Dykes trending ENE-

WSW in the Agali-Coimbatore area constitute another important dyke swarm (Radhakrishna et al., 1994b; Radhakrishna and Joseph, 1992a,b). The detailed geochemical, palaeomagnetic and isotopic data of Agali-Coimbatore dykes have been discussed by Radhakrishna et al. (1994b) and Radhakrishna and Joseph (1994). K-Ar ages (1660-1700 Ma) and palaeomagnetism were also reported for the Dharmapuri and north Kerala dykes (Radhakrishna et al. 1986; 1991; Radhakrishna and Joseph, 1994).

The isotope ages of these dyke swarms indicate that the southern granulite terrain was affected by large scale basic magmatic events during mid-Proterozoic (2000-1600 Ma) period. The exposures as dykes may be due to deep erosional levels or otherwise these magmatic episodes may not have given rise to large volcanic sequences.

1.4 TIRUVANNAMALAI DYKES

1.4.1 PREVIOUS WORK

Two groups of geologists, one from the Geological Survey of India (GSI) and the other from the National Geophysical Research Institute (NGRI), Hyderabad have focussed their study on the mafic dykes of Tiruvannamalai area. Sugavanam et al. (1978) of the GSI have published the geological map of the area. The NGRI group has reported palaeomagnetic and geochemical data on seven dykes (Venkatesh et al. 1987). The palaeomagnetic study involves initial natural remanent magnetism (NRM) measurements and AF/thermal demagnetisations following the pilot specimen approach. The dykes were regarded as three distinct groups. Geochemical studies were based mainly on major elements and few

compatible trace elements of seven dykes. According to them, the dykes were crystallised from two different tholeiitic magmatic suites.

1.4.2 SCOPE AND IMPORTANCE OF FURTHER STUDY

The geochemical and palaeomagnetic data of the previous works are inadequate to argue convincingly the different phases of magmatism or mantle source characteristics. Although three different palaeomagnetic groups are deciphered from the pilot specimen approach in AF demagnetisation, it would be important to conduct detailed demagnetisations at each sample level to identify the secondary magnetic overprints and to arrive at a primary characteristic remanent magnetism. Therefore, palaeomagnetic study on more dykes has an advantage in the case of Tiruvannamalai dykes. First, the data would more convincingly test the suggested occurrences of three phases of igneous (dyke) activity. Alternatively, if the different directions correspond to discrete phases of magmatism, then the increase in number of sites and samples would result in a more precise palaeomagnetic pole, averaging out the palaeosecular variation. Further, the lack of isotope ages remains to be a hindrance for a comparison with other dykes and to use the data for drawing the apparent polar wander path.

Petrogenetic studies of the Proterozoic basic magmatism in the south Indian shield have been long overdue. The petrogenetic aspects of dykes of several continents have been worked out. The Scourie dykes of Scotland, dykes of Superior Province etc have contributed significantly to the understanding of continental magmatism during the Proterozoic time. Unfortunately, a comparable information over the Indian shield is not available owing to the lack of the incompatible element, rare earth element (REE) and isotope data on dykes or other

magmatic suites of Proterozoic age. Geochemical investigation incorporating such data of the Tiruvannamalai dykes, which is one of the most prominent and well exposed Proterozoic dyke swarms in south India, would provide information on the Proterozoic continental magmatism in the Indian shield. A comparison with other similar dyke swarms of Gondwanaland would provide in general, the geodynamics of mantle processes during Proterozoic in the combined Gondwanaland.

1.5 OBJECTIVES OF THE PRESENT STUDY

The Tiruvannamalai dykes were taken up for study with the following objectives:

1. The geochemical study is envisaged to characterise the Tiruvannamalai dykes, using a large data set of major and trace elements including more incompatible elements, REE and oxygen isotopes. Further, the various petrogenetic problems associated with continental magmatism, like fractional crystallisation, crustal contamination and the nature of mantle source (s) would be evaluated.

2. The characteristic palaeomagnetic directions of Tiruvannamalai dykes will be determined through incremental AF and thermal demagnetisation at each sample level in close intervals (25 Oe). These data would be properly screened to isolate primary magnetisation from secondary magnetism and to derive mean palaeomagentic pole for the dyke swarm after averaging out palaeosecular variations. Further, K-Ar isolate dating is envisaged to assign age(s) for the palaeomagnetic pole(s) in the Tiruvannamalai dykes.

3. The study proposes to test whether the dykes of NW-SE and NE-SW trends represent petrogenetically related suites using geochemistry, palaeomagnetism and isotope data.

4. The data from the field, geochemical, palaeomagnetic, isotope dating would be interdigitated to probe into the development of Proterozoic south Indian lithosphere and relative motions of lithospheric plates.

GEOLOGICAL SETTING

2.1 INTRODUCTION

Evaluation of petrogenetic and geotectonic problems of the dyke intrusion require a knowledge about the geology of host rocks for the dyke intrusions and the regional geological setting of the terrain. Therefore, the chapter is devoted to review first the regional geology of the south Indian terrain under three broad tectono-thermal units namely Granite-Greenstone Terrain, Eastern Ghat Mobile Belt and Southern Granulite Terrain. It follows a more detailed description on the Tiruvannamalai host rock geology including the metamorphic and deformation history. Then, the field characteristics of the dykes and their petrographic details are described. These descriptions guided the sample selections for the geochemical study, selection of palaeomagnetic sites and isotope dating and further to evaluate the data more meaningfully in the subsequent chapters.

2.2 REGIONAL GEOLOGY

The south Indian shield is a classic terrain which has recorded much of the Precambrian geological history. Recently, various workers (Swami Nath and Ramakrishnan, 1981; Drury et al., 1984; Naqvi and Rogers, 1983 and 1987; Radhakrishna and Ramakrishnan, 1993) have discussed the geology of the region. The present description is based on these reviews.

The south Indian shield comprises rocks of diverse origin, age and metamorphism (figure 2.1). Precambrian rocks ranging from 3800 Ma to late Precambrian constitute about

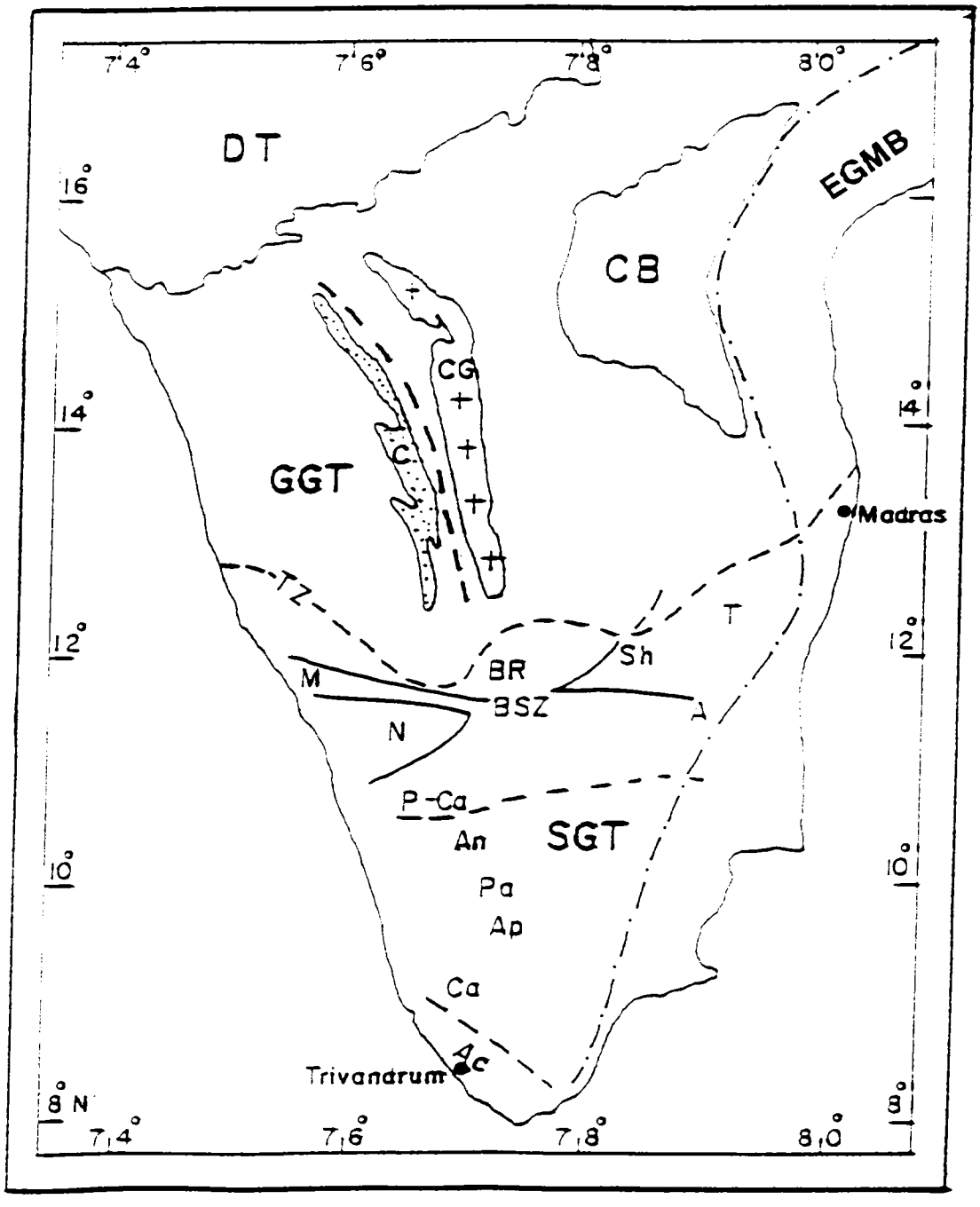

Figure 2.1: Tectonic map of south Indian shield (mostly based on Drury et all, 1984). Ac = Achankovil lineament (or shear zone); Ca = Cardamom Hills; Ap = Anttipatti; Pa = Palani; An = Anamalai; N =Nilgiri massif; BR = Biligirirangana Hillls; M = Moyar shear zone; BSZ = Bhavani shear zone; P-Ca = Palghat-Cavery lineament; T = location of Tiruvannamalai dykes.

two thirds of the surface exposures of the peninsular Indian shield. The other important lithologies are the late Cretaceous Deccan Traps and Proterozoic sedimentary basins of Cuddapah and Kurnool. Based on the tectono-metamorphic history, the south Indian shield is divided into the Granite-Greenstone Terrain (GGT), Southern Granulite Terrain (SGT) and Eastern Ghat Mobile Belt (EGMB). The orthopyroxene isograde (Fermor, 1936) is generally regarded as the boundary between the low grade GGT and high grade SGT. The EGMB constitute the crustal terrain exposed on the east coast (figure 1.1) and is suggested to extend all along the Tamil Nadu coast up to Kanyakumari (figure 2.1). The western boundary of the EGMB shows a thrust contact.

The GGT and SGT were suggested to have come into contact involving subduction and/or collision tectonics (Peucat et al., 1989, Radhakrishna, 1989). Gravity studies across the Transition zone do not indicate any anomaly like in the case of Eastern Ghat front (Hari Narain and Subrahmanyam, 1986). A continuous gradation of metamorphism and palaeopressures have also been indicated (Janardhan et al., 1982; Hansen et al. 1984).

2.2.1 GRANITE-GREENSTONE TERRAIN (GGT)

The Granite Greenstone Terrain of south India is one of the most critically studied cratons of the world. The terrain is divided into western Dharwar craton and eastern Dharwar craton by the N-S trending Closepet Granite.

In the western Dharwar craton, the Older Gneissic Complex (OGC) is the dominant lithologic unit. They are Tonalite-Trondhjemite-granodiorite (TTG) gneisses metamorphosed

to amphibolite facies. The Rb-Sr and Pb-Pb ages of the OGC range from 3.4 Ga to 3.0 Ga. Their low initial $^{87}Sr/^{86}Sr$ ratio of 0.7009-0.7033 indicate mantle- like source for their protoliths. The 3000 Ma old poorly foliated to massive trondhjemite diapirs mark the final stage of cratonisation of the western Dharwar craton.

The western craton is a host to many nearly N-S trending mafic schist belts. These schist belts can be broadly grouped into three types. The oldest of these are exposed in the southern part of the craton. They are high grade mafic schist belts metamorphosed to upper amphibolite to granulite facies and are seen as small enclaves. Typical rock types include quartzites, carbonates, metapelite, iron stones, mafic and ultramafics. These have been deposited in a shallow, volcanically active basin. They are characterised by the absence of clastic sediments. These are generally referred to as Sargur type.

The schist belts Nuggihalli, Krishnarajpet and Javanahalli which are older than 3000 Ma and are characterised by the abundance of komatiitic ultramafics, aluminous and ferrugenous metapelites and absence of quartz and clastic sediments constitute the second group. The rocks are metamorphosed to amphibolite facies and are intruded by 3000 Ma trondhjemite diapirs.

The younger schist belts are characterised by metamorphism predominantly of greenschist facies but occasionally grades into epidote amphibolite or low amphibolite facies. Major belts are Chitradurga, Bababudan, Shimoga and Western Ghat. In several places the belts lie unconformably on 3.0 Ga basement rocks. These belts have been formed during 3.0-2.5 Ga in long linear basins formed by the faulting and rifting of the 3.0 Ga crust. The

depositional environment of the younger schist belts indicate tectonically unstable basin evolution. The initial shallow water assemblages of cross-bedded quartzites, carbonates and metapelites are followed by deep water facies like greywacks, argillites and cherts in association with pillowed and variolitic bimodal lava units.

The Eastern Dharwar craton extends towards east of the Closepet granite up to Cuddapah Basin and Nellore schist belt. The boundary between the Eastern Dharwar and Western Dharwar was defined by the Closepet granite. Drury (1983) proposed a N-S trending shear zone along the eastern margin of the Chitradurga belt. This is spatially correlated with an east dipping thrust revealed by deep seismic sounding (Kaila et al., 1979) and is now considered to be the boundary between the two terrains. The Younger Granitic Complex (YGC) constitutes basement granodioritic to granitic gneisses of this terrain. The major difference of YGC from the OGC is that the YGC is dominated by granitoids. These are metamorphosed at a high T/low P than rocks of the OGC. Based on the earlier Rb/Sr isotope data, the ages of the YGC have been placed between 3.0 and 2.5 Ga. Recently, more precise U-Pb ages (2630-2530 Ma) on gneisses of Kolar region have been reported by Krogstad et al. (1991). These data also support the view that the metamorphism and cratonisation of this terrain must have taken place at 2.5 Ga.

The eastern Dharwar craton is characterised by the famous gold belts of Kolar, Ramagiri and Hutti. Other schist belts are Maski and Pamidi belts. These belts are correlated with the Bababudan Group of the Dharwar supergroup, while the Sakarsanahalli supracrustal enclaves near the Kolar belt have been correlated with the Sargur enclaves of the western Dharwar craton. These belts are characterised by the scarcity of metasedimentaries and

dominance of various types of amphibolites including Mg rich-komatiitic amphiboles (Rajamani, 1991). The komatiitic amphibolites of Kolar were dated at 2.9 Ga.

Within the GGT, there are three major Proterozoic platformal sequences, which are mostly undeformed. They are represented by Cuddapah, Bhima and Kaladgi Basins. The Bhima and Kaladgi Basins which occur in the western Dharwar craton do not show metamorphism or deformation. On the other hand, the Cuddapah Basin experienced extensive deformation along the Eastern Ghat front towards the eastern boundary while the western basin is devoid of deformation or metamorphism. The Deep Seismic Sounding (DSS) data indicate low angle easterly dipping thrust between the Cuddapah and the Eastern Ghat Mobile belt.

The crescent shaped Cuddapah Basin contains two sub-basins, the Cuddapah and the Kurnool. The Cuddapah sediments unconformably overlie the YGC and are composed predominantly of arenaceous and argillaceous sediments of shelf facies, intercalated with volcanic flows/tuffs. Drury (1984) has discussed the thermal model for the formation of this basin. The Kurnool sediments overlie unconformably the Cuddapah suite of rocks. The sub-basin has a western transgression contact while at the eastern contact Cuddapah sediments are thrust over the Kurnool rocks. The rocks are mainly calcareous of near shore to shallow depositional condition. The Banganapalli quartzite at the base of the Kurnool Group is diamond bearing. As the kimberlites of Wajrakarur have yielded Rb-Sr mineral isochrons of 1091±20 Ma and 1092±15 Ma (Anil Kumar et al., 1993) and the dykes cutting Cuddapah have yielded 980±110 Ma (Crawford and Compston, 1973), the age of the Kurnools can be assigned to be ~1000 Ma.

2.2.2 EASTERN GHAT MOBILE BELT (EGMB)

The Eastern Ghat Mobile Belt is comprised mostly of high grade granulite facies gneisses. The western boundary of this belt is defined by a thrust fault (Kaila and Bhatia, 1981). The northern boundary is defined by the Sukinda thrust. Major rock suites include charnockite, khondalite, leptinitic gneisses. Many occurrences of anorthosite complexes and alkaline plutonic rocks are reported.

The terrain hosts two schist belts, Nellore and Khammam. The Nellore schist belt has been equated with the older mafic schist belts of the Dharwar craton. It includes lower metasedimentary Kandikur Formation and the upper metavolcanic Kandra Formation. The age of original deposition of the Nellore sediments is difficult to trace, but from the regional setting it seems to have undergone final metamorphism in the late Proterozoic around 1000 Ma (cf: Radhakrishna and Ramakrishnan, 1993). Recently, Leelanandam (1990) interpreted the Kandra volcanics from the Nellore mica belt as an ophiolite suite.

Anorthosites, gabbros and ultramafic rock occurrences constitute the magmatic units in this terrain. They are generally deformed but do not show granulite facies metamorphism. Major post-tectonic alkaline suites occur at Koraput, Kunavaram and Elchuru. They include syenite, alkali diorite, monzodiorite, nepheline syenite, minor occurrence of carbonatite and lamprophyre. Available geochronology of these rocks is only of preliminary nature; the ages on the anorthosites and alkaline rocks fall in the Mid-Proterozoic period (1400-1200 Ma). High precision dating is yet to be done to ascertain the age of these igneous activity.

Recent U-Pb ages on zircon and monazites as well as Sm-Nd, U-Pb and Rb-Sr ages from the granulites of this belt place the granulite metamorphism at ~1100-900 Ma and granite intrusion at 900-1000 Ma (Grew and Manton, 1986; Aftalion et al., 1988; Paul et al., 1990). This Proterozoic granulite event can be traced in Antarctica but is not traced in the GGT. It appears that, following the granulite facies metamorphism, the Eastern Ghat unit came into a thrust contact with the granite greenstone block (Radhakrishna and Ramakrishnan, 1993). Naqvi and Rogers (1987) have indicated the probability of the thrust fault in the western margin of this belt to be caused by the continent-continent collision. This major geotectonic process is considered to have caused folding in the eastern Cuddapah Basin and also in the eastern parts of Kurnool sub-Basin and a N-S structural grain in the whole terrain.

2.2.3 SOUTHERN GRANULITE TERRAIN (SGT)

The region to the south of the orthopyroxene isograde (Transition Zone; figure 2.1) is termed as the Southern Granulite Terrain characterised by the upper amphibolite to granulite facies (high grade) metamorphic rocks. Major rock types of the terrain include banded gneisses, charnockite and khondalite suite of rocks. Satyamangalam Group (Gopalakrishnan et al., 1975) and Wynad schist belt (Nair et al., 1975) constitute important supracrustal units of higher amphibolite facies in this terrain. Anorthosite-Gabbro complexes are the characteristic of layered sequences in the granulite region and do not occur outside the granulite terrain. Mafic dyke intrusions and several post or late tectonic granitic bodies represent important igneous activity in the terrain.

The southern granulite region is characterised by a number of highland regions and shear zones. The Nilgiri massif, Biligirirangana Hills massif and Shevory Hills are the prominent highland regions (figure 2.1). These highland regions are all comprised of charnockite massifs recrystallised in high temperature (700-800°C) and high pressure (7-8 kb) compared to the temperature (700±20°C) and pressure (4-6 kb) of recrystallisation within the low land charnockites or supracrustals. The charnockites and other granulites on the Transition zone show lithological, structural and metamorphic continuity with the GGT, suggesting them to be deep crustal sections of the Dharwar craton (Ramakrishnan, 1993).

Drury et al. (1984) have proposed a number of shear zones traversing the southern granulite terrain (figure 2.1). The Moyar shear zone borders the Nilgiri massif on the north while Bhavani shear zone marks the southern boundary of the Nilgiri massif. These two join together to the east of the massif and continue east ward as the Moyar-Bhavani-Attur shear zone for several kilometers almost parallel to the transition zone. According to Drury et al. (1984) several tens of kilometers of displacement has occurred along the Moyar-Bhavani shear zone between Biligirirangana Hills and Nilgiri massif. Drury et al. (1984) proposed that E-W trending Palghat-Cauvery shear zone is another prominent shear in southern granulite terrain. It is suggested to extend along the low lands from Palghat in the west to the Cauvery delta in the east. To the south of this shear zone are the prominent hills of Anamalai, Palani, Andipatti and Cardamom Hills (figure 2.1) consisting of charnockite and migmatite gneiss. Thick sequences of supracrustal units of khondalite group occur in the southern Kerala extending to Tamil Nadu and generally referred as Kerala khondalite belt (KKB). The boundary between these lithologies follow closely the Achankovil lineament which has been proposed as Achankovil shear zone by Drury et al. (1984). Drury et al. (1984) and a few

other researchers suggested that the Achankovil demarcates the zone along which the KKB has been welded to the SGT. Naqvi and Rogers (1987) indicated that the sense of movement or magnitude of displacement along the shear zone is not yet clearly worked out. While Radhakrishna et al. (1991b) interpreted it as a topographic expression of neotectonic event and it does not represent a zone of tectonic contact between crustal blocks in the absence of characteristic features of shearing.

Compared to GGT, the isotope ages from the southern granulite terrain are very sparse. Majority of published isotope ages are on the rocks of the transition zone which includes Nilgiri massif, Biligirirangana Hills, Kabbal and Pallavaram. The Rb-Sr, Nd-Sm and Pb-Pb ages range between 2900-2500 Ma (Peucat et al., 1989; Friend and Nutman, 1992 and the compilation of Naqvi and Rogers, 1987). For the charnockite occurring in khondalite in the southern khondalite belt, Srikantappa et al. (1985) reported U-Pb zircon data which lie close to the lower intercept of a discordia through c.540 Ma and c.1930 Ma. Hansen et al. (1985) have also reported 550 Ma for gneisses retrograded from charnockite near Madurai. Late Proterozoic magmatic activity in the SGT is manifested in the form of many small granitic plutons whose ages lie between 980-665 Ma (cf. Kroner, 1991). The Ezhimala granite-granophyre complex was dated at 678 Ma age (Rb-Sr method; Nair and Vidyadharan, 1982).

2.3 GEOLOGY OF TIRUVANNAMALAI AREA

2.3.1 GEOLOGICAL SETTING

The area under investigation falls in the North and South Arcot districts of Tamil Nadu. It forms a part of the southern high grade Granulite terrain to the south of the

orthopyroxene isograde. The geological description is mainly based on the work of Sugavanam et al (1978).

The geological map of the study area is shown in figure 2.2. High grade metamorphic crystalline rocks (charnockite and khondalite groups and migmatites) constitute the main lithology. Magnetite quartzites and pyroxene granulites are subordinate lithologies in the area. Distinctly well developed foliation is noteworthy in the charnockites of this area and it is intensely co-folded with magnetite-quartzite and pyroxene granulite (Sugavanam et al., 1978). Migmatitic gneiss is extensively exposed as flat outcrops in plain areas. Migmatisation of charnockite appear to have developed biotite gneiss exposed towards the centre of the area with many relicts of charnockite patches.

The metasedimentary rocks represented by khondalite group of rocks comprise magnetite-quartzite, gneiss with garnet + sillimanite + quartz + feldspar ± graphite, garnet-biotite-quartz-feldspar gneiss and sillimanite-quartzite. Magnetite-quartzite occurs as distinct bands traceable over considerable distance. Sillimanite schists and Kyanite-sillimanite-staurolite schist are exposed near the Sattanur Dam.

Garnetiferous quartz-pyroxene granulite with pyrite and pyrhotite occur in the sulphide bearing band intercalated with magnetite quartzite. The only metaliferous deposite of economic significance is located in Mamandur in Kallakurichi, south Arcot. This is a polymetal sulphide deposit comprising zinc, lead, copper and silver with significant traces of tellurium and gold.

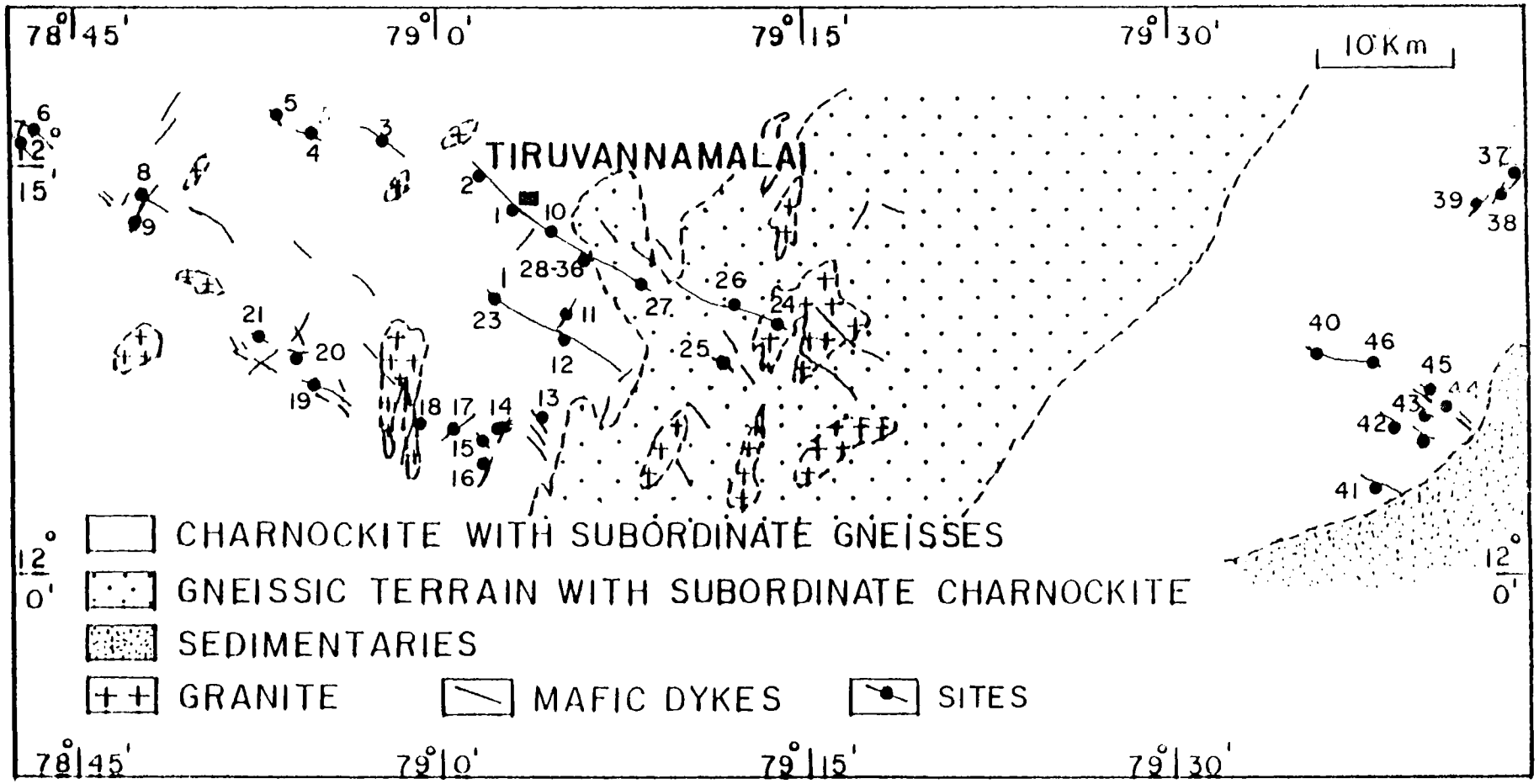

Figure 2.2: Geological map of Tiruvannamalai area (modified after Sugavanam et al 1978) with sample location.

The ultramafic rocks include pyroxenite, dunite and anorthosite. They occur as concordant impersistent bands and lenses. Impure talcose rocks developed occasionally within the ultramafics. Magnesite also occurs within some of the altered ultrabasic rocks.

Pink granites essentially composed of perthitic feldspar and quartz form concordant bands and lenses. Porphyritic granite forms a narrow but distinct zone between the migmatite and the massive non-foliated Gingee granite.

Alkali syenite of Elagiri and the associated carbonatite represent the youngest igneous activity in the Tiruvannamalai area. They are enriched in pink and grey alkali feldspar. The dolerite dyke north of Andiyappam abuts against the Elagiri syenite. The syanite shows assimilation of dyke indicating that the dykes are older than the syenite (Sugavanam et al., 1978).

Overlying the crystalline rocks of Precambrian age are the fossiliferous upper Cretaceous Formations (seen on the eastern extreme; figure 2.3) . They occur near the high ground of Tiruvakkarai. Overlying the Cretaceous rocks are the Mio-Pliocene Cuddalore Formation. This formation is composed of sandstone often ferrugeneous, pebble bed, sand and clay with lignite seams and silicified wood at places. These in turn are overlain by the rocks of the Coromandal Formation of Holocene and composed of sandstone, clayey sand, sandy clay and clay.

2.3.2 METAMORPHISM AND DEFORMATION

The Tiruvannamalai terrain exhibits multi-structural and polymetamorphic complexity. Various phases of deformation were inferred from highly warped and contorted foliation trends and variable amounts of dip. Except the basic dykes and the alkali intrusives, all other formations have well developed foliation. The major structural markers in the area are bands of magnetite-quartzite, pyroxene granulite and pink granite. Sugavanam et al. (1978) reported the metamorphic and structural history of this area and it is the basis for the brief description below.

The repeated deformation, complex folding and the interaction of these deformation phases have resulted in tightening earlier folds, warping earlier fold axes, superposition of new foliations, development of lineations, plunges, domes and basins.

The original layering in the rocks were disrupted and the rocks were folded isoclinally with an axial trace in the NNE-SSW trend. The granulite facies metamorphism which resulted in the formation of charnockite and pyroxene granulites was correlated with this deformation. This deformation appears to have resulted local anatexis and migmatisation.

The refolding of the isoclinal folds are generally marked by kinks on the limbs of the longitudinal isoclinal folds. They have an ENE-WSW trend with low plunge to ENE. The granitic activity appears to be associated with the late stage of earlier folding and seems to have extended into this later deformation and culminated in the formation of Gingee granitic massif.

The subsequent deformation resulted in NS trending folds in all the lithologies. They are very much restricted in their development and areal extent and are seen mostly to the north-east of Tiruvannamalai. This deformation has resulted in local remelting, fusion and epidotisation.

Regional fracturing and shearing appear to have facilitated emplacement of large alkali syenite, carbonatite and galena bearing quartz baryte veins. These processes mark the final phases of tectonic activity in the Tiruvannamalai area. Sugavanam et al. (1978) placed the last tectonic event between 1000 and 750 Ma.

No direct isotope ages are available on charnockites in Tiruvannamalai region. However, a few isotope ages are now available on charnockites of Nilgiri, Kabbal, Biligirirangana Hills and Pallavaram in the Transition zone which are the extensions of the charnockite rocks of Tiruvannamalai (compilations of Naqvi and Rogers, 1987; Peucat et al., 1989; Friend and Nutman, 1992). Based on these studies the charnockite formation of the area may be regarded as 2.6 Ga.

In summary, the basement rocks in Tiruvannamalai terrain has undergone major deformation and granulite facies metamorphism ~2600 and 2500 Ma. The dykes occurring in NW-SE and NE-SW strike trends and a few syenites and associated carbonatite constitute the Proterozoic magmatic phases. In the light of the attributed age of 2500 Ma for the basement regional metamorphism and 750 Ma for the syenite bodies (which have incorporated the dolerite dyke material), it may be inferred that the unmetamorphosed mafic dykes intruded sometime during the early to mid-Proterozoic in age.

2.4 DESCRIPTION OF MAFIC DYKES

2.4.1 FIELD DESCRIPTION OF THE DYKES

Mafic dykes of the Tiruvannamalai area occur in a 50 km wide zone for over 100 km. The dykes are medium grained black dolerites. They trend in the NW-SE and NE-SW strike directions. Even though the dykes occur in two directions, their relative chronology based on cross-cutting relationship could not be established in the field.

Generally the dykes could be traced for more than 4 km along the strike. The dyke cutting through the Tiruvannamalai town was traced for more than 20 km. The widths usually vary between 20-60 m and rarely attain 80-100 m. The dykes display steep to vertical contacts with the country rocks. The contacts are always knife sharp and show development of chilled margins.

The dykes frequently occur as well exposed ridges while in the low lands they may be flat lying or are exposed as boulders in the soil cover. Below the boulder zones, the dykes are massive and devoid of fractures and alteration. These dykes are regarded as one of the best dimension stones in the international market.

2.4.2 PETROGRAPHIC DESCRIPTION

The mafic dykes are medium-coarse grained dolerites. The samples from the margin are fine grained while the dyke centres are medium grained. The rocks are essentially composed of plagioclase, clinopyroxene and opaques. Olivine and micropegmatites constitute

the accessory mineral phases while minor biotite, amphibole (actinolite) and quartz occur rarely as secondary components. All samples possess typical ophitic to sub-ophitic intergrowth of plagioclase and pyroxene. Selected photomicrographs are shown in plate 1.

Plagioclase (usually labradoritic) occurs as laths and shows polysynthetic twinning. In few samples, it occurs as phenocrysts within the ophitic matrix. The plagioclase is generally fresh and constitute more than fifty percent of the rock. Clouding of plagioclase is observed in a few samples (T8, T9, T10, T12, T13). Micropegmatitic intergrowths of quartz and plagioclase near the plagioclase grain boundary.

Augite is the most common clinopyroxene occurring in these dykes. It is seen as subhedral microphenocryst or cumulus phases and constitute more than forty percent. These are commonly fresh. A few clinopyroxenes alteration along grain boundaries or cleavages. The alteration product is uralite or rarely hornblende. However, in T9 and T18, the alteration is more pronounced, but the igneous textures are well preserved. Therefore, alterations are judged to be deuteric.

Olivine occurs as euhedral to subhedral grains in a few samples (T11, T15, T16, T25, T37 and T39). They occur as cumulates/microphenocryst. These can be distinguished by their high relief and irregular microcracks within the grains. A few grains show garlanding of dusty opaques along the grain boundaries.

Opaque minerals are mainly titanomagnetites. They occur as dispersed as euhedral and subhedral grains. A few opaque minerals are skeletal shaped and show development of biotite at the grain boundary. Pyrite is rarely present.

Only one sample (T31) among the total collection is highly altered and its original mineralogy and texture are completely destroyed. It is from the contact of the large dyke passing through Tiruvannamalai margin. The chlorite and calcite are the secondary mineral. Micro-veinlets of quartz and calcite are also present in them.

Typical ophitic texture from the centre of the dyke T2 (Scale 1 cm = 0.3 mm)

Microphenocrysts of plagioclase and pyroxene within the ophitic matrix from the centre of dyke T16 (Scale 1 cm = 0.3 mm)

Olivine cumulates within the ophitic matrix in the centre of the dyke T11 (Scale 1 cm = 0.3 mm).

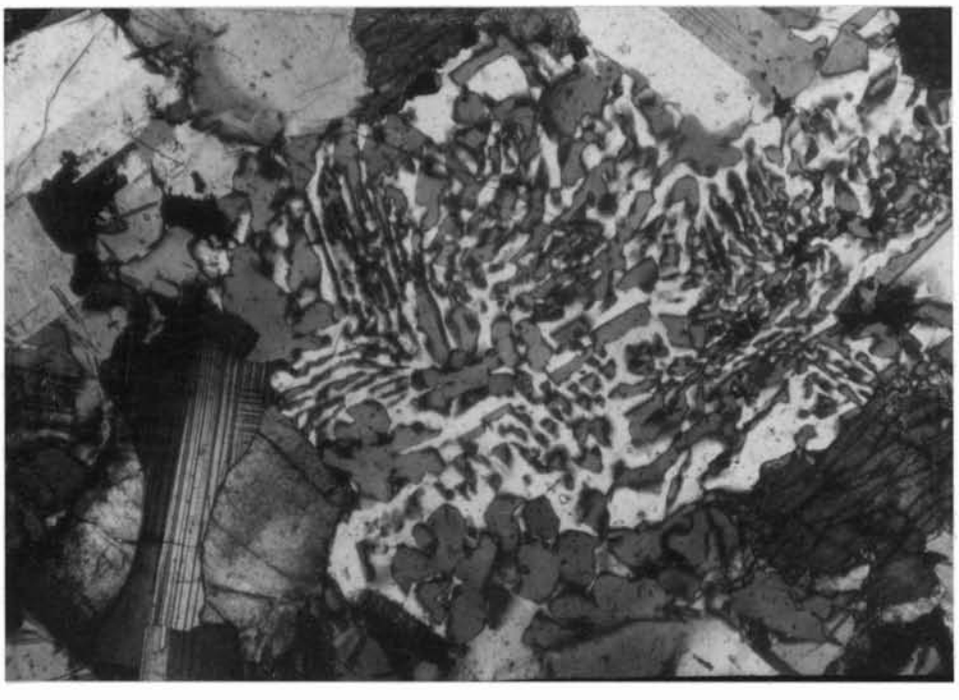

Micropegmetitic intergrowth from the centre of the dyke T 4 (Scale 1 cm = 0.1 mm).

ISOTOPE AGES

3.1 INTRODUCTION

Mafic dykes are considered difficult for radiometric dating because primary minerals that provide stable sites for radio-isotopes are often absent, or present in quantities that preclude acquisition of precise isochrons (Halls and Fahrig, 1987). The problems are exacerbated in Precambrian dykes that have experienced a long and potentially complex history (Hanes, 1988). But assigning absolute ages for dykes have become inevitable as they play a vital role in elucidating the tectono-thermal history, palaeogeography and mantle geochemical evolution. Dating of Precambrian dykes is much more important as they are the major time markers due to their episodic occurrence in a dominantly unfossiliferous period. Precise ages are therefore required for regional correlation of igneous activity, timing of basin formation over wide areas, and for reliable calibration of apparent polar wander paths.

K-Ar, Rb-Sr, Sm-Nd, U-Pb isotopic methods are potentially of value in obtaining ages of dyke swarms. Lanyon et al. (1993) have shown that late stage felsic differentiates of the mafic dykes provide precise crystallisation ages for the dykes, but favourable lithologies (pegmatoid portion of dykes, quartz bearing phases, coarse gabbros and diorites) are generally absent. Application of the whole rock Rb-Sr isotopic technique has proved to be of limited use because of the small spread in Rb/Sr ratios and initial isotopic heterogeneity or perturbation of the isotopic system due to chemical exchange with wall rocks or metamorphic fluids. Internal Rb/Sr or Sm/Nd isochrons using different mineral fractions (plagioclase, pyroxene, magnetite) as well as whole rock samples have proved of value (Armstrong, 1988),

but it is essential to obtain multiple dates on several dykes of a swarm in order to distinguish geologically significant ages (Heaman et al., 1988).

In view of these limitations, dating of dolerite dykes has been done using the K-Ar method. Precambrian dykes often yield anomalous K-Ar ages because of their long and potentially complex post emplacement history which has caused loss or inheritance of Ar and exchange of potassium. Though these factors are unavoidable, judicious sample selection after careful petrographic examination can still provide geologically significant results (Hanes, 1988).

In the case of Tiruvannamalai dyke swarms, no attempts were madeearlier to determine isotope ages. K-Ar isotope technique has been employed on petrographically alteration free Tiruvannamalai dykes. The isotope dating of these dykes is most significant to probe the relative chronology and timing of both NW-SE and NE-SW dykes and also to assign an age for the palaeomagnetic directions to help drawing the apparent polar wander path and to understand the implications of geodynamic.

3.2 K-Ar ANALYTICAL METHOD AND TREATMENT OF DATA

K-Ar ages were determined for ten whole rock dolerites of different dykes from the Tiruvannamalai area. Fresh samples displaying the least alteration features were selected on the basis of petrographic observation. The whole-rock samples were prepared by crushing and sieving to 177-149μ size followed by thorough washing in deionised water and drying at 120°C. Where possible, the powder particle size was kept approximately equal to the natural

grain- size of the whole rock because fine pulverising is recognised to cause loss of radiogenic ^{40}Ar. The K-Ar isotopic measurements were carried out at the University of Newcastle upon Tyne, UK. Potassium was determined on a Corning EEL 450 Flame Photometer with lithium as an internal standard and using sodium buffering. A modified Kratos MS-10 Mass Spectrometer was used to determine the radiogenic argon contents by means of isotope dilution with a ^{38}Ar tracer. Modifications to the MS-10 included use of a 4.2 Kilogauss permanent magnet (to improve resolution) and a high gain chopper amplifier (to improve sensitivity and stability). The sensitivity achieved is about 1 X 10^{-5} A/torr allowing a lower limit of detection for ^{36}Ar of about 4 X 10^{-8} cc STP. The quoted uncertainties (table 3.1) are based on reproducibility of measurements and are generally better than 0.3%. Ages were calculated using the decay constants of Steiger and Jager (1977).

The timing of dyke intrusions was inferred from the K-Ar ages on the basis that a geological event has initially "set" the potassium-argon isotopic system. Very few minerals respond in exactly the same way to geological conditions that are capable of affecting potassium-argon dates (Dalrymple and Lanphere, 1969) because the loss of argon, in general, proceeds at different rates in different minerals for any given set of conditions. Thus whole rock analyses performed on independent but related samples having variable proportion of mineral phases, if yielding concordant ages, are indicative of a lack of geological disturbance, and therefore are of an "age" which relates to an identifiable geological event in the history of the suite of related samples.

Where concordancy exists at the 2σ level among a subset of analysed samples from the dyke sets, a mean age was calculated on the basis that the same geological event is being

recorded in all of the samples. The analytical uncertainties attached to individual dates vary considerably and so it has been necessary to adopt a weighting factor (the inverse variance; Topping, 1958) favouring the most precisely determined values, and a weighted mean (and standard error) calculated (the Inverse Variance Weighted Mean; IVWM) for each set of concordant dates. The analytical uncertainties of individual analyses could, under no circumstances, be used as a basis for assessing the geological significance of the date in question.

3.3 K-Ar AGES OF TIRUVANNAMALAI DYKES

Ten dolerite dyke samples, five each from NW-SE and NE-SW dykes, were selected covering the entire geographical distribution of the area. Data are presented in table 3.1. In conventional K-Ar dating of diabase dykes, the main difficulty is to locate samples which have suffered minimal argon loss. The margins of the dykes can act as channel ways to later hydrothermal fluids. This can alter the isotopic systematics. But there are views that chilled margin samples normally yield dates older and more reliable than the coarse interior (cf: Mohr, 1987). But Hanes and York (1979) demonstrated reverse behaviour for an early Proterozoic dyke, with older dates from centre samples. Hunziker (1979) argued that central portion of the dyke are to be collected for K-Ar dating. The margins are also prone to crustal contamination and this will upset the isotopic concentration. Moreover, the contact samples of Tiruvannamalai dykes are highly fractured and altered. In view of this, samples from the contact zones have been avoided.

In the Tiruvannamalai dykes, four samples have shown dates higher than 1800 Ma. In the context of the tectonothermal history of the area, the highest age (c.2550 Ma) obtained from a sample T-12 can have no geological significance. Sample T-16 (which has given an age of 1870 Ma) shows minor alteration to amphibole and may not be entirely deuteric. There is a strong likelihood, therefore, that its K-Ar system was perturbed by "initial" ^{40}Ar or later K-Ar exchange. Among the other samples, six of the ages are concordant with inverse variance weighted mean age of 1650 ±10 Ma. Two of the remaining ages are concordant with a mean of 2240±30 Ma. These data provide strong evidence of a geologically significant event at 1650±10 Ma. One scenario would be that the dykes were intruded at this time in which case the older ages would be attributed to excess ^{40}Ar; alternatively the dykes may have been intruded at 2240 Ma with a regional event (metamorphism ?) at 1650 Ma. Since the dykes are devoid of metamorphism and are fresh with typical igneous textures, the 1650 Ma event is ascribed to the actual intrusion of the dykes.

Table 3.1: K-Ar isotope ages of the Tiruvannamalai dykes

Sample No.	K_2O wt.%	Radiogenic ^{40}Ar (mm^3g^{-1})	%Atmospheric contamination	Age (Ma±1σ)
Northwest-Southeast Dolerite Dykes				
T1	0.815±0.013	$(6.94\pm0.07)10^{-2}$	2.0	1630±30
T8	0.585±0.009	$(8.54\pm0.10)10^{-2}$	1.9	2270±40
T12	0.576±0.006	$(10.45\pm0.09)10^{-2}$	2.1	2550±30
T15	0.434±0.004	$(3.78\pm0.05)10^{-2}$	9.1	1650±30
T45	0.745±0.003	$(6.59\pm0.08)10^{-2}$	4.0	1670±20
Northeast-Southwest Dolerite Dykes				
T9	0.647±0.003	$(9.08\pm0.08)10^{-2}$	3.6	2210±20
T11	0.470±0.008	$(4.12\pm0.04)10^{-2}$	8.3	1660±30
T16	0.458±0.006	$(4.85\pm0.07)10^{-2}$	6.0	1870±40
T17	0.759±0.011	$(6.60\pm0.05)10^{-2}$	7.6	1650±30
T39	1.094±0.010	$(9.48\pm0.09)10^{-2}$	1.8	1640±20

Concordancy of the ages from both the NW-SE and NE-SW dykes suggests that both NW-SE and NE-SW dolerite swarms in Tiruvannamalai were intruded at 1650±10 Ma. The data suggest that the Tiruvannamalai dykes of both NW-SE and NE-SW trends are penecontemporaneous and relate to a single magmatic episode.

Appendix:

The K-Ar ages of the dyke samples were calculated using the following equation:

$$t = \frac{1}{\lambda}\ln\left[\left(^{40}Ar^{*}/^{40}K\right)\left(\frac{\lambda}{\lambda_e}\right) + 1\right]$$

Where, $^{40}Ar^{*}$ is the Argon produced by the disintegration of ^{40}K after the formation of the rock excluding the initial argon if any, λ is the total decay constant of ^{40}K and λ_e refers to the decay of ^{40}K to ^{40}Ar. The decay constants recommended by the IUGS Subcommission on Geochronology (Steiger and Jäger, 1977) are $\lambda = 5.543 \times 10\text{-}^{10}y^{-1}$ and $\lambda_e = 0.581 \times 10^{-10}y^{-1}$.

GEOCHEMISTRY

4.1 INTRODUCTION

Forty dolerite samples from both the NW-SE (32 samples) and NE-SW (8 samples) dykes were chosen for geochemical studies. It was ensured that the samples were fresh and least altered based on petrography. Samples were collected generally from the central portion of the dykes while a few samples (T16, T28, T29, T30 and T31) were from the dyke margins. One long dyke was sampled along and across the length to assess within-the-dyke variation. Samples were crushed, washed in distilled water and dried. About five hundred grams of each sample were pulverised to fine powder. All samples were analysed for major and trace (Rb, Sr, Ba, Th, Pb, V, Cr, Ni, Co, Zn, Y, Zr, Nb) elements. Representative samples, selected based on the degree of fractionation were analysed for more incompatible trace elements including REE. Oxygen isotope content of eight samples were determined. The analytical techniques are briefly summarised and then the results of Tiruvannamalai dykes are presented below.

4.2 ANALYTICAL TECHNIQUES

The major element analysis was done using X-ray Fluorescence (XRF) techniques. These analyses were performed at the Airborne Mineral Surveys and Exploration Wing of Geological Survey of India, Bangalore. Among the trace elements, all the samples of major element analysis were analysed for transition metals and large ion lithophile elements using the XRF methods. These trace element analysis were performed at Geology Department,

Rhode University, South Africa. Selected samples were analysed for REE and more incompatible elements including the duplication of the trace elements determined by XRF method by ICP-MS techniques at the National Geophysical Research Institution, Hyderabad. Details of analytical methods are briefly summarised below:

4.2.1 X-RAY FLUORESCENCE (XRF) TECHNIQUE

4.2.1.1 Major elements

The major rock forming oxides (SiO_2, TiO_2, Al_2O_3, $Fe_2O_3^t$, MgO, CaO, Na_2O, K_2O, P_2O_5, MnO) were analysed adopting the XRF (Phillips PW1410) techniques in which the sample powders were fused with lithium tetraborate and lithium carbonate flux and fused into

Table 4.1: Comparative major element (XRF) data for the USGS (DR-N) standard.

	Observed values	Reported values	Percent of difference
SiO_2	52.83	52.87	<1
TiO_2	1.08	1.08	<1
$Al2O_3$	17.73	17.53	<2
Fe_2O_3	9.61	9.69	<1
MgO	4.32	4.47	<4
CaO	7.04	7.09	<1
Na2O	2.85	3.00	<5
K_2O	1.72	1.73	<1
P_2O_5	0.24	0.25	<4
MnO	0.20	0.21	<5

glass disks. These disks were then analysed using K- alpha line for each of the major elements. Background corrections were effected based on counts made from blank materials in the same fusion mixture at the analytical peak positions. USGS and other international rock standards were used as reference samples. Detailed analytical methods were described by Rao et al (1993). A sample USGS rock standard data are given in table 4.1 indicating the accuracies.

4.2.1.2 Trace elements

The trace elements determined using XRF techniques are Cr, Co, Ni, Zn, Rb, Sr, Pb, Ba, Y, Zr, Nb, Th and V. Pressed sample powder briquette were used for XRF analysis. The K-alpha spectral line was used for analysis of most trace elements but L spectral line was used for Ba, Pb and Th. Matrix effects were corrected using appropriate mass absorption coefficients (details in Norish and Chappell, 1967). Background corrections were made by counting at spectral position chosen as interference free and calculating background corrections factors from measurments on high purity SiO_2 and SiO_2+Fe_2O_3 blank samples. Spectral line interferences were corrected by determining interference correction factors from specially prepared interference standards. The following elements were corrected for spectral line interferences (the interference elements are given in brackets) Nb (Y, U, Th); Zr (Sr, Th, U); Y (Rb, Th, U); Sr (Th); Rb (U); Th (Pb); Pb (Th) ; Ba (Ti, Sc); Co (Fe); Cr (V); V (Ti). USGS and other International Rock Standards (BHVO, BCR, AGV, DTS, NIM-P, GSP, PCC, KRF-13) were used to provide calibration for the trace elements analysed. Analytical counting errors, precision and accuracies of the analysis are given in table 4.2.

Table 4.2: Comparative trace element (XRF) data for the USGS rock standards.

	Reported values	Observed values	Difference. absolute	Difference. percent	Error
*Ba	675	703	-28.3	4.2	3.0-4.2
+Co	53	54	-1.5	2.8	0.7-0.8
+Cr	309	305	+3.7	1.0	0.8-1.6
+V	330	320	+9.8	2.9	1.1-1.5
*Th	6.4	4.8	+1.6	24.0	1.2-9.2
*Pb	35	33.6	+1.4	4.1	0.6-1.0
*Zn	84	81	+3.0	3.5	0.8-1.6
@Ni	117	126	-9.4	8.0	1.1-1.7
*Nb	15.0	15.2	-2.0	1.3	0.3-0.9
*Zr	225	221	+4.0	1.7	0.3-0.9
*Y	21.3	21.2	+0.1	0.4	0.3-0.8
*Sr	657	653	+3.1	0.5	0.4-1.0
*Rb	67	66.8	+0.2	0.3	0.3-0.8

* = AGV; + = BHVO; @ = BCR

4.2.2 INDUCTIVELY COUPLED PLASMA - MASS SPECTROMETRY

The PlasmaQuad (VG Elemental, Winsford, Cheshire, UK) ICP-MS instrument interfaced with an IBM PC-XT has been used for determination of REE (La, Ce, Pr, Nd,Sm, Eu, Gd, Tb, Dy, Ho, Er, Tm, Yb, Lu) and many trace elements (Sc, V, Cr, Co, Ni, Cu, Zn, Ga, Rb, Sr, Y, Zr, Nb, Ba, Hf, Ta). 0.1 gm of sample powders, in Teflon beaker, were moistened with few drops of water and then mixed with 7 ml of HF, 3 ml of HNO_3 and 1 ml

Table 4.3:Comparative trace element (XRF) data for the Standard JB-1.

	Reported values	Observed values	Percent of error
Sc	32	29	10
V	200	220	8
Co	38	39	2
Zn	84	82	3.5
Ga	16.8	18	6.3
Rb	40	41	2.2
Sr	461	443	4.2
Y	25.3	25	1.3
Zr	119.6	144	16.9
Nb	18.51	27	31
Ba	486	490	2.1
La	38.08	38.2	<1
Ce	62.99	63.8	5.9
Pr	7.76	6.54	15
Nd	27.29	25	8.3
Sm	3.48	4.7	33
Eu	1.4	1.47	6
Gd	3.8	4.3	12
Tb	0.63	0.70	10
Dy	3.27	3.82	16
Ho	0.74	0.78	5
Er	1.88	2.15	18
Tm	0.32	0.34	5
Yb	1.91	1.96	4.5
Lu	0.26	0.27	4
Hf	3.97	3.40	16
Ta	2.17	2.0	8.5

of $HClO_4$ and digested overnight and evaporated to dryness on a hot plate at 200°C. The process of evaporation with 3 ml of HF and 1 ml of $HClO_4$ been repeated. Rhodium and bismuth (1 ml of 10 μg/ml) was added to act as internal standards. The contents were dissolved in 1:1 HNO_3 (10 ml) medium and made clear solutions to 100 for the ICP-MS analysis. The ion - detection system and the data acquisition system consists of a Channeltron Electron Multiplier (CEM) and a multichannel analyser (Tracor Northern). More details of the instrument and operating parameters are given by Balaram et al. (1990) and Manikyamba et al. (1993). The analytical precision and accuracies were calculated using USGS Rock Standards and are listed in table 4.3.

4.2.3 OXYGEN ISOTOPES

The gas samples were prepared for mass spectrometric analysis by standard vacuum techniques in routine use at the Stable Isotope Laboratory, University of Georgia, USA. Oxygen was extracted from 15-28 mg whole rock powder by reaction with BrF_5 and converted to CO_2. Isotope analyses were made using a VG Micromass 602 C double collecting Mass spectrometer. Oxygen isotope compositions are reported on the standard delta ($\delta^{18}O$) notation in units of per mil (‰) relative to Standard Mean Ocean Water (SMOW). Repeated analyses on an internal quartz sand (RQS) standard ($\delta^{18}O$ value +17.5 ‰) gave errors within ±0.3 ‰.

4.3 RESULTS AND MAGMA CLASSIFICATION

4.3.1 MAJOR ELEMENTS

The major elements are those generally expressed as weight percentages (wt%) of oxides. These include SiO_2, TiO_2, Al_2O_3, Fe_2O_3, MgO, Na_2O, K_2O, P_2O_5 and MnO. These elements control the general abundances and the occurrence of mineral phases and their assemblages. It is of a general practice to transform the major oxide percentages into mineral compositions which are known as norm composition and present in the form of tables along with major elemental abundances. The major element chemistry and the norm compositions of Tiruvannamalai dykes are listed in tables 4.4 and 4.5.

Generally, the major element concentrations of the Tiruvannamalai dykes are restricted within basalt to basaltic andesite compositional range. The average SiO_2 content in the NW-SE dykes is 51.45 wt% with a range between 49.62 and 53 wt%. However, two samples, T15 and T25 have lower SiO_2 of 46.06 and 46.15 wt% respectively. These samples contain cumulus/phenocryst olivine phase. T31 has the highest content (53.26 wt%) and this sample is from the margin of a dyke and contains microveinlets of quartz and the mineralogy is altered. The NE-SW dykes have also similar SiO_2 concentrations varying between 50 and 53 wt% (avg: 51.42 wt%). In these also, two samples (T11 and T16), which contain cumulus/phenocryst olivine, have lower content of SiO_2 (46.54 and 46.21 wt.%). The samples T37 and T39 have high SiO_2 content (53.42 and 53.98 wt% respectively).

$Fe_2O_3^t$, in both the NW-SE and NE-SW Tiruvannamalai dykes, show a pronounced enrichment relative to MORB (avg: 10.0 wt%; cf: Condie, 1987) and OIB (avg: 12.4 wt%;

Table 4.4: Major element and Norm Composition of NW-SE dykes

	T-15	T-25	T-42	T-12	T-8	T-45	T-27	T-2	T-7	T-3	T-36	T-10
SiO2	46.06	46.18	52.67	52.36	52.22	51.11	52.20	51.69	52.23	52.32	51.12	51.38
TiO2	0.88	0.84	0.62	0.63	0.64	0.99	1.08	1.10	1.10	1.10	1.00	1.14
Al2O3	14.51	15.26	13.92	14.27	14.62	13.23	13.42	13.68	13.99	13.88	13.66	13.56
Fe2O3	13.14	11.91	10.48	10.55	10.55	13.52	13.93	13.80	13.92	14.08	13.45	14.18
MgO	12.09	10.39	8.49	7.03	6.59	6.13	5.98	5.88	5.91	5.90	5.56	5.79
CaO	10.55	10.41	11.88	11.06	11.09	10.54	10.37	10.21	10.16	10.20	10.07	10.44
Na2O	1.92	2.03	1.33	1.25	1.64	1.88	2.10	1.80	1.88	1.82	2.01	2.12
K2O	0.46	0.47	0.52	0.59	0.55	0.68	0.71	0.73	0.72	0.75	0.64	0.77
P2O5	0.09	0.10	0.08	0.08	0.08	0.14	0.15	0.16	0.16	0.15	0.13	
MnO	0.19	0.17	0.17	0.16	0.16	0.18	0.20	0.19	0.19	0.19	0.19	0.20
Total	100.32	98.27	100.72	98.29	98.30	98.80	100.42	99.44	100.68	100.73	98.10	100.14
Mg.no.	0.65	0.64	0.62	0.57	0.56	0.48	0.46	0.46	0.46	0.46	0.45	0.45
qz	0.00	0.00	4.54	6.81	5.86	3.60	3.56	4.77	4.65	4.85	4.28	2.26
ab	16.26	17.57	11.24	10.49	14.14	16.17	17.74	15.35	15.87	15.34	17.39	18.01
or	2.72.	2.84	3.07	3.34	3.31	4.08	4.19	4.35	4.24	4.42	3.87	4.57
an	29.65	31.85	30.43	31.69	31.49	26.07	25.06	27.30	27.54	27.38	26.94	25.32
di	18.03	16.55	2.79	19.09	19.8	21.76	21.12	18.92	18.09	18.4	19.41	22.29
hy	0.39	4.88	24.31	23.49	21.64	23.10	22.91	23.83	24.14	24.15	22.88	22.28
ol	28.21	21.8	0	0	0	0	0	0	0	0	0	0
mt	2.86	2.65	2.27	2.31	2.33	2.99	3.03	3.02	3.02	3.05	2.99	3.10
il	1.67	1.63	1.18	1.21	1.24	1.91	2.05	2.11	2.08	2.08	1.94	2.17
ap	0.21	0.24	0.19	1.6	0.19	0.33	0.35	0.37	0.37	0.35	0.31	0

Table 4.4: cont'd

	T-24	T-32	T-22	T-1	T-26	T-35	T-29	T-33	T-46	T-23
SiO2	51.83	52.42	51.69	52.03	52.03	51.50	51.63	52.47	52.90	52.36
TiO2	1.02	1.16	1.21	1.13	1.06	1.27	1.08	1.19	1.14	1.24
Al2O3	13.57	13.05	13.05	14.06	14.32	12.99	13.46	13.30	13.68	13.07
Fe2O3	13.77	14.23	14.38	14.08	13.50	14.50	13.45	14.56	14.08	14.63
MgO	5.61	5.74	5.79	5.55	5.28	5.67	5.18	5.57	5.38	5.52
CaO	10.35	9.99	10.21	10.03	10.09	9.87	11.04	10.08	10.07	9.79
Na2O	2.20	2.33	1.96	2.31	1.94	1.85	1.63	2.16	1.94	2.01
K2O	0.72	0.78	0.77	0.80	0.75	0.78	0.70	0.78	0.79	0.80
P2O5	0.14	0.16	0.17	0.16	0.16	0.17	0.16	0.17	0.17	0.17
MnO	0.20	0.20	0.19	0.19	0.20	0.20	0.18	0.21	0.20	0.19
Total	99.72	100.31	99.98	100.53	99.71	99.21	99.45	100.88	100.78	100.04
Mg.no.	0.45	0.45	0.45	0.44	0.44	0.44	0.44	0.43	0.43	0.43
qz	3.23	3.30	4.08	2.66	5.16	4.96	6.19	3.98	5.80	5.09
ab	18.73	19.70	16.68	19.48	16.52	15.84	14.00	18.19	16.36	17.05
or	4.28	4.61	4.58	4.71	4.46	4.67	4.20	4.59	4.65	4.74
an	25.17	22.83	24.68	25.55	28.34	25.14	27.76	24.17	26.19	24.33
di	21.35	21.43	21.01	19.23	17.57	19.47	22.41	20.49	18.82	19.45
hy	21.96	22.48	23.13	22.82	22.59	23.90	20.02	22.81	22.59	23.42
ol	0.00	0.00	0.00	0.00	0.00	0.00	0.00	0.00	0.00	0.00
mt	3.02	3.09	3.15	3.05	2.96	3.20	2.97	3.15	3.05	3.18
il	1.95	2.20	2.31	2.14	2.03	2.44	2.08	2.25	2.16	2.36
ap	0.33	0.37	0.40	0.37	0.37	0.40	0.38	0.39	0.39	0.39

Table 4.4: cont'd

	T-41	*T-4*	*T-30*	*T-19*	*T-34*	*T-28*	*T-21*	*T-20*	*T13*	*T-31*
SiO2	52.59	52.72	50.46	51.03	51.68	52.39	49.62	49.78	50.41	53.26
TiO2	1.22	1.11	1.17	1.27	1.27	1.25	2.27	2.27	2.30	1.00
Al2O3	13.22	13.56	13.20	12.33	13.85	14.37	12.76	12.54	12.28	13.13
Fe2O3	14.64	13.94	16.03	15.78	14.66	14.37	17.12	17.28	17.40	12.57
MgO	5.42	5.09	5.82	5.54	5.04	4.91	4.69	4.55	4.56	2.88
CaO	10.13	9.79	5.06	10.31	9.96	9.38	9.16	9.07	8.58	13.91
Na2O	2.13	2.11	1.65	1.78	2.21	2.03	2.28	2.31	2.98	
K2O	0.80	0.74	1.55	0.75	0.66	0.90	1.02	1.03	1.19	0.20
P2O5	0.17	0.16	0.17	0.17	0.16	0.18	0.37	0.39	0.48	0.15
MnO	0.20	0.19	0.23	0.22	0.20	0.22	0.22	0.23	0.22	0.17
Total	100.85	99.70	98.25	99.71	100.09	101.22	100.04	100.06	100.76	100.06
Mg.no.	0.43	0.42	0.42	0.41	0.41	0.41	0.35	0.34	0.34	0.31
qz	4.38	5.87	6.38	4.16	3.95	5.45	1.84	2.17	0.00	11.15
ab	17.93	17.96	14.64	15.19	18.76	17.18	19.39	19.65	25.12	12.85
or	4.70	4.40	9.61	4.47	3.91	5.32	6.06	6.12	7.00	1.20
an	24.02	25.49	25.16	23.63	26.00	27.44	21.68	20.92	16.55	28.86
di	20.83	18.70	0.00	22.51	18.90	15.05	18.20	18.40	19.21	34.05
hy	22.27	22.04	37.80	23.76	22.49	23.65	23.90	23.72	22.24	6.85
ol	0.00	0.00	0.00	0.00	0.00	0.00	0.00	0.00	0.66	0.00
mt	3.17	3.05	3.65	3.46	3.20	3.13	3.74	3.78	3.77	2.77
il	2.31	2.12	2.33	2.43	2.42	2.37	4.33	4.34	4.35	1.92
ap	0.39	0.37	0.41	0.40	0.37	0.42	0.86	0.91	1.11	0.35

Table 4.5: Major element and Norm Composition of NE-SW dykes

	T-37	*T-11*	*T-39*	*T-16*	*T-14*	*T-18*	*T-9*	*T-17*
SiO2	53.42	46.54	53.98	46.21	52.60	50.34	50.01	51.17
TiO2	0.92	0.84	0.96	0.87	0.67	1.23	1.54	1.14
Al2O3	9.06	14.74	9.65	14.13	14.35	14.04	13.19	13.40
Fe2O3	13.54	12.65	12.89	13.31	10.99	13.91	15.91	14.29
MgO	12.86	11.87	11.82	12.09	7.12	6.73	5.86	5.25
CaO	7.35	10.19	7.37	10.57	11.63	11.25	10.68	9.84
Na2O	1.87	1.61	1.03	1.64	1.50	1.90	2.13	1.98
K2O	1.00	0.45	1.10	0.45	0.51	0.56	0.64	0.74
P2O5	0.12	0.10	0.12	0.09	0.08	0.14	0.17	0.16
MnO	0.18	0.18	0.17	0.19	0.11	0.21	0.23	0.19
Total	100.69	99.62	99.55	99.93	99.86	100.76	100.61	98.52
Mg.no.	0.66	0.65	0.65	0.64	0.56	0.49	0.42	0.42
qz	0.63	0.00	6.65	0.00	5.53	0.83	0.49	4.61
ab	15.77	13.74	8.80	13.94	12.75	16.03	17.96	17.07
or	5.89	2.68	6.56	2.67	3.03	3.30	3.77	4.46
an	13.33	31.93	18.63	30.00	31.05	28.04	24.45	25.97
di	18.07	14.45	14.22	17.98	21.70	22.15	22.81	19.02
hy	41.35	11.53	40.20	6.67	22.09	24.00	23.78	23.13
ol	0.00	20.56	0.00	23.98	0.00	0.00	0.00	0.00
mt	2.94	2.77	2.83	2.91	2.40	3.02	3.45	3.17
il	1.74	1.61	1.84	1.66	1.28	2.30	2.91	2.21
ap	0.28	0.23	0.28	0.21	0.19	32.00	0.39	0.38

Condie, 1987). Most NW-SE dykes have $Fe_2O_3^t$ >13 wt% up to 17wt% except four least fractionated samples (T25, T42, T12, T8). Similarly, in the NE-SW dykes also, the $Fe_2O_3^t$ contents are between 12 and 16 wt% except one sample (T14) which has low $Fe_2O_3^t$ of 10 wt%. Such higher $Fe_2O_3^t$ are common in many continental basalts (Condie, 1987).

In the NW-SE dykes, two samples T15 and T25 which contain cumulus/phenocryst olivine have high MgO (12.90 and 10.39 wt%) while the sample T31 which is an altered sample from the dyke contact has the lowest MgO content (2.85 wt%). If these sample are excluded, the MgO ranges between 8.49 and 4.55 wt %. Similarly, in the NE-SW dykes also the MgO content ranges between 5.25 and 7.12 wt%, if we exclude the samples with cumulus/phenocryst olivine (samples T11, T16, T37 and T39 have MgO >11 wt%).

The MgO and Fe_2O_3 data have been used to calculate the Magnesium numbers (Mg number). The Mg number is calculated using the formula,

$$Mg\ number = \frac{\frac{MgO}{40.404}}{\frac{MgO}{40.404} + \frac{85}{100}\left[\frac{\Sigma Fe_2O_3 \times 0.6994}{0.7773 \times 77.84}\right]}$$

The Mg number is widely used in the description of basaltic rocks. As the total iron content of the samples are expressed as $Fe_2O_3^t$, the Fe_2O_3 content was calculated using the relation $Fe_2O_3/FeO = 0.15$. In the basic magmas, as the ferromagnesian minerals crystallise the Mg number decreases. In the early stages of crystallisation the decrease will be steep as olivine and pyroxene will have higher Mg/Fe ratios than the liquids from which they crystallise. The advantage of this index is that the value in residual liquid during fractionation is not affected

by the crystallisation of plagioclase. The Mg number, after excluding the samples with cumulus olivine and the margin sample, ranges between 0.62 and 0.34 in the NW-SE dykes, while in the NE-SW the range is between 0.56 and 0.42. Only the samples with cumulus/phenocryst olivine have the high Mg number of about 0.64-0.65.

CaO content generally vary between 9 and 11.88 wt% for NW-SE dykes and it varies between 7.35 and 11.63 wt% in NE-SW dykes. Two contact samples from the same dyke, T31 and T30 have the highest and lowest CaO content of 13.91 and 5.06 wt% respectively, falling outside the general range. Among the alkalies the Na_2O content has a nearly uniform distribution with average values of 1.99 wt% in the NW-SE dykes and 1.98 wt% in the NE-SW dykes.

The Al_2O_3 content in the NW-SE dykes has a range from 12.28 to 15.26 wt%. Exceptions to this range are the samples with phenocryst mineralogy. The highest contents (>14.5 wt%) are found in samples T15 and T25 which have plagioclase phenocrysts. Among the NE-SW dykes, two samples (T37 and T39) which have olivine aggregates are lower in Al_2O_3 content (~9 wt%). One sample (T11), with plagioclase phenocrysts, has the highest Al_2O_3 (14.7 wt%). Otherwise the range is similar to that of the NW-SE dykes. In general, the distribution of Al_2O_3 in both NW and NE dykes is comparable to that found in the tholeiitic rocks.

The K_2O content in the NW-SE dykes is less than 1.0 wt% and always more than 0.4 wt%. However, four samples, T13, T20, T21 and T30 have higher K_2O (>1 wt%). The altered sample T31 from the margin has given a significantly low value of 0.2 wt%. The NE-SW dykes also have similar K_2O content ranging between 0.46 and 1.1 wt%. These values

are markedly higher than the K_2O content in MORB (0.14 wt%) and are within the reported values of many continental basalts (avg: 0.66 wt%; cf: Condie, 1987).

TiO_2 is present mostly as ilmenite which is associated in the form of exsolution lamellae with magnetite and is also present in ferromagnesian minerals. The Ti is relatively immobile and insensitive to secondary alteration processes. Three NW-SE dykes (T13, T20 and T21) have higher TiO_2 content (2.3, 2.27 and 2.27 wt% respectively). These three samples are the most fractionated among the NW-SE dyke samples. Other NW-SE dyke samples have lower TiO_2, ranging between 0.62 and 1.27 wt%. The NE-SW dykes also have similar TiO_2 range which varies between 0.67 and 1.54 wt%. The samples with high TiO_2 have also high Fe_2O_3. The spread of TiO_2 in both NW and NE dykes are within the values of MORB to continental tholeiitic basalts.

The P_2O_5 in the NW-SE dykes generally range between 0.8 and 0.18 wt% with the exception of three most fractionated TiO_2 rich samples (T13, T20 and T21). These three samples have higher P_2O_5 values of 0.48, 0.39 and 0.37 wt% respectively. In the case of the NE-SW, dykes the variation is between 0.08 and 0.17 wt%. In terms of P_2O_5, the Tiruvannamalai dykes are comparable with the tholeiitic rocks (0.15 wt%; Wilson, 1989).

The major element data were recalculated as normative minerals using the method introduced by Cross, Iddings, Pirsson and Washington (C.I.P.W). The Tiruvannamalai dykes are mostly quartz normative (figure 4.1) with normative quartz content varying from <1 to 7%. However, the contact sample (T31) has higher normative quartz (11.15%). None of the samples contain nepheline in the norm. The samples T11, T15, T16 and T25 which contain olivine aggregates also have a high normative olivine (>20%). The normative anorthite varies

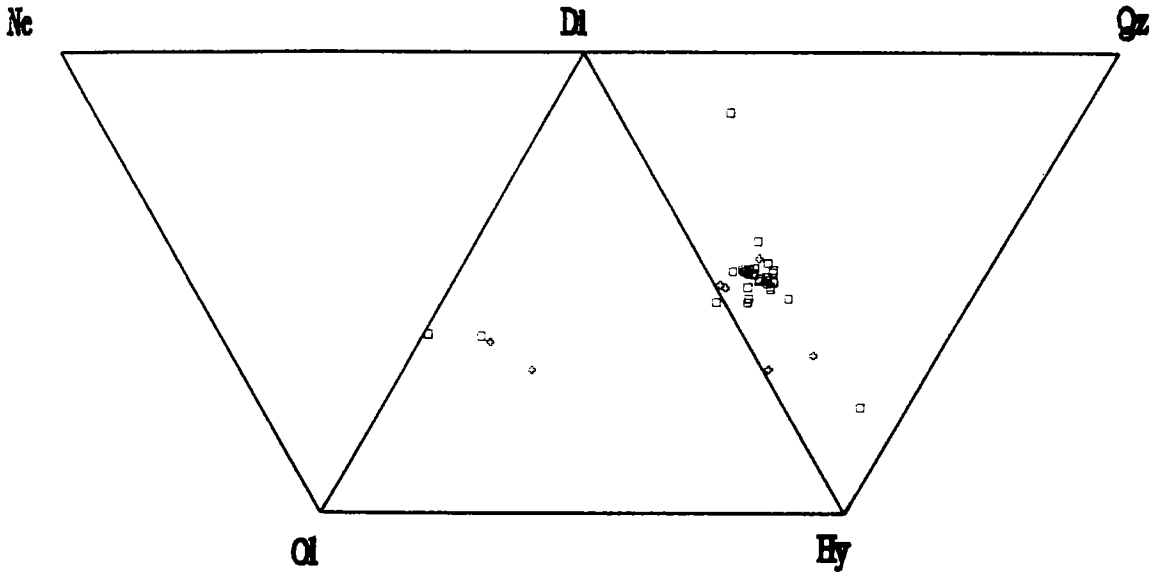

Figure 4.1: Plot of relative proportions of normative olivine, hypersthene, diopside, nepheline and quartz in Tiruvannamalai NW-SE (open square) and NE-SW (open cross) dykes.

between 15-30%. All samples are hypersthene normative (4 to 41% normative hypersthene). In general, the normative characters of the Tiruvannamalai dykes are within the tholeiitic distribution.

SiO_2 vs (K_2O+Na_2O) diagrams have been widely used for magma classification. Macdonald and Katsura (1964), Irvine and Baragar (1971), Middlemost (1975), Le Maitre (1989) and Le Bas et al. (1992) have proposed the Alkali-Silica diagrams to distinguish between the tholeiitic and alkaline magmas. They provide a useful way of displaying the magma series containing rocks with both basic and acidic composition. These diagrams are applicable to classify the commonly occurring non-potassic rocks. Middlemost (1975), proposed SiO_2 vs K_2O and SiO_2 vs Na_2O diagrams to differentiate between alkalic and sub-alkalic series within the basaltic series and therefore used to geochemically characterise the

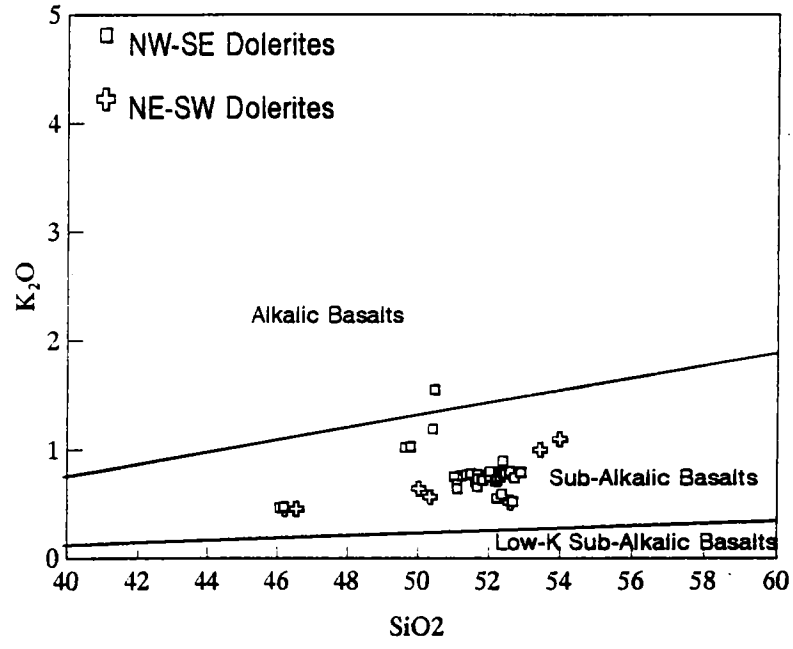

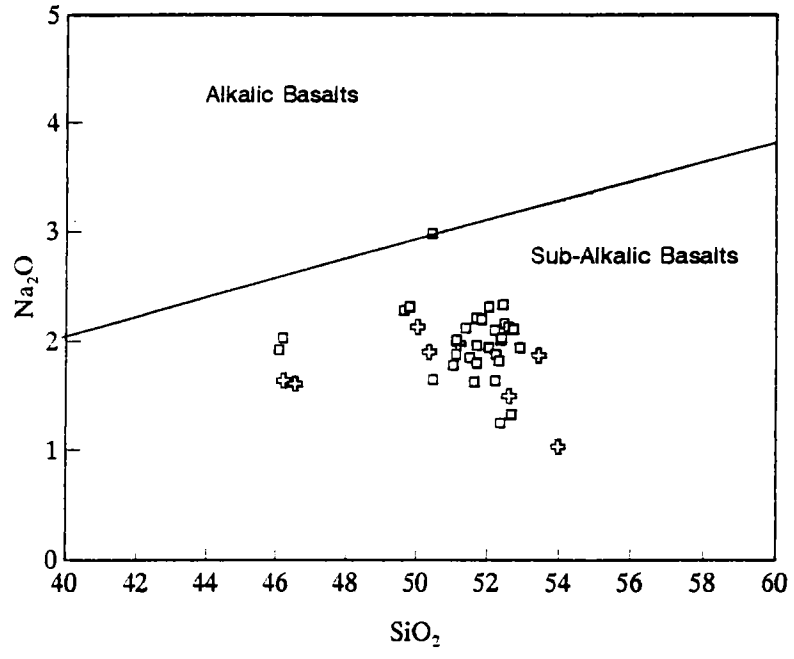

Figure 4.2: Variation plots of SiO_2 vs K_2O and SiO2 vs Na_2O of Tiruvannamalai dykes (field boundaries are from Middlemost, 1975).

Tiruvannamalai dyke. In both the diagrams (figure 4.2 a, b), the Tiruvannamalai dyke samples fall into the sub-alkaline field.

Within the sub-alkalic basalts there exist two sub-series. They are calc-alkali series and tholeiite series. The calc-alkali series will be high in alumina while the tholeiites are high in iron. The AFM triangular diagram has been conventionally used to discriminate these two series. The three corners, A, F and M of the triangle are represented by A = ($Na_2O + K_2O$), F = ($FeO + Fe_2O_3$) and M = MgO. The tholeiitic rocks show a strong iron enriched trend while the calc-alkaline rocks trend across the diagram and the iron enrichment is suppressed. The AFM plot (figure 4.3) of both the NW-SE and NE-SW Tiruvannamalai dyke samples show an iron enriched tholeiitic trend. As the samples have relatively high Al_2O_3 content, Al_2O_3 vs Alkali Index (A.I = $(Na_2O+K_2O)/(SiO_2-43)$ x 0.17) was also plotted (figure 4.4). Both the NW-SE and NE-SW dyke samples fall in the tholeiitic field.

In terms of absolute concentrations and distribution of major elements, both the NW-SE and NE-SW dykes are continental tholeiites in character.

4.3.2 TRACE ELEMENTS

Trace elements behave different from the major elements and they usually do not form any mineral phase in the rock. Still, they are very fundamental in understanding the classification of magma types and igneous processes. As new and improved analytical techniques developed, the trace elements became most important in the geochemical evaluation of different rock types. The trace element concentrations are generally expressed in parts per million (ppm) ie, in practice the measured unit is mg/kg. An element which is a

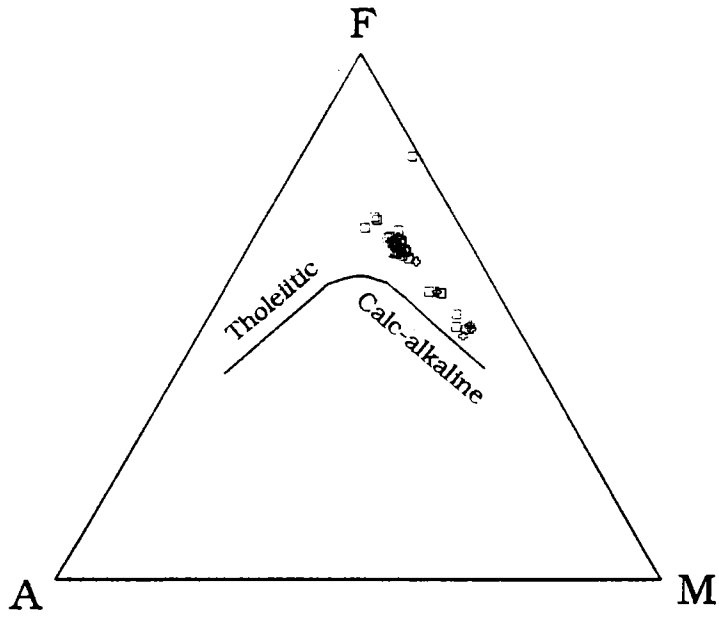

Figure 4.3: AFM diagram of Tiruvannamalai dykes (symbols are as in figure 4.1).

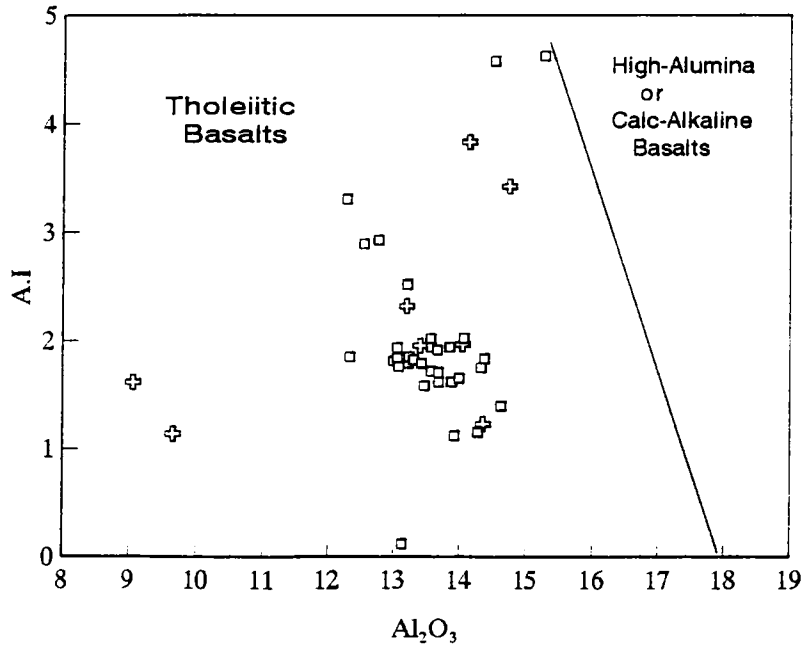

Figure 4.4: Alkali Index vs Al2O3 variation of Tiruvannamalai dykes (fields are after Middlemost, 1975). Symbols are as in figure 4.1.

trace element in one rock can be a major element in some other rock. Therefore, Cox et al. (1981) proposed to use the term trace element for elements which are present in a few thousand ppm or below in a particular rock. In the case of basaltic rocks, the more commonly determined trace elements include Rb, Ba, Sr, Y, Zr, Nb, Ta, Ti, K, P and REE. However, Ti, K, P which are reported along with major elements are discussed in association with trace elements. The trace elements show much more sharp distinction between the different types of basaltic rocks than the major elements. The trace elements based on their ionic potential, charge and radii have been broadly grouped into transition metals, high field strength elements, large ion lithophile elements and rare earth elements. The trace element data are provided in table 4.6 and table 4.7 and the nature of distribution within and between the NW-SE and NE-SW dykes in the Tiruvannamalai area are discussed under these headings.

4.3.2.1 Transition elements

Among the transition elements, Cr, Ni, Co, and Sc are generally compatible in basaltic rocks. These are easily incorporated into the crystallising phases and their content reflects the minerals which have crystallised. However, V is generally incompatible in the basaltic magmas, but sometimes may show compatible nature.

Both the NW-SE and NE-SW dyke sets of Tiruvannamalai have similar kind of variations in the Cr content. The values vary from about 300 ppm and 60 ppm with a little higher values in the NE-SW dykes. Only the samples with high Mg number (>0.60) and olivine phase have higher Cr concentrations (>400 ppm). The Cr^{3+} is identical to Fe^{3+} and preferentially enter into Fe position due to its ionic nature of the bond. They are incorporated into the clinopyroxene where the trivalent cations are readily accommodated. In the

Table 4.6: Trace element chemistry of NW-SE dykes

	T-15	*T-25*	*T-42*	*T-12*	*T-8*	*T-45*	*T-27*	*T-2*	*T-7*	*T-3*	*T-36*
Rb	10.10	11.30	18.20	24.50	20.80	24.30	28.00	27.00	28.90	26.20	24.20
Sr	169.90	269.90	123.00	130.50	137.49	143.50	138.60	146.60	144.30	137.70	150.10
Ba	152	157	159.3	150	187	177	189	243.5	258.8	252.3	306.8
Th	2.33	1.51	2.23	2.02		2.35	2.22	2.18	3.07	2.33	3.04
U									1.07		
Pb	37.24	11.60	4.55	4.67		5.64	8.14	67.58	15.74	10.02	74.33
V	246.60	241.40	247.20	247.90	200.00	356.80	346.40	358.00	367.10	365.50	348.50
Cr	577.5	499	459	294.3	248	127	108	172.5	166.9	159.4	89
Ni	370.3	289	152.8	126.6	89	116.5	104	123.6	107.5	111.1	102.3
Co	70.2	63	49	45.3	47	54	53	52.3	52.4	52.5	54
Zn	91.7	74.5	71.8	73.5	65	97.8	98.5	95.2	102.6	96.5	92
Y	23.5	18.1	18.4	18.3	17.5	32.7	31.7	31.8	30.3	31.6	29.3
Zr	59.9	53.1	50.3	55.2	56	77.8	88.6	89.1	87.1	90	80
Nb	2.66	2.37	1.9	3.2	2	2.4	4.5	4.7	2.2	3.3	3.7
Sc	41	43		41	39	37	44.59		41		
Cu	473	98		109	113	124	175		126		
Ga	15.2	14.8		13	13.3	19.6	16.2		15.7		
Hf	2.46	2.66		1.72	1.88	1.77	2.53		2.27		
Ta	0.2	0.48		0.56	0.55	0.3	0.38		0.27		
La	5.49	5.83		5.64	5.11	6.98	6.86		15.14		
Ce	13.28	14.31		12.55	12.63	15.71	17.15		23.48		
Pr	1.69	2.04		1.56	1.66	2.04	2.21		3.44		
Nd	7.63	8.06		7.2	6.77	10.49	8.3		14.14		
Sm	2.21	1.99		1.48	1.7	2.72	2.85		4.12		
Eu	0.98	0.8		0.55	0.65	0.56	0.89		1.42		
Gd	3.24	2.8		2.26	2.41	3.34	3.49		4.57		
Tb	0.46	0.5		0.27	0.34	0.55	0.61				
Dy	3.03	2.94		2.22	2.18	3.26	3.53		5.17		
Ho	0.61	0.67		0.52	0.46	0.72	0.86				
Er	1.94	2.01		1.43	1.54	3.37	2.16		2.42		
Tm	0.22	0.28		0.18	0.25	0.24	0.38				
Yb	1.46	1.55		1.35	1.56	2.48	2.52		2.47		
Lu	0.3	0.28		0.22	0.23	0.55	0.39		0.41		
$\delta^{18}O$				+5.5			−6.0				

Table 4.6: cont'd

	T-10	*T-24*	*T-32*	*T-22*	*T-1*	*T-26*	*T-35*	*T-29*	*T-33*	*T-46*	*T-23*
Rb	26.50	26.60	31.40	31.70	29.90	26.10	31.70	30.00	29.40	30.30	28.00
Sr	161.00	134.90	151.00	140.40	149.50	157.50	145.00	142.70	129.40	141.00	126.90
Ba	464	214.2	322	277.5	272.7	283	293	392.4	245	259	286.8
Th	0.80	2.02	4.40	1.54	1.98		1.60	2.93	2.71	4.39	4.24
U									0.63		
Pb		12.58		16.43	7.23			78.44	10.01	263.81	18.88
V	217.00	342.20	273.00	381.40	365.20	247.00	276.00	357.55	352.20	370.50	392.90
Cr	179	79	97		146.9	97	87	90	98.5	104.3	
Ni	83	100	65	113	109.3	61	63	91.4	95.9	97.9	106
Co		49		54	53			51.8	52	53.5	55
Zn	96	92.5	92	98.4	107.8	83	89	96.4	614.2	102.2	102.8
Y	32.7	27.4	32.6	33.2	32	31.9	32.8	32.7	31.5	33	31.3
Zr	100	78.7	99.7	99.2	91.4	101	106	91.8	94.6	97.2	91.1
Nb	3.8	2.1	4.1	3.6	2.4	3.3	4.2	2.5	2.2	4	1.6
SC									54		
Cu									161		
Ga	21		20			20	21		18.1		
Hf									1.98		
Ta									0.34		
La	13.3		14.7			14.5	13.5		33.74		
Ce	27.9		25.6			25.2	27.1		26.78		
Pr									3.6		
Nd	15.2		14.5			14.3	15.7		17.18		
Sm									4.3		
Eu									1.17		
Gd									4.11		
Tb											
Dy									5.26		
Ho											
Er									2.94		
Tm											
Yb									2.76		
Lu									0.41		
$\delta^{18}O$											

Table 4.6: cont'd

	T-41	*T-4*	*T-30*	*T-19*	*T-34*	*T-28*	*T-21*	*T-20*	*T13*	*T-31*
Rb	32.00	30.30	51.70	28.20	25.10	31.90	35.60	37	43.20	2.30
Sr	142.30	150.00	131.90	131.10	156.00	196.60	144.80	154.00	148.30	1195
Ba	264.7	288	416.5	252.5	294	358.3	357.5	317	317	56
Th	2.57	1.60	1.57	2.39	2.90	1.17	2.99	2.90	3.27	3.00
U	0.61			0.57						
Pb	5.79		6.49	7.12		20.15	33.94		9.76	
V	394.10	280.00	381.50	403.70	330.00	361.70	510.30	409	450.30	268.00
Cr	120.3	82	67.4	100	90	61	91	107	127.6	114
Ni	100.3	59	98.5	105	62	84	82	53	93.3	45
Co	52.7		57.7	62		51	52		50.7	*30
Zn	109.3	90	371.4	110.6	100	101.1	132.7	140	139.4	81
Y	34.1	31.2	30.5	34.2	32.4	33.1	50.2	52.9	57	30
Zr	93.9	100	97.7	95	102	100.1	171.4	200	204.5	63
Nb	1.5	4.1	3.7	1.8	4.9	3	9.6	9.2	11.4	3
SC	53			51					39	43
Cu	153			152					190	308
Ga	17.8	20		17.6	19			22	20.5	13
Hf	2.2			2.48					4.34	1.96
Ta	0.38			0.44					1.06	0.27
La	23.97	14.5		14.68	13.2			21.6	18.32	7.14
Ce	25.53	21.7		24.81	22.1			50	44.02	15.46
Pr	3.42			3.2					6.37	2.1
Nd	16.27	13.3		15.62	13.6			28.2	25.29	8.88
Sm	2.93			3.33					6.05	2.93
Eu	1.18			1.27					2.05	0.79
Gd	3.97			3.81					8.05	3.43
Tb									1.22	0.44
Dy	4.9			5.52					7.6	3.29
Ho									1.93	0.85
Er	3.06			2.85					4.99	2.13
Tm									0.78	0.28
Yb	2.98			2.92					4.61	1.85
Lu	0.52			0.4					0.73	0.3
$\delta^{18}O$									+5.5	

Table 4.7: Trace element chemistry of NE-SW dykes

	T-37	*T-11*	*T-39*	*T-14*	*T-18*	*T-9*	*T-17*
Rb	42.90	10.70	47.50	19.30	12.80	14.80	26.60
Sr	148	176	160	128	236	254	147
Ba	259	143	267.8	166	292.6	181	268
Th	7.90	3.19	9.23	1.19	1.37	0.97	2.80
U				0.78	0.48		
Pb	120	11	15	8	5	19	
V	203	242	200	240	330	384	284
Cr	1471	546	1350	326	243	144	98
Ni	458	360	414	137	103	78	68
Co	74	68	69	46	66	57	57
Zn	91	82	88	7	87	113	97
Y	21.4	23.9	21.5	18.5	25.2	30	32.2
Zr	111	56	123	54	75	99	100
Nb	6.9	2.22	9.1	1.2	2.7	4.4	3.7
SC	32	39		46	48	43	46
Cu	127	99		92	91	89	207
Ga	17.3	14		14	17.6	17.4	17.7
Hf	3.67	1.6		1.46	1.77	2.24	2.6
Ta	0.68	0.4		0.18	2.61	0.43	0.37
La	21.39	5.77		9.2	14	9.48	7.18
Ce	38.12	12.85		15.4	26.79	23.55	18.15
Pr	4.76	1.7		1.96	3.61	3.33	2.56
Nd	25.58	7.15		8.95	18.3	13.19	8.45
Sm	3.99	2.12		2.62	4.3	4.38	2.92
Eu	0.8	0.96		0.6	1.34	1.01	1.02
Gd	3.89	2.43		2.43	4.34	4.41	3.41
Tb	0.68	0.46				0.62	0.65
Dy	3.37	3.19		2.81	3.88	4.06	4.17
Ho	0.86	0.52				0.87	1.01
Er	2.56	1.69		1.7	2.07	2.2	2.68
Tm	0.16	0.25				0.39	0.37
Yb	2.36	2.02		1.51	2.27	2	2.34
Lu	0.3	0.27		0.25	0.27	0.42	0.4
$\delta^{18}O$	+6.0					+5.5	+5.6

Tiruvannamalai dykes the Cr values show a broad sympathetic behaviour with Mg number.

The Ni content nearly follows the same variation pattern as that of Cr. The lowest value of 45 ppm is recorded in T31 which has altered mineralogy, while the highest values (289 and 370 ppm) are from the samples with olivine aggregates. In other samples from both NW and NE dykes, Ni ranges from 150 ppm to 55 ppm. In the NE-SW dolerites also, the Ni has similar range (137-68 ppm) in the olivine-free samples. The higher values (360-458 ppm) being restricted to the samples containing olivine.

Cobalt and scandium have a limited range in the concentration. In basic rocks Co prefers to enter the olivine structure and to a lesser extend into the pyroxene. The Co again is higher in the olivine bearing samples (> 60 ppm), otherwise it ranges within the 45-57 ppm. Sc content varies between 54 and 37 ppm in NW-SE dyke similar to that in the NE-SW dykes (48 to 32 ppm).

The vanadium concentration in the three most fractionated NW-SE dyke samples (T13, T20 and T21) are >400 ppm. In the other NW-SE samples, V ranges between 200 to 394 ppm. The NE-SW dykes also have similar range between 384 and 200 ppm.

4.3.2.2 Large ion lithophile elements

The large ion lithophile elements are those elements with large ionic radius and low ionic charge. Usually their radius will be more than 0.92A°. Wood et al. (1979) have classified these elements along with the more hygromagmatophile elements (ionic radius/ionic

charge >0.2) as their bulk distribution coefficients are far less than 1 ($D \leq 0.01$). Rb, Sr, Ba, Pb, U and Th are included into this group.

The Rb content in many of the NW-SE dykes is between 18 and 31. The most fractionated three samples (T13, T20 and T21) are rich in Rb (35-43 ppm). Olivine bearing T15 and T25 have the lowest Rb (10 and 11 ppm respectively). The altered contact sample (T31) has an anomalously low Rb value of 2 ppm. The sample T30 which is also from contact zone has recorded highest value of 51 ppm. This sample also contains highest K_2O (1.55 wt%) and Ba (416 ppm). In the NE-SW dykes, samples without olivine aggregates have Rb between 12 and 27 ppm. Two samples (T37 and T39 respectively) which have high MgO and have olivine aggregates have higher values of Rb (42 and 47 ppm respectively). While one olivine bearing sample (T11) has low Rb (10.7 ppm). Generally, the Rb content in the Tiruvannamalai dykes are much higher than the NMORB and EMORB and are distinctly lower than that in alkali basalts. The values are within the range of continental tholeiitic basalts (avg: 31; cf: Condie, 1987).

In the NW-SE dykes Sr content varies from 123 to 196 ppm except in the altered contact sample T31 (1195 ppm). Similarly, the NE-SW dykes also have Sr generally ranging from 128-176 ppm. Only two samples (T9 and T18) have higher Sr values (236 and 254 ppm respectively). Although, the Sr values in the Tiruvannamalai dykes are lower than the average values (350 ppm) of continental tholeiites of Condie (1987), they are comparable with the values reported in Deccan basalts (for example, Mahoney, 1988).

Ba generally ranges between 150 and 300 ppm in both NW-SE and NE-SW dykes. However, highly evolved samples (T13, T20 and T21) rich in Ti, Zr, K_2O and Rb have higher

Ba abundances (317 to 360 ppm). Apart from them, the Ba is significantly higher in T30 (416 ppm) which is also rich in K_2O (1.55 wt%) and Rb (51 ppm) but not enriched in TiO_2 or Zr. In terms of Ba values, the Tiruvannamalai dykes are much higher than the MORB and EMORB (6.3 and 57 ppm respectively; Sun and McDonough, 1989), but are comparable with the continental flood tholeiites of Deccan (100-280 ppm; Mahoney, 1988).

Except the anomalous content of 263 ppm Pb in sample T46, all other NW-SE dykes have a Pb content ranging from 4.55 to 78 ppm. Among the NE-SW dykes, the sample T37 has a content of 120 ppm. Otherwise, the range is between 5 and 19 ppm. The average Pb content in OIB is 3.2 ppm while many continental tholeiites have the range between 2-6 ppm. All these averages are much lower than the average Pb content in the Tiruvannamalai dykes.

Th is uniformly low (1-4.5 ppm) in all the Tiruvannamalai dykes. Similar values were recorded in many continental rift tholeiites (avg: 1.5 ppm; Condie, 1987). Only two NE-SW dykes (T37 and T39) have higher Th content (7.9 and 9.23 ppm respectively). Four NW-SE and two NE-SW dyke samples were analysed for uranium. In these samples the U range from 0.5 to 1 ppm. These values are within the general range of tholeiitic rocks.

4.3.2.3 High field strength elements

The high field strength elements (HFSE) have small ionic radii and are highly charged. Therefore, they do not have great affinity for lattice sites in many common rock forming minerals. These elements are highly immobile and are insensitive to secondary alterations. The HFSE include Ti, Ta, Nb, Zr, Hf, Y and HREE

The Zr content in the NW-SE dykes generally vary between 50 to 106 ppm. Higher values (170-205 ppm) are observed in samples T13, T20 and T21. These samples are highly evolved in terms of their Mg number and rich in LIL elements and TiO_2. The NE-SW dykes also have similar range (54 to 123 ppm) of Zr. These values generally range between EMORB (avg: 73 ppm; Sun and McDonough, 1989) and continental tholeiites (200 ppm) and also are comparable to the values in Deccan volcanics (80-250 ppm; Mahoney, 1988).

Y content in both NW-SE and NE-SW dykes have an indistinguishable range of 17-34 ppm. The three, more evolved NW-SE dyke samples (T13, T20 and T21) have higher Y contents (>50 ppm). These values are within the general ranges of continental basalts (for example Deccan; Mahoney et al., 1988). The Hf content in both the NW-SE and NE-SW dykes range between 1.4 to 2.6 ppm.

Nearly all the Tiruvannamalai dykes have Nb concentrations ranging from 1.5 to 5 ppm. Two NE-SW dyke samples (T37 and T39) have higher Nb contents of 6.9 and 9.1 ppm respectively. Among the NW-SE dykes the more fractionated samples (T13, T20 and T21) also have high Nb concentration (9-11 ppm). In these samples the high Nb is positively correlated with the Zr, Ti and LIL elements. The Ta closely follows the nature of Nb distribution. It is generally low in the Tiruvannamalai dykes (0.2-0.5 ppm).

HFSE have been widely used by various authors in the preparation of tectonomagmatic discrimination diagrams. These are useful to elucidate the tectonic setting of ancient volcanic suites. The Tiruvannamalai samples are plotted in some of these discrimination diagrams in figure 4.5. In the Ti/100-Zr-Y3 ternary diagram (Pearce and Cann, 1973) and in the 2Nb-Zr/4-Y diagrams (Meschede, 1986), both NW-SE and NE-SW dyke samples plot in the MORB

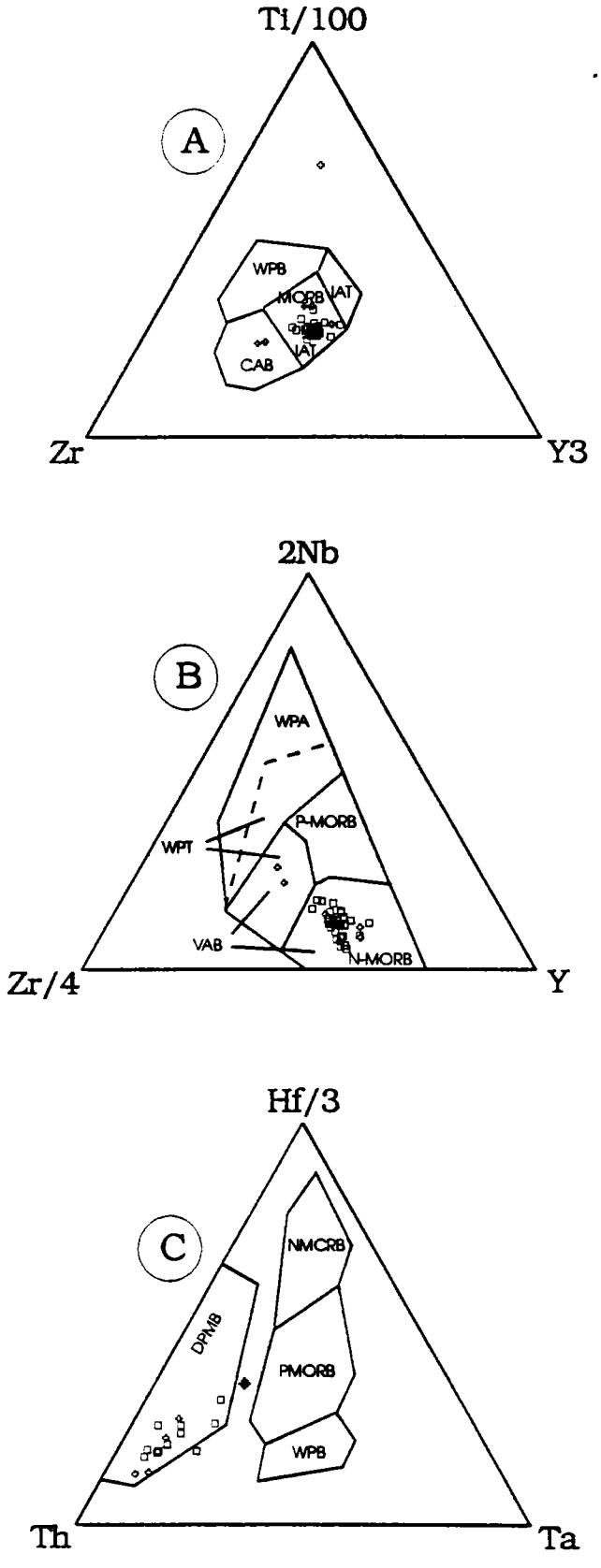

Figure 4.5: Tectonomagmatic discrimination diagrams for tiruvannamalai dykes. The field demarcations in (A) are after Pearce and Cann (1973), (B) are after Meschede (1986) and (C) are after Wood (1980). Symbols are as in figure 4.1.

field. The samples fall in the island arc field in the Th-Hf/3-Ta ternary diagram (Wood, 1980). However, continental tholeiites which are poor in Ta (and Nb), also plot in the IAB fields and these characteristics would indicate crustal contamination or involvement of subduction components in the mantle sources which are discussed in the section 6.2.1.2.

4.3.2.4. Rare earth elements

The rare earth elements (REE) are a coherent group of fifteen elements with mutually similar behaviour. It includes the elements from atomic number 57 to 71. These are La, Ce, Pr, Nd, Pm, Sm, Eu, Gd, Tb, Dy, Ho, Er, Tm, Yb and Lu. The elements which have lower atomic number and mass and higher ionic radii are termed as light rare earth elements (LREE) while HREE are those elements which have higher atomic number and mass and lower ionic radii. Their electronegativity and ionisation potential values are similar. The major difference among them is the steady decrease in ionic radii with increasing atomic number which makes them segregate into different minerals. Generally the REE are trivalent with exception of Eu and Ce. In igneous systems Eu can occur as Eu^{2+} in reducing conditions and as Eu^{3+} in oxidising conditions. In extreme oxidation conditions Ce can occur as Ce^{4+}.

The conventional practice in comparison of REE in different rocks is through graphic presentation. The concentration of individual rare earth element in a rock is normalised to their concentration in a standard. As chondrites are considered to be primitive solar system material which may have been parental to the earth, the REE abundances of chondrites have been chosen for normalising. This will reduce the Oddo-Harkins effect to produce a smooth pattern. Moreover, as there is no fractionation between the LREE and HREE in a chondrite, the normalisation will bring out clearly the fractionation, if any, present in the sample. The

chondrite normalised patterns are dependent on the mineral phases involved and degrees of partial melting of the source region and the fractional crystallisation. Thus different magma types will have different patterns unique to their setting. In general, the N-MORB rocks have an LREE depleted pattern reflecting earlier episodes of magma extraction from the source and higher degrees of partial melting. The E-MORB posses a flat to slightly enriched LREE pattern. The calc-alkaline basalts will have highly enriched LREE. The alkali basalts show highly enriched total REE along with LREE enrichment. Depending up on the involvement of plagioclase the Eu position in the trend may lie away from the general trend of other elements. This deviation is known as Europium anomaly. The anomaly will be positive if the normalised value of Eu is greater than the normalised value of the adjacent Sm and Gd, and negative if vice versa. The chondrite normalised elemental ratios also express the fractionation among different elements.

Twelve sample (T7, T8, T12, T13, T15, T19, T25, T27, T31, T33, T41 and T45) from the NW-SE dykes and six samples (T9, T11, T14, T17, T18 and T37) from the NE-SW dykes were analysed for the rare earth contents. These samples representing various stages of differentiation were selected based on Mg number. The REE concentrations have been normalised using the chondrite values reported by Haskin et al (1968). The chondrite normalised REE distribution patterns of samples are plotted in figure 4.6.

Both NW-SE and NE-SW dykes show similar REE patterns. The patterns are subparallel and are moderately fractionated with enriched LREE. The $[Ce/Yb]_N$ varies between 1.4 and 2.2 in the NW-SE and 1.4-3.7 in NE-SW trending dykes. The $[Tb/Yb]_N$ is ~1 indicating no fractionation among HREE. The abundances of LREE are within 20-40 x chondrite while the HREE abundance generally vary between 10-20 x chondrite. The more

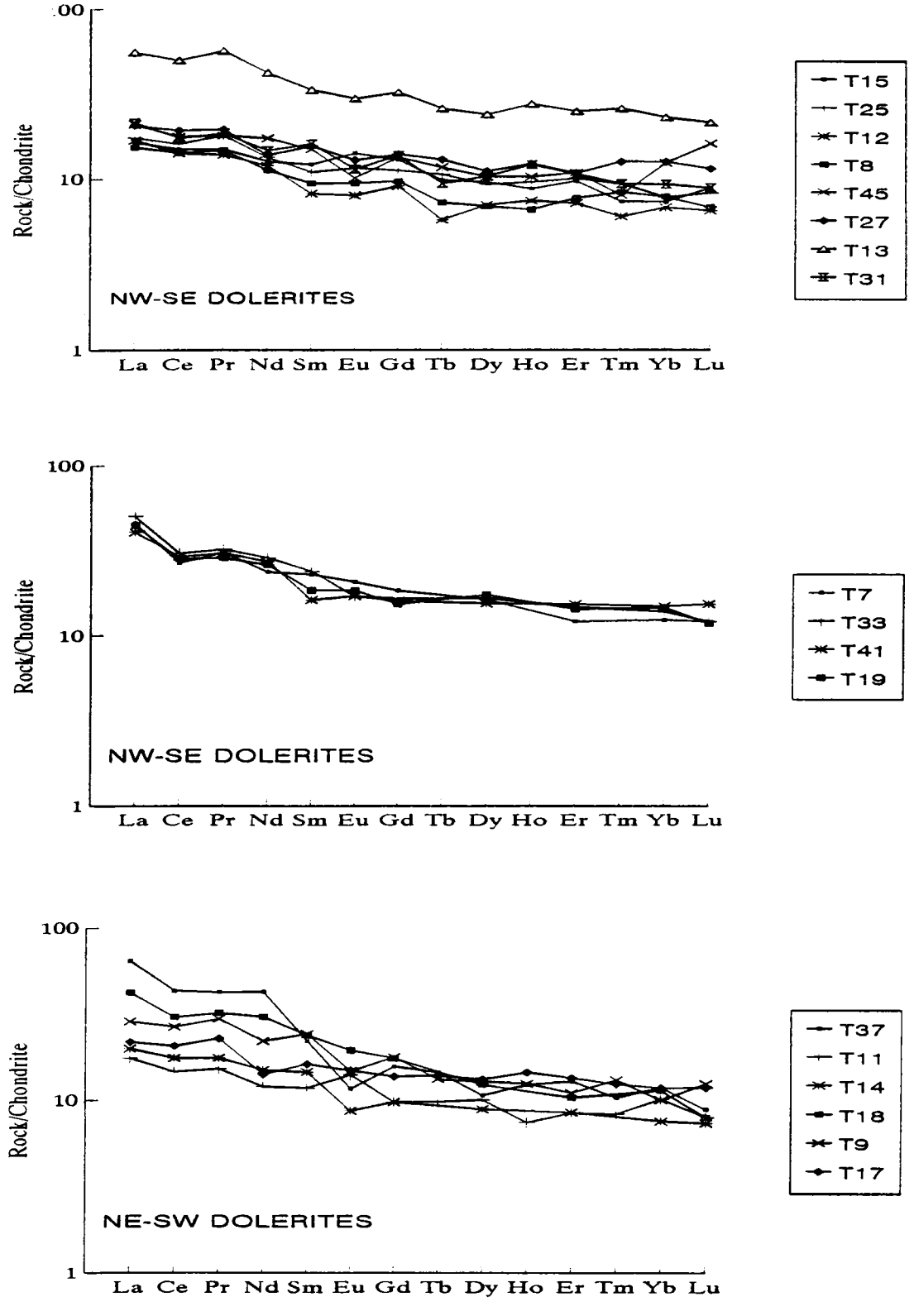

Figure 4.6: Chondrite normalised REE plots of the Tiruvannamalai dykes.

evolved samples display relatively higher levels of REE abundances. Sample T13 shows an REE pattern distinctly higher than that for other samples (about 60 x chondrite level). Sample T37, in spite of high MgO values, has higher LREE abundances. This sample is the most evolved with low Mg number (0.34) and higher incompatible element chemistry. None of the samples have a prominent Eu anomaly.

4.3.2.5 Oxygen isotope

The variation in isotopic composition of elements are related to the difference in mass of individual isotopes. The difference in mass is more pronounced between the stable isotopes of light elements. Their physical properties based on the mass will also be different. The isotopic composition of the light elements in rocks and minerals contain important information about their origin and conditions of formation. Among the stable light elements, the isotopic composition of H, O, S and C are used in the study of igneous rocks. Stable isotopes of oxygen are directly relevant to the study of the lithospheric mantle because oxygen is the major component in H_2O or CO_2 rich metasomatic fluids. Further, oxygen is the most abundant element in the continental lithosphere. It forms approximately 50 wt% of the silicate minerals and melts, 92 weight percent of water and 75 weight percent of CO_2.

Oxygen exist as three isotopes, ^{16}O, ^{17}O and ^{18}O. ^{16}O is the most abundant isotope comprising 99.76 % of all oxygen; ^{17}O is 0.04 % and ^{18}O which makes up to 0.2 % of all oxygen. Among these three isotopes, the greatest fractionation is between the heaviest (^{18}O) and the lightest (^{16}O) isotopes. The isotopic fractionation is temperature dependent and is greatest at low temperature. At magmatic temperatures isotopic fractionation is much less pronounced than at atmospheric temperature. In order to compare variations in isotope ratios

it is necessary to eliminate any laboratory bias introduced during analysis. This is achieved by reporting results relative to an internationally agreed standard (SMOW - Standard Mean Ocean Water). Fractionations are usually reported using the notation $\delta^{18}O$. This is the difference between the $^{18}O/^{16}O$ ratio of the sample and that of SMOW. The value is expressed as per mil (‰). Fractionation of oxygen isotopes is given by,

$$\delta^{18}O = \left[\frac{(^{18}O/^{16}O)_{Sample} - (^{18}O/^{16}O)_{SMOW}}{(^{18}O/^{16}O)_{SMOW}}\right] \times 10^3$$

Most silicate rocks have $\delta^{18}O$ values between +5 to +15‰. The isotope composition of igneous, sedimentary and metamorphic rocks display systematic variations that provide insight into the involvement of such rocks in the genesis of the rocks under study. Epstein and Taylor (1967) listed the tendency of minerals of igneous rocks to concentrate ^{18}O. Magnetite, ilmenite, biotite, olivine, hornblende and pyroxene contain less amount of ^{18}O. While quartz has the maximum content of ^{18}O followed by alkali feldspar, calcite, intermediate plagioclase, muscovite and anorthite. This is reflected in the isotopic composition of mantle and crustal rocks. The difference is greater than that can be produced by liquid-crystal fractionation (Kyser et al. 1982; Faure, 1986). Therefore, oxygen isotopes are extensively used to assess the effects of crustal contamination and the nature of magmatic sources. James (1981) reported a very narrow range of ^{18}O values (+5.5 to +6‰) for the mantle derived magmas compared to the crustal rocks which have $\delta^{18}O$ values >+6‰. Kyser et al. (1982) have indicated a wider range from +4.9 to +8.3‰ for the $\delta^{18}O$ of the oceanic basalts suggesting oxygen isotope heterogeneity in the mantle source. MacGregor and Manton (1981) have suggested that different portions of the oceanic crust may have distinct $\delta^{18}O$ values (+2 to +15‰) because of systematic effects of hydrothermal alterations. Oxygen isotope studies on mantle derived rocks provide constraints on the processes of magma genesis and mantle metasomatism. Therefore, oxygen isotopes of basaltic rocks, peridotite

massifs and mantle xenoliths are found useful to probe the petrogenetic problems. Kyser (1990) has reviewed in detail these aspects. In spite of its significance, there has been no attempt of oxygen isotope study on the mafic/ultramafic igneous rocks of mantle origin in India except a few preliminary results reported on Deccan volcanics (Matsuhisa et al., 1986).

Eight samples (T9, T12, T13, T17, T25, T27, T31 and T37) were analysed for oxygen isotopes. These values are well within the range reported from the MORB rocks (Faure, 1986). The range of $\delta^{18}O$ in the samples are restricted within +5.0 to +6.0‰ (tables 4.6 and 4.7). The sample which has the highest SiO_2 content of 53.42 wt%, high Mg number (0.65) and marked LREE enrichment has also given a maximum $\delta^{18}O$ value of +6‰ only. It is significant to note that the sample T31, which is from the dyke margin and has highly altered mineralogy and chemistry has also given $\delta^{18}O$ value of +5.5‰, indistinguishable from that of the fresh dykes.

4.3.2.6 Elemental ratios

The elemental ratios are useful in characterising and classifying the magma types and to probe the processes involved in the petrogenesis. The elemental ratios are shown in tables 4.8 and 4.9. The Dolerites of Tiruvannamalai are characterised by constant and low CaO/Al_2O_3 values ranging between 0.65 and 0.84. Only the contact samples (T30 and T31) have values out side this range (0.38 and 1.06 respectively). The CaO/MgO values in both NW and NE dykes show a similar range. In the NW-SE dykes the CaO/MgO ranges between 0.87 to 2.13 except the altered T31 (4.83). In the NE-SW the range is between 0.57 and 1.87.

Table 4.8: Elemental ratios of NW-SE dykes.

	T-15	*T-25*	*T-42*	*T-12*	*T-8*	*T-45*	*T-27*	*T-2*	*T-7*	*T-3*	*T-36*
CaO/Al2O3	0.73	0.68	0.85	0.78	0.76	0.80	0.77	0.75	0.73	0.73	0.74
Al2O3/CaO	1.4	1.5	1.2	1.3	1.3	1.3	1.3	1.3	1.4	1.4	1.4
TiO2/P2O5	9.78	8.40	7.75	7.88	8.00	7.07	7.20	6.88	6.88	7.33	7.69
K2O/P2O5	5.11	4.70	6.50	7.38	6.88	4.86	4.73	4.56	4.50	5.00	4.92
K/Rb	378	345	237	200	219	232	210	224	207	238	219
Rb/Sr	0.06	0.04	0.15	0.19	0.15	0.17	0.20	0.18	0.20	0.19	0.16
Ba/La	28	27		27	37	25	28		17		
Nb/La	0.48	0.41		0.57	0.39	0.34	0.66		0.15		
Zr/Nb	23	22	26	17	28	32	20	19	40	27	22
Zr/Y	2.55	2.93	2.73	3.02	3.20	2.38	2.79	2.80	2.87	2.85	2.73
Y/Nb	8.83	7.64	9.68	5.72	8.75	13.63	7.04	6.77	13.77	9.58	7.92
Ti/Zr	88	95	74	68	69	76	73	74	76	73	75
La/Ta	27	12		10	9	23	18		56		
K/Zr	64	73	86	89	81	73	66	68	69	69	66
Sr/Nd	22	33		18	20	14	17		10		
Ba/Nb	57	66	84	47	94	74	42	52	118	76	83
Ti/V	21	21	15	15	19	17	19	18	18	18	17
Ce/Y	0.57	0.79		0.69	0.72	0.48	0.54		0.77		
Sr/Y	7.2	14.9	6.7	7.1	7.9	4.4	4.4	4.6	4.8	4.4	5.1
Ba/Y	6.5	8.7	8.7	8.2	10.7	5.4	6.0	7.7	8.5	8.0	10.5
La/Nb	2.1	2.5		1.8	2.6	2.9	1.5		6.9		
Sm/Hf	0.9	0.7		0.9	0.9	1.5	1.1		1.8		
Eu/Ti	0.0002	0.0002		0.0001	0.0002	0.0001	0.0001		0.0002		
Ti/Eu	5388	6300		6873	5908	10607	7281		4648		
Th/Ta	11.7	3.1		3.6		7.8	5.8		11.4		
Rb/Nb	3.80	4.77	9.58	7.66	10.40	10.13	6.22	5.74	13.14	7.94	6.54
Ti/K	1.38	1.29	0.86	0.77	0.84	1.05	1.10	1.09	1.10	1.06	1.13
Zr/Hf	24.3	20.0		32.1	29.8	44.0	35.0		38.4		
Nb/Ta	13.3	4.9		5.7	3.6	8.0	11.8		8.1		
Y/Ho											
Lu/Hf	0.12	0.11		0.13	0.12	0.31	0.15		0.18		
Hf/Lu	8.2	9.5		7.8	8.2	3.2	6.5		5.5		
Nb/Th	1.14	1.57	0.85	1.58		1.02	2.03	2.16	0.72	1.42	1.22
Nb/U									2.06		
Zr/Sm	27	27		37	33	29	31		21		
Hf/Sm	1.11	1.34		1.16	1.11	0.65	0.89		0.55		
Rb/La	1.84	1.94		4.34	4.07	3.48	4.08		1.91		
Th/La	0.42	0.26		0.36	0.00	0.34	0.32		0.20		
Ba/La	28	27		27	37	25	28		17		
[La/Yb]	2.28	2.28		2.53	1.99	1.71	1.65		3.71		
[Ce/Yb]	2.07	2.10		2.11	1.84	1.44	1.55		2.16		
[Ce/Sm]	1.24	1.48		1.74	1.53	1.19	1.24		1.17		
[Tb/Yb]	1.34	1.37		0.85	0.93	0.94	1.03				

Table 4.8: cont'd

	T-24	*T-32*	*T-22*	*T-1*	*T-26*	*T-35*	*T-29*	*T-33*	*T-46*	*T-23*
CaO/Al2O3	0.76	0.77	0.78	0.71	0.70	0.76	0.82	0.76	0.74	0.75
Al2O3/CaO	1.3	1.3	1.3	1.4	1.4	1.3	1.2	1.3	1.4	1.3
TiO2/P2O5	7.29	7.25	7.12	7.06	6.63	7.47	6.75	7.00	6.71	7.29
K2O/P2O5	5.14	4.88	4.53	5.00	4.69	4.59	4.38	4.59	4.65	4.71
K/Rb	225	206	202	222	238	204	194	220	216	237
Rb/Sr	0.20	0.21	0.23	0.20	0.17	0.22	0.21	0.23	0.21	0.22
Ba/La		22			20	22		7		
Nb/La		0.28			0.23	0.31		0.07		
Zr/Nb	37	24	28	38	31	25	37	43	24	57
Zr/Y	2.87	3.06	2.99	2.86	3.17	3.23	2.81	3.00	2.95	2.91
Y/Nb	13.05	7.95	9.22	13.33	9.67	7.81	13.08	14.32	8.25	19.56
Ti/Zr	78	70	73	74	63	72	71	75	70	82
La/Ta								99		
K/Zr	76	65	64	73	62	61	63	68	67	73
Sr/Nd		10			11	9		8		
Ba/Nb	102	79	77	114	86	70	157	111	65	179
Ti/V	18	25	19	19	26	28	18	20	18	19
Ce/Y		0.79			0.79	0.83		0.85		
Sr/Y	4.9	4.6	4.2	4.7	4.9	4.4	4.4	4.1	4.3	4.1
Ba/Y	7.8	9.9	8.4	8.5	8.9	8.9	12.0	7.8	7.8	9.2
La/Nb		3.6			4.4	3.2		15.3		
Sm/Hf								2.2		
Eu/Ti								0.0002		
Ti/Eu								6103		
Th/Ta								8.0		
Rb/Nb	12.67	7.66	8.81	12.46	7.91	7.55	12.00	13.36	7.58	17.50
Ti/K	1.02	1.08	1.14	1.02	1.02	1.18	1.12	1.10	1.04	1.12
Zr/Hf								47.8		
Nb/Ta								6.5		
Y/Ho										
Lu/Hf								0.21		
Hf/Lu								4.8		
Nb/Th	1.04	0.93	2.34	1.21		2.63	0.85	0.81	0.91	0.38
Nb/U								3.49		
Zr/Sm								22		
Hf/Sm								0.46		
Rb/La		2.14			1.80	2.35		0.87		
Th/La		0.30			0.00	0.12		0.08		
Ba/La		22			20	22		7		
[La/Yb]								7.41		
[Ce/Yb]								2.21		
[Ce/Sm]								1.28		

Table 4.8: cont'd

	T-41	*T-4*	*T-30*	*T-19*	*T-34*	*T-28*	*T-21*	*T-20*	*T13*	*T-31*
CaO/Al2O3	0.77	0.72	0.38	0.84	0.72	0.65	0.72	0.72	0.70	1.06
Al2O3/CaO	1.3	1.4	2.6	1.2	1.4	1.5	1.4	1.4	1.4	0.9
TiO2/P2O5	7.18	6.94	6.88	7.47	7.94	6.94	6.14	5.82	4.79	6.67
K2O/P2O5	4.71	4.63	9.12	4.41	4.13	5.00	2.76	2.64	2.48	1.33
K/Rb	207	203	249	221	218	234	238	231	229	722
Rb/Sr	0.22	0.20	0.39	0.22	0.16	0.16	0.25	0.24	0.29	0.002
Ba/La	11	20		17	22			15	17	8
Nb/La	0.06	0.28		0.12	0.37			0.43	0.62	0.42
Zr/Nb	63	24	26	53	21	33	18	22	18	21
Zr/Y	2.75	3.21	3.20	2.78	3.15	3.02	3.41	3.78	3.59	2.10
Y/Nb	22.73	7.61	8.24	19.00	6.61	11.03	5.23	5.75	5.00	10.00
Ti/Zr	78	67	72	80	75	75	79	68	67	95
La/Ta	63			33					17	26
K/Zr	71	61	132	66	54	75	49	43	48	26
Sr/Nd	9	11		8	11			5	6	135
Ba/Nb	176	70	113	140	60	119	37	34	28	19
Ti/V	19	24	18	19	23	21	27	33	31	22
Ce/Y	0.75	0.70		0.73	0.68			0.95	0.77	0.52
Sr/Y	4.2	4.8	4.3	3.8	4.8	5.9	2.9	2.9	2.6	39.8
Ba/Y	7.8	9.2	13.7	7.4	9.1	10.8	7.1	6.0	5.6	1.9
La/Nb	16.0	3.5		8.2	2.7			2.3	1.6	2.4
Sm/Hf	1.3			1.3					1.4	1.5
Eu/Ti	0.0002			0.0002					0.0001	0.0001
Ti/Eu	6203			6000					6732	7595
Th/Ta	6.8			5.4					3.1	11.1
Rb/Nb	21.33	7.39	13.97	15.67	5.12	10.63	3.71	4.02	3.79	0.77
Ti/K	1.10	1.08	0.55	1.22	1.39	1.00	1.61	1.59	1.40	3.62
Zr/Hf	42.7			38.3					47.1	32.1
Nb/Ta	3.9			4.1					10.8	11.1
Y/Ho										
Lu/Hf	0.24			0.16					0.17	0.15
Hf/Lu	4.2			6.2					5.9	6.5
Nb/Th	0.58	2.56	2.36	0.75	1.69	2.56	3.21	3.17	3.49	1.00
Nb/U	2.46			3.16						
Zr/Sm	32			29					34	22
Hf/Sm	0.75			0.74					0.72	0.67
Rb/La	1.34	2.09		1.92	1.90			1.71	2.36	0.32
Th/La	0.11	0.11		0.16	0.22			0.13	0.18	0.42
Ba/La	11	20		17	22			15	17	8
[La/Yb]	4.87			3.05					2.41	2.34
[Ce/Yb]	1.95			1.93					2.17	1.90
[Ce/Sm]	1.79			1.53					1.50	1.09
[Tb/Yb]									1.13	1.01

Table 4.9: Elemental ratios of NE-SW dykes.

	T-37	*T-11*	*T-39*	*T-16*	*T-14*	*T-18*	*T-9*	*T-17*
CaO/Al2O3	0.81	0.69	0.76	0.75	0.81	0.80	0.81	0.73
Al2O3/CaO	1.2	1.4	1.3	1.3	1.2	1.2	1.2	1.4
TiO2/P2O5	7.67	8.40	8.00	9.67	8.38	8.79	9.06	7.13
K2O/P2O5	8.33	4.50	9.17	5.00	6.38	4.00	3.76	4.63
K/Rb	193	349	192	2196	219	363	359	231
Rb/Sr	0.29	0.06	0.30	0.06	0.15	0.05	0.06	0.18
Ba/La	12	25			18	21	19	37
Nb/La	0.32	0.38			0.13	0.19	0.46	0.52
Zr/Nb	16	25	13	35	45	28	23	27
Zr/Y	5.19	2.33	5.71	2.36	2.91	2.96	3.30	3.11
Y/Nb	3.10	10.77	2.36	14.67	15.42	9.33	6.82	8.70
Ti/Zr	50	90	47	502	75	99	93	68
La/Ta	31	14			51	5	22	19
K/Zr	75	67	74	359	79	62	54	61
Sr/Nd	6	25			14	13	19	17
Ba/Nb	38	64	29	597	138	108	41	72
Ti/V	27	21	29	22	17	22	24	24
Ce/Y	1.78	0.54			0.83	1.06	0.79	0.56
Sr/Y	6.9	7.4	7.4	7.0	6.9	9.4	8.5	4.6
Ba/Y	12.1	6.0	12.5	40.7	9.0	11.6	6.0	8.3
La/Nb	3.1	2.6	0.0	0.0	7.7	5.2	2.2	1.9
Sm/Hf	1.1	1.3			1.8	2.4	2.0	1.1
Eu/Ti	0.0001	0.0002			0.0001	0.0002	0.0001	0.0001
Ti/Eu	6900	5250			6700	5507	9149	6706
Th/Ta	11.6	8.0			6.6	0.5	2.3	7.6
Rb/Nb	6.22	4.82	5.22	5.67	16.08	4.74	3.36	7.19
Ti/K	0.67	1.35	0.63	1.40	0.95	1.59	1.74	1.11
Zr/Hf	30.2	34.9			36.9	42.2	44.2	38.5
Nb/Ta	10.1	5.6			6.7	1.0	10.2	10.0
Y/Ho	25	46					34	32
Lu/Hf	0.08	0.17			0.17	0.15	0.19	0.15
Hf/Lu	12.2	5.9			5.8	6.6	5.3	6.5
Nb/Th	0.87	0.70	0.99	3.33	1.01	1.97	4.54	1.32
Nb/U					1.54	5.63		
Zr/Sm	28	26			21	17	23	34
Hf/Sm	0.92	0.75			0.56	0.41	0.51	0.89
Rb/La	2.01	1.85			2.10	0.91	1.56	3.70
Th/La	0.37	0.55			0.13	0.10	0.10	0.39
Ba/La	12	25			18	21	19	37
[La/Yb]	5.49	1.73			3.69	3.74	2.87	1.86
[Ce/Yb]	3.67	1.45			2.32	2.68	2.68	1.76
[Ce/Sm]	1.97	1.25			1.21	1.28	1.11	1.28
[Tb/Yb]	1.23	0.97					1.32	1.18

The incompatible elemental ratios which are insensitive to secondary processes, can be more reliably used to characterise magma types and to compare different rock units. The ratios are also not affected by varying degrees of partial melting or fractional crystallisation. The elemental ratio averages of NW-SE and NE-SW dykes along with the values of chondrite, primordial mantle, NMORB, EMORB, upper crust, lower crust, gneisses and charnockites of Tiruvannamalai area are given in table 4.10.

The Tiruvannamalai dykes are characterised by high Rb and low K/Rb ratios (avg: 230 and 290 for NW-SE and NE-SW respectively). These ratios are much lower than average NMORB (avg: 1071) and EMORB (avg: 417). The NW-SE dolerites samples, free of olivine mineral phase, have Rb/Sr ratios between 0.15 to 0.30, and the higher values (>0.25) are restricted to the more fractionated samples. Similarly, the NE-SW dykes also have similar Rb/Sr values between 0.15 to 0.18, if the samples with olivine aggregates and anomalous (high) Sr values are excluded. These values are much higher compared to the ratios in NMORB and EMORB. The Ba/La ratio (avg: 22 for NW-SE and 22 for NE-SW dykes) and the K/Zr ratio (avg: 69 for NW-SE and 63 for NE-SW dykes) are much higher than those in the NMORB (avg: 8) and EMORB (avg: 29).

The high field strength elemental ratios (Zr/Nb, Zr/Y, Y/Nb) are similar to that of NMORB. Zr/Nb values in the NW and NE dykes (avg: 28 and 30 respectively) are similar to the ratios of NMORB. The Zr/Y ratio also are more close to NMORB and EMORB values. Y/Nb ratio in both NW and NE dykes (avg: ~10) are comparable with NMORB values of 12. While Ti/Zr ratio (avg: 74 and 82) is less than NMORB and chondrite values.

Table 4.10: Average incompatible elemental ratios of the Tiruvannamalai dykes

	AVG1	AVG2	Chondr	PM	NMORB	EMORB	U.C	L.C	TNMGn	TNMCh
K/Rb	230	290	235	394	1071	417	316	329	740	1131
Rb/Sr	0.20	0.17	0.32	0.03	0.01	0.03	0.06	0.04	0.03	0.02
Ba/La	23	24	10	10	3	9	17	28	40	48
Zr/Nb	30	28	16	16	32	9	10	12	32	19
Zr/Y	3.0	2.8	2.5	2.5	2.6	3.3	4.5	4.9	31.5	34.0
Y/Nb	10	10	6	6	12	3	2	3	1	1
Ti/Zr	74	82	115	116	103	82	61	67	10	6
La/Ta	25	24	17	17	19	13			323	263
K/Zr	69	63	141	22	8	29	29	58	153	133
Sr/Nd	13	17	16	16	12	17	12	30	132	148
Ba/Nb	88	88	10	10	3	7	16	52	195	109
Ti/V	21	21		15	20-50		50			
La/Nb	3.8	3.3	1.0	1.0	1.1	0.8	0.9	1.8	4.9	2.3
Ti/Eu	6549	6427	7672	7738	7451	6593	5735	4962	1277	1024
Th/Ta	6.7	5.4	2.1	2.1	0.9	1.3			26.7	23.3
Hf/Lu	6.4	5.9	4.2	4.2	4.5	5.7	18.0	17.2	131.3	95.7
Ce/Y	0.74	0.72	0.39	0.39	0.27	0.68	1.00	1.56	7.50	6.00
Sr/Y	5.07	6.9	4.6	4.6	3.2	7.1	7.0	23.2	231.0	222.5
Sm/Hf	1.28	1.63	1.44	1.44	1.28	1.28	1.23	0.69	0.20	0.17
Zr/Sm	29	23	25	25	28	28	31	26	147	179
Nb/Th	1.7	1.9	8.5	8.4	19.4	13.8	24.1	4.4	2.5	5.0
Nb/La	0.35	0.33	1.04	1.04	0.93	1.32	1.06	0.54	0.21	0.44

Average of NW-SE Tiruvannamalai (AVG1) and NE-SW Tiruvannamalai (AVG2) dykes. Average values of NMORB, EMORB, chondrite and primitive mantle are from Sun and McDonough (1989); Upper Crust (U.C) from Weaver and Tarney (1984); Lower Crust (L.C) from Kempton et al (1991); Country rocks for the dykes TNMGn (Tiruvannamalai gneiss) and TNMCh (Tiruvannamalai charnockite) are from Allen et al (1985).

La/Nb values in both NW-SE and NE-SW Tiruvannamalai dykes (avg: 4.7 and 3.6 for NW-SE and NE-SW dykes respectively) are significantly higher than the ratios in MORB (avg: ~1) and are comparable with island arc basalts (avg: 3.3). La/Ta values (avg: 34 and 20 for NW-SE and NE-SW dykes respectively) are also higher than EMORB (avg: 13).

The enrichment of Ba is indicated by the Ba/Nb ratio. Both the NW-SE and the NE-SW dykes have high Ba/Nb (avg: 88 and 78 respectively). This is distinctly higher than the

NMORB and EMORB values (avg: ≤10). Similar high values are seen only in island arc basalts (avg: 50) and andesites (avg: 100).

The average Ti/V ratio values in both NW-SE and NE-SW dykes are similar and comparable to the values of NMORB (avg: 20). The Ti/Eu ratio in NW-SE (avg: 6549) and NE-SW (avg: 6427) dykes are similar to MORB values (avg: 6593).

The Th/La values of NW-SE (avg: 6.7) and NE-SW (avg: 4.2) are higher than that found in MORB (avg: <1.3). The Hf/Lu ratios (avg: ~6) of Tiruvannamalai dykes are within the average MORB range. The Ce/Y ratio of NW-SE and NE-SW dykes show a range between 0.48 to 0.95 and between 0.54 to 1.78 respectively.

In summary, both NW-SE and NE-SW trending dolerite dykes of Tiruvannamalai area are sub-alkalic iron rich tholeiites. These samples are characterised by enriched LILE and LREE abundances while HFSE are lower than the MORB values. Their $\delta^{18}O$ values are within the MORB range. The elemental ratios involving HFSE are generally within the MORB range while some of the incompatible element ratios like Rb/Sr, Ba/Nb, La/Ta etc. are very high as in island arc basalts.

4.4 GEOCHEMICAL VARIATIONS WITHIN THE DYKE

The composition of an individual dyke may vary along or across the dyke. As there may be a time difference in the crystallisation between the contact zone and the centre of the dyke, there is a possibility of developing a chemical zonation due to fractional crystallisation. The fractionation can be post-emplacement or pre-emplacement phenomenon. In the case of

post-emplacement fractionation, a highly evolved centre will be resulted due to the segregation of residual liquids during fractional crystallisation. In the case of pre-emplacement fractionation, a differentiated magma from a chamber is injected to form the zoned dyke. The dyke margins which are in contact with the country rock having contrasting composition can assimilate the wall rock and develop a different chemistry from the dyke centre.

Karlsbeek and Taylor (1985, 1986) have noted the within dyke chemical variation for the Proterozoic dykes in southern and western Greenland and attributed the variation in incompatible element concentration to the amount of primocryst material and the degree of fractionation of the magma. The margins of these dykes are more fractionated and the dyke centre was characterised by more primitive material. This may be due to the enrichment of early formed crystals in the central part of the dyke which dilutes the concentration of the incompatible elements. The magmas were intruded from a zoned magma chamber such that more fractionated magma was first intruded to form the dyke margins followed by more primitive magma to form the dyke centres.

The variations within the individual dykes of Mackenzie dykes, Ontario have been studied by Gibson et al. (1987). Unlike the Greenland dykes, Mackenzie dyke centres are more evolved than the margins. The centres are enriched in P_2O_5, TiO_2, Fe and incompatible trace elements and depleted in MgO and CaO. Major element composition of the dyke centre can be produced by fractionally crystallising plagioclase, orthopyroxene and clinopyroxene from the marginal magma.

In view of the above, a NW-SE dyke passing through Tiruvannamalai town which was traced for more than 24 km and has a width of about 55-60 m was selected to study the within dyke variations. About fifteen samples were collected from this dyke. Eight samples

from Kilnachipattu (12° 12': 79° 5') were collected across the dykes. Samples T29 and T31 are from the western margin, while the samples T28 and T30 are from the eastern margin. T32 is about 5m from the western margin. T33 is about 8 m towards the centre, from the sample T32. Samples T34 and T35 are from the dyke centre. T36 is 7 m from the eastern margin. The samples T2, T1, T10, T35, T27, T26 and T24 have been taken from the same dyke from north to south to study variations along strike extension of the dyke.

The variations of major and trace elements in samples collected along the dyke are shown in figure 4.7. The Mg number does not show any systematic variation along the length (43-46). The major element content is also coherent without any traceable patterns. The SiO_2 content is within a small range of 51.38-52.2 wt%. The Al_2O_3, Fe_2O_3, MgO, CaO, Na_2O, K_2O and P_2O_5 also have restricted range. Among the trace elements although T10 shows a deviation towards lower V and Th, others do not show any consistent trend along the strike of the dyke.

Figure 4.8 shows major and trace element variations across the dyke. The contact sample T31, from the western margin, which shows petrographical evidence of post magmatic alteration is exceptionally depleted in the LILE and LREE, while the sample T30 from the eastern margin is enriched in K_2O, Ba and Rb, a case that can be explained through contamination processes. Among the major elements TiO_2, Fe_2O_3, P_2O_5 and K_2O show a mild increase towards the centre from the western margin, while there are no noticeable trends for SiO_2, MgO, Al_2O_3 and Na_2O. Among the trace elements Rb, V, Sr, Ni, Y and Nb do not show any pattern in the variation. But, the content of Zr is found to increase mildly towards the centre, while the Ba content decreases towards the centre. Based on the increasing trends of TiO_2, Fe_2O_3 K_2O, P_2O_5 and Zr, the centre of the dyke appear to have been mildly fractionated compared to the dyke margin.

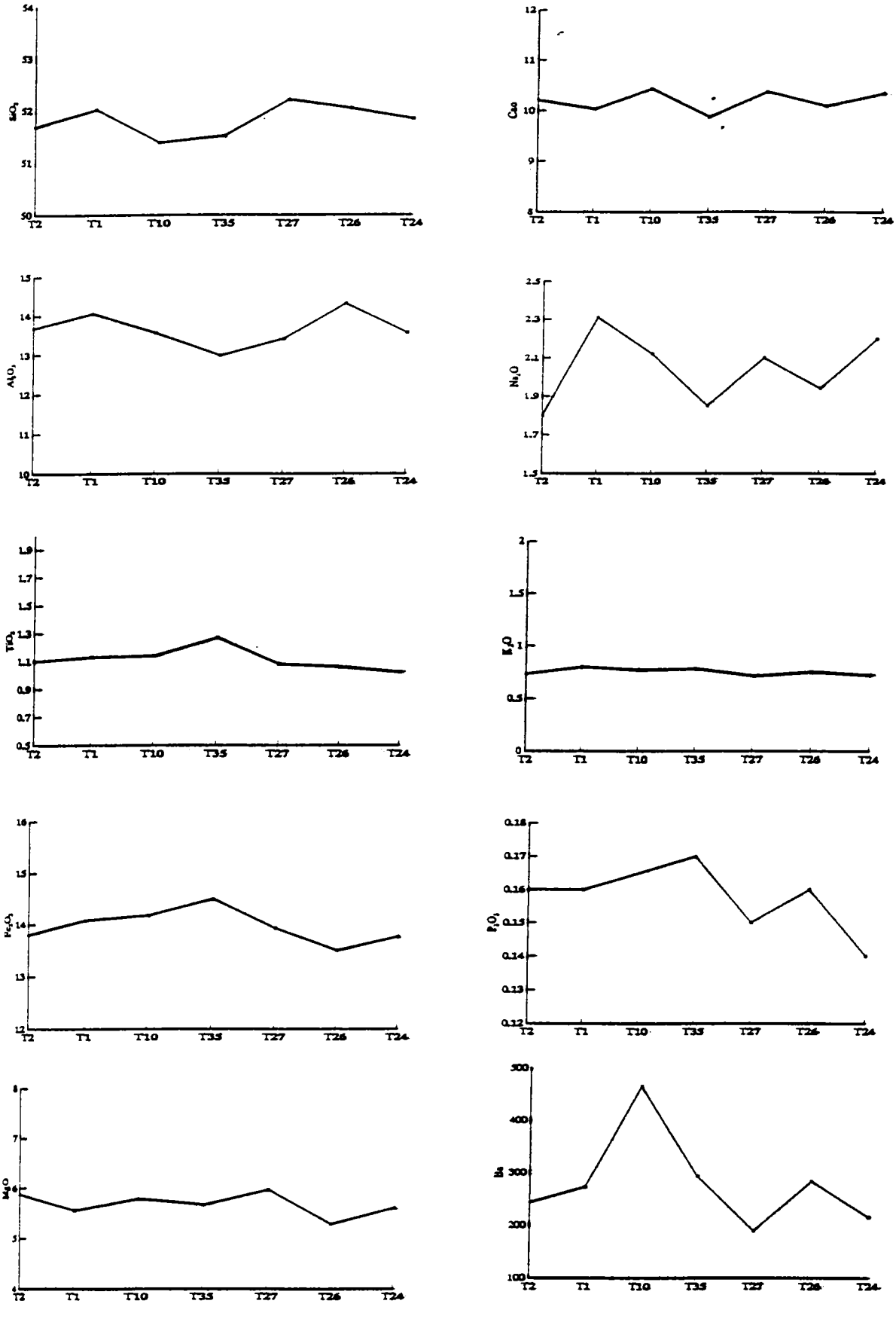

Figure 4.7: Selected major and trace element variations along the long dyke passing through Tiruvannamalai town.

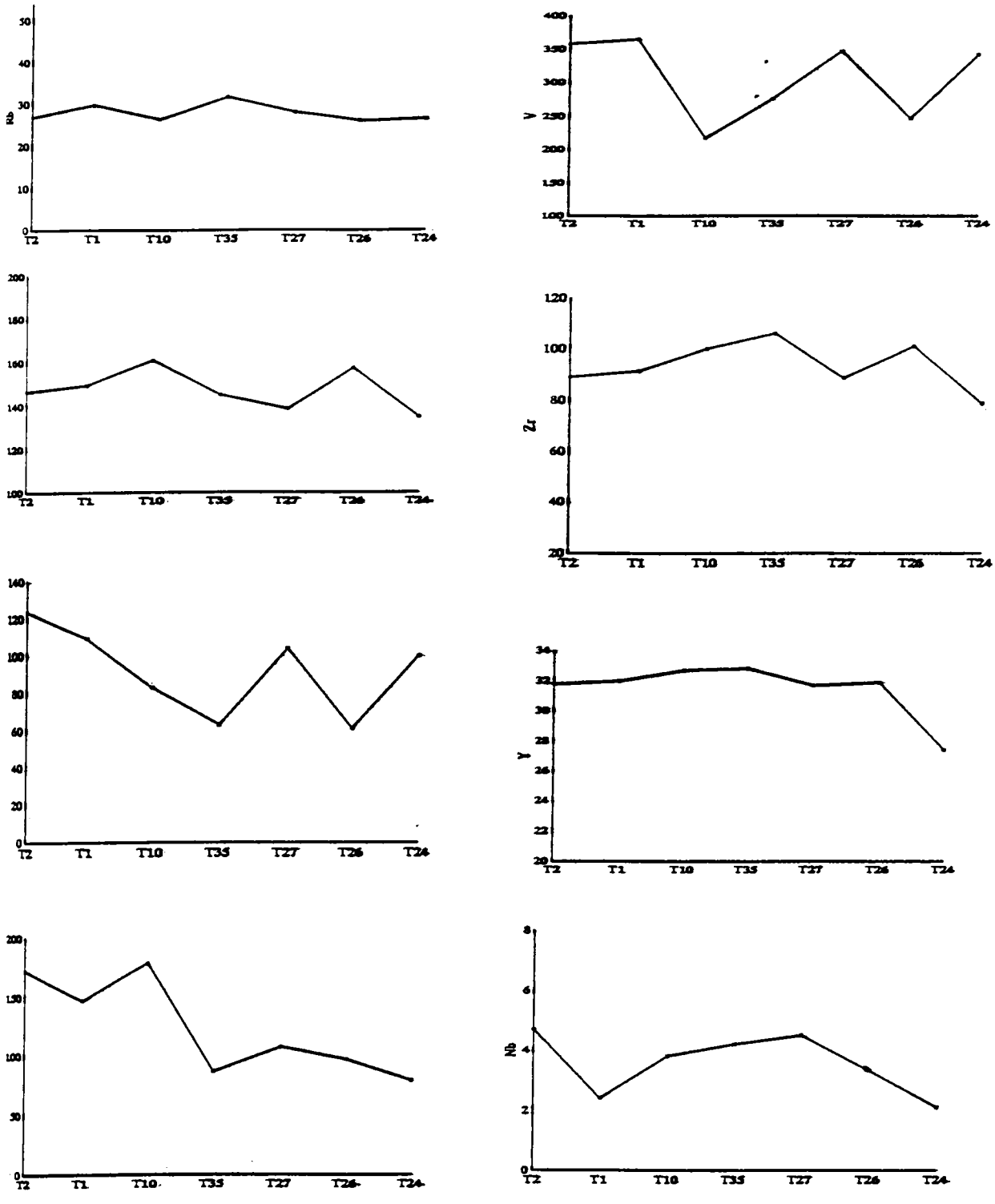

Figure 4.7 continued

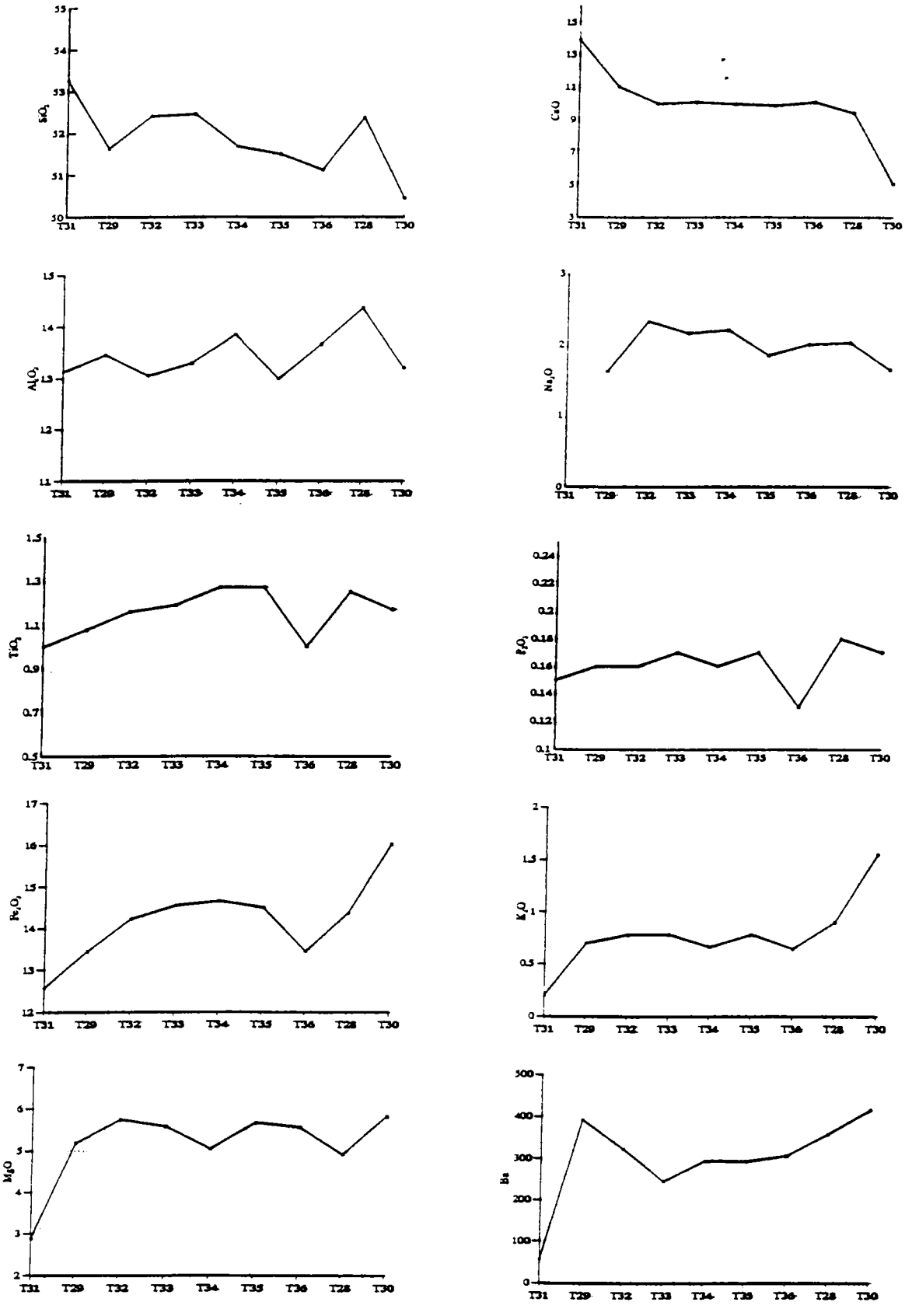

Figure 4.8: Selected major and trace element variations across the long dyke passing through Tiruvannamalai town

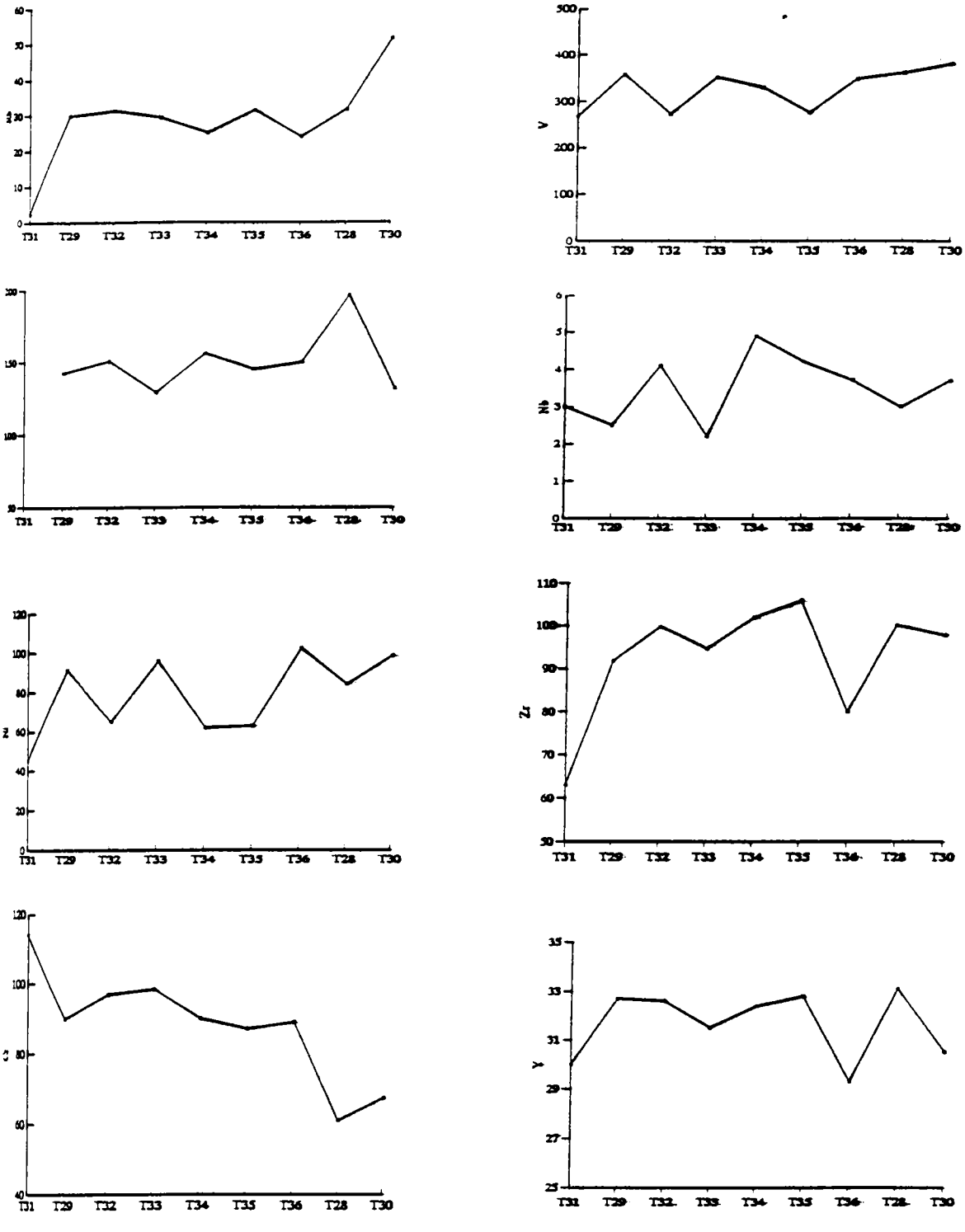

Figure 4.8 continued

PALAEOMAGNETISM

5.1 INTRODUCTION

Magnetism in rocks has been reported many centuries ago. The magnetism leaves some traces of original values in favourable conditions facilitating their measurement and provides vital information regarding the past. During the middle of this century, with the advent of Plate tectonics the study of palaeomagnetism attained importance in the field of Earth Sciences. Palaeomagnetism has provided qualitative confirmation to the observation of continental drift and sea-floor spreading to evolve these into the theory of Plate Tectonics. The application of palaeomagnetism has become a vital tool in different fields of earth science including palaeoclimatology, palaeogeography and geotectonic reconstruction of continental blocks. Here, the fundamental information of magmatism has been reviewed, first, to give the background history of this subject. Subsequently, the methodology adopted in the present study of Tiruvannamalai dykes and then the results are presented.

5.2 MAGNETISM IN RELATION TO EARTH'S HISTORY

5.2.1 GEOMAGNETISM

The presence of geomagnetic field has been recognised for centuries. But its application in geology, geophysics and archaeology have achieved importance only recently. Eventhough the Earth's magnetism is one of the earliest geophysical properties to be studied, its origin remains a matter of speculation. The field produced is similar to that of a bar magnet, but the process is not simple. To assume that the interior of the Earth is permanent

magnet is not possible because the Curie temperature of magnetic minerals is reached at 20-30 km below the surface.

The generation of geomagnetic field within the fluid outer core of the Earth, by some form of magnetohydrodynamic dynamo, has been widely accepted. But a complete dynamical model is yet to be accomplished (Butler, 1992). If a weak stray magnetic field was present, movement in the fluid iron core would generate an electrical current which would then produce its own magnetic field. The interaction between the magnetic field and the electrically conducting Fe-Ni produces positive feed back and allow the core to operate as a self-exiting magnetohydrodynamic dynamo.

The movement of fluid in the outer core is sufficient to produce the field, but a part is lost through electrical resistivity. Thus there is a requirement for energy input to drive the fluid motion. The most reasonable source is associated with the gradual cooling of the earth's core with accompanying freezing of the outer core and growth of solid inner core. This will effectively provide energy for fluid motion, in the outer core, required to generate the geomagnetic field.

The dominant portion of the geomagnetic field is due to the dipole. Almost 90% of the present geomagnetic field can be best described by a geocentric dipole inclined at an angle ~11.5° with the Earth's axis of rotation. The points on the surface where extensions of the inclined dipole intersect the earth's surface is the geomagnetic poles. But the magnetic poles, where the dip is 90°, do not coincide with the geomagnetic pole. Therefore, the geomagnetic field is more complex than can be explained by a dipole at the earth's centre. To account for

this discrepancy, an eccentric dipole positioned about 500 km from the geocenter towards the northwestern part of the Pacific basin was proposed. In most places the eccentric dipole perfectly accounts for the field, but it fails to account for the observed field in other places. This difference between the observed and the calculated field is generally ascribed to non-dipole field which is resulted due to the fluid eddy currents within the core near the boundary with the overlying mantle.

5.2.2 SECULAR VARIATIONS

Geomagnetic data over periods of a few thousand to a million years showed that there is a constant variation in the direction and magnitude of surface geomagnetic fields. The short term fluctuations occur on time scales ranging from few seconds to a few years and these are largely due to solar effects. The long term variations are termed as secular variations. They include the westward drift of the magnetic field, decay in the magnetic field and drift of magnetic poles. These are evident even in rocks which have cooled through a large period of time.

The magnetic data for the past one million years show that the variations in the north magnetic pole were in a path around and within a few degrees of the rotational pole. The time-averaged geomagnetic fields correspond with a Geocentric Axial Dipole where variation in field and other features would be averaged out (Opdyke and Henry, 1969; Kovacheva, 1980). In this model, the magnetic field is considered to be produced by a single dipole at the centre of the earth and aligned with the rotational axis and this concept is central to the principles of palaeomagnetism.

5.2.3 POLARITY REVERSALS

Major change observed in the geomagnetic field is the insertion of its polarity. The present alignment with the magnetic north pole lying close to the geographical north pole is regarded as normal polarity, while when the north pole is close to the present south pole is considered to be reverse polarity. There is no fixed periodicity in the intervals between reversals. However, Marzocchi and Mulargia (1992) proposed a 15 Ma periodicity in the rate of reversal occurrence.

Opdyke et al. (1966) recorded a major reversal from the deep ocean sediments from Antarctica region at different depth from different cores. All these reversals were dated at 73,000 years. Cox et al. (1965) had also reported reversal in the volcanic rocks of the same age from Alaska. Reports of coincidence of reversal across the globe in sedimentary and igneous rocks of identical ages were overwhelming evidence to consider that the geomagnetic field itself got reversed. These are largely considered as due to processes within the Earth's core. The time spent in one or the other polarity ranges from 10^4 to 10^7 years, while the transition takes about 10^3 to 10^4 years. As the transition is an instantaneous event on a geological time scale and the process is global, the reversals have became a tool in magneto-stratigraphic correlation in establishing geomagnetic polarity time scale. The mechanism behind this process of reversal is yet to be clearly understood. The extraterrestrial origin linked with solar magnetic dipole does not seem to be valid because the solar field shows a 22 year cycle in its polarity which is not reflected in the geomagnetic reversals. Early workers proposed self-reversal as a mechanism (Neel, 1951; Nagata, 1961). However, the self-reversal mechanism can only occur in minerals that have or have had specific composition (cf: Tarling,

1983). Parker (1969) and Levy (1972) suggested outer core cyclones as the source for origin of reversals. Stacey and Loper (1983) proposed that a dynamic layer 8-10 km thick at the base of the mantle, where vigorous horizontal flow takes place, originates a number of uprising plumes. Such a layer is not in thermal equilibrium and has a thermal relaxation time of approximately 10 Ma. The frequency of reversals has always been correlated with the vigour of convection in the outer core. McFadden and Merrill (1984) and Gubbins (1987) observed that the energy input in the mechanism of reversal generation is increasing with time which can be explained with a long term change in the lower mantle and core-mantle boundary temperature distribution.

5.3 PALAEOMAGNETISM AND POLAR PATH

5.3.1 MAGNETIC DIRECTIONS

The direction of natural remanent magnetism in a rock is expressed in terms of polar co-ordinates, Declination (D) and Inclination (I). Declination is the angle between the direction of magnetism in the horizontal plane and the geographical north measured clockwise in degrees. The inclination is the angle of the dip of magnetisation measured in degrees from the horizontal plane. The strength of the magnetisation is expressed as intensity (F).

The magnetisation can also be expressed as magnitude of its components in cartesian co-ordinates, x, y and z. The total intensity (F) can be resolved into a horizontal component H and a vertical component z. The horizontal component H is further resolved into x and y components. The north direction coincides with +x and east direction coincides with +y. The positive z is considered to be pointing down.

The relation between polar and cartesian co-ordinates are as follows:

$H = F \cos I$

$z = F \sin I$

$x = H \cos D$

$y = H \sin D$

$$[F^2=H^2+Z^2 = x^2+y^2+z^2]$$

In determining the declination and inclination of a rock, the conventional practice is to measure the x, y, z and F components and then get the D and I. Usually to derive D and I of any rock unit, 6-8 samples are collected from the rock unit. The location from which the samples are collected is referred to as palaeomagnetic site. D and I of individual samples are measured first and then averaged for all samples in the site to get a mean D and I of the rock unit. The mean direction is calculated by finding the direction of the vector sum of all the individual magnetic vectors (x', y', z').

Thus $x = \Sigma x'/R$

$y = \Sigma y'/R$

$z = \Sigma z'/R$

where $R^2=\Sigma x'^2+\Sigma y'^2+\Sigma z'^2$

Mean Declination, $D = \tan^{-1} y/x$

Mean Inclination, $I = \sin^{-1} z$

The precision of the calculated mean direction is represented by the "precision parameter κ" and "circle of 95% confidence". The parameter κ determines the dispersion of the points. The precision κ refers to the absolute total population of vector points on a sphere.

As it is never possible to measure individually the magnetisation of every individual magnetic grain of an absolute value of the standard deviation and precession must be estimated from the samples taken from the population. Fisher (1953) proposed the best estimate of precision to be κ = N-1/N-R, where N is the total number of samples. When the value of κ is zero the data are scattered randomly. As the κ value increases, the points cluster about the mean direction. Values greater than ten indicate that the observed mean is close to true mean. Higher values are preferable for a more reliable estimate of the mean direction.

Fisher (1953) introduced another parameter called cone of confidence (α) usually expressed as α_{95}. This means that there is a 95% probability that the true mean direction lies within the cone of confidence around the observed mean. The mean will be more reliable if the value is small. Values more than 20 is generally regarded as less reliable. The value is given by the equation, $\alpha_{95} = 140/(\kappa N)^{1/2}$.

5.3.2 PALAEOMAGNETIC POLE

The primary NRM vectors from a rock provide information of the declination and inclination of that particular rock unit. This is dependent on the location of the site. The declination and inclination of rocks of the same age for different locations around the earth will be different. It is worthwhile to compare rocks of a single continental block as well as from different continents with same and different ages. To make a meaningful comparison, there should be a parameter which will serve as a common reference system to all rock units across the globe. Unlike the declination and inclination of a dipolar magnetic field, which

change with the position on the globe, the geomagnetic pole of a geocentric dipole is independent of observation location.

The palaeomagnetic pole (λ', Φ') can be determined from the palaeomagnetic mean direction of the rock (D, I) and latitude (λ_s) and longitude (ϕ_s) of the sampling site. It refers to the palaeopole position with respect to the present latitude and longitude. The colatitude (p), which is the great circle distance from the site to the pole, is calculated to determine the palaeopole position. The colatitude is given by,

$$p = \cot^{-1}(\frac{1}{2}\tan I)$$

Then, the palaeopole latitude is given by,

$$\lambda' = \sin^{-1} (\sin \lambda_s \cos p + \cos \lambda_s . \sin p . \cos D)$$

and the palaeopole longitude is given by,

$$\Phi' = \Phi_s + \beta \qquad (\text{if, } \cos p \geq \text{Sin } \lambda . \text{Sin } \lambda')$$

or,

$$\Phi' = \Phi_s + (180 - \beta) \qquad (\text{if, } \cos p < \text{Sin } \lambda . \text{Sin } \lambda')$$

where, β is the longitudinal difference between the site and the palaeo-pole and is given by,

$$\beta = \sin^{-1} [(\sin p . \sin D)/\sin \lambda']$$

Palaeopole position may also have associated angular errors. The ellipse of confidence about the calculated pole position has a semi-axis *dp*, along the site to pole meridian and a

semi-axis *dm* perpendicular to *dp*. The error dp in the ancient colatitude p is given by,

$$dp = \alpha_{95} \left(\frac{1 + 3\cos^2 P}{2} \right)$$

The error dm perpendicular to dp is given by,

$$dm = \alpha_{95} \left(\frac{\sin P}{\cos I} \right)$$

The palaeo-latitude position of the continental block with respect to the palaeo-latitude (λp) can be determined from the calculated palaeopole. Usually the palaeo-latitude is calculated for a reference town (λ_r : Φ_r) centrally located to a particular continental block. The is given by,

$$\text{Sin } \lambda p = \text{Sin } \lambda_r \text{ Sin } \lambda' + \text{Cos } \lambda_r \text{ Cos } \lambda' \text{ Cos } (\Phi' - \Phi_r)$$

In the present calculation, Nagpur (21.09 N : 79.09 E) which is centrally located in India is taken as the reference town.

5.3.3 APPARENT POLAR WANDER PATH

The palaeomagnetic information of a given region can be represented by means of palaeogeographic maps of different epochs. Creer et al. (1954) introduced the technique of plotting apparent polar wander path (APWP). Now this has become the standard method of presenting palaeomagnetic data covering significant geological time interval. The APWP is a plot of the sequential positions of palaeomagnetic poles from a particular continent, usually drawn on the present geographical grid. To develop an APWP, a set of palaeomagnetic poles of varying geological age is presented in a single diagram with an assumption that the continents are stationary. Thus, the APWP represents the apparent motion of the rotational

axis with respect to the continents. In reality, the major portion of apparent polar wander is due to the motion of lithospheric plate carrying the continents over the earth's surface.

APWP diagrams are made on equal-area projection of the earth relative to the present position of continents. In the APWP diagrams usually the north pole is plotted. If a reversal is encountered, then it will be rotated to normal and plotted so that there will be a smooth path. When more data are handled, more details of APWP could be determined by averaging poles within time intervals shorter than geological time periods. In the sliding-time-window technique (Van Alstine and de Boer, 1978) an absolute age is assigned to available palaeomagnetic pole, a time duration for the time window is chosen and all poles with ages falling within the time window are averaged and plotted as 95% confidence ellipse surrounding each mean pole. This will average out random noise but limit the details.

Another approach is to construct the APWP from more reliable palaeomagnetic poles without applying time averaging. More rapid variations in the APWP, such as the sharp corners are resolved by this technique. The drawback is that the interpreted pattern of APWP is strongly dependent on the accuracy of individual palaeomagnetic poles.

Matching of APWP of continents is the fundamental palaeomagnetic method in proposing and testing relative positions in the past. If the poles from rocks of different ages from a single continent falls on a curve, it indicates that the continental block was a single tectonic unit at least over the period of time represented by the APWP and the different parts of the continent did not drift relative to each other. When the poles of certain continents are plotted, they show that the path was formed by the convergence of two paths. This indicates

that the continent is made up of two tectonic blocks which drifted separately and collided to from the present configuration as in the case of India and Eurasia. The convergence of APWP suggests closing of ocean, continental collision and the suturing of plates. In the case of opening of an ocean, the APWP of two continental blocks are similar initially with slight offset followed by divergence of the path in two different directions.

5.4 NATURAL REMANENT MAGNETISM AND MAGNETIC OVERPRINTING

5.4.1 NATURAL REMANENT MAGNETISM AND ITS MEASUREMENT

The measurement of the magnetic parameters in rocks, which have formed in the geological past, will provide insight into the nature of geomagnetism of the past. The palaeomagnetic principals are based on the geocentric axial dipole model of the Earth's magnetic field. Almost all rocks contain iron or other magnetic minerals like iron oxides (magnetite, ilmenite etc.), oxyhydroxides, sulphides. In the igneous rocks magnetite and ilmenite form a solid-solution series with compositions varying between magnetite (Fe_3O_4) and ulvöspinel (Fe_2TiO_4).

When rocks crystallise, they cool through the Curie temperature and acquire magnetism parallel to the prevailing earth's magnetic field. This is referred to as primary magnetism. Later to its formation rocks can acquire secondary magnetism (detailed below). The combination of these two magnetism is retained in the rock as Natural Remanent Magnetisation (NRM).

Astatic magnetometer was the primary instrument during the initial stage of palaeomagnetic study. It is composed of a system of two magnets that are equally and oppositely magnetised. These magnets are held in an aluminium beam of 1 mm square cross section. The beam also carries a small mirror. This unit is suspended on a torsion fibre. The fibre may be of phosphor-bronze or quartz. The whole system is placed within a three-component Helmholtz set. This will cancel the influence of earth's magnetic field on the measured value. The system responds to the magnetic field of the specimen while it is insensitive to geomagnetic and laboratory disturbance. When the specimen is placed near the astatic magnetometer, the magnet system twists in response to the direction and intensity of magnetisation of the specimen. The deflections are monitored using an optical arrangement. This arrangement consist of a light source the mirror fixed between the magnets and a scale. The reflected beam should fall perpendicular to the scale. The deflections produced by the specimen at different positions are used to calculate the magnetic vectors.

The major difficulty with this instrument is its sensitivity to vibrational disturbances. This can be reduced by vibrationless mounting and selection of torsion fibres. The measurements are also time consuming. In spite of the difficulties, it has a fairly good sensitivity and can be used for measurement of even irregularly shaped samples.

Spinner magnetometer: In the spinner magnetometer the specimen is spun within a pickup coil. This will allow filtering of external noise. The magnetic moment of the specimen produces an alternating voltage in the coil. The direction and intensity of magnetisation can be determined from the phase and amplitude of this signal. The

improvement by adding ring fluxgate pickup coil has made the instrument fastest and most sensitive.

5.4.2 OVERPRINTING OF MAGNETIC DIRECTION

The rocks, after acquisition of primary magnetism at the time of formation, are exposed to fluctuation of temperature and magnetic field. These can induce secondary magnetism. The secondary magnetism can also provide useful information if the time of acquisition is accurately known. But usually these soft components are just strong enough to mask the primary magnetism. The secondary magnetism can be acquired in many ways. Important among them are described below.

Viscous remanent magnetisation (VRM)

Rocks acquire this magnetism when exposed to weak fields for long periods. The grains with short relaxation periods will gradually align parallel with the ambient field. The intensity will be proportional to the ambient field strength and generally to the logarithm of the time of exposure to the field.

Partial thermo remanent magnetism (PTRM)

Rocks which have been subjected to thermal fluctuations by burial by overlying deposits or intrusives can acquire this magnetism. If the temperature exceeds the blocking temperature of any magnetic grain present they will be magnetised, on cooling, parallel to the ambient field which will be different from that acquired originally during crystallisation.

Isothermal remanent magnetisation (IRM)

IRM is a relatively rare type of magnetism in natural rocks. This type of secondary magnetism will be acquired due to lightning strikes, when a large field acts for a short time. Usually the lightning struck samples will show anomalous behaviour with high intensity of NRM in rocks causing deflections in the compass when brought near to the outcrop.

Laboratory induced magnetisation

Secondary magnetism can be created within the laboratory also. If a rock is subjected to an alternating field superimposed on a small direct field and the alternating field is decreased to zero, the sample will acquire an Anhysteretic Remanent Magnetisation (ARM). Sample can also acquire magnetism when they are rotated in the presence of an alternating magnetic field. This type of secondary magnetism is known as Rotational Remanent Magnetism (RRM).

The VRM and the PTRM are the most frequent secondary magnetisation that are encountered in the rocks. It is essential to erase the secondary magnetisation in order to obtain the primary magnetisation direction. Therefore, demagnetisation (cleaning) techniques to remove the secondary magnetisation have become a routine part of palaeomagnetism. These techniques allow preferential removal of secondary NRM by leaving the particles of secondary magnetism randomly oriented in terms of their magnetisation. The routine demagnetisations currently employed are Alternate Current (AC) and thermal methods in which magnetic and thermal energy supply are used to randomise the secondary NRM. These methods in many cases help to identify and isolate primary magnetisation in the rocks.

5.5 METHODOLOGY OF THE PRESENT STUDY

5.5.1 SAMPLING AND PREPARATION OF SPECIMENS

The palaeomagnetic study is centred upon direction of magnetism within the rocks. Therefore, samples should be taken from undisturbed areas and if disturbed, proper correction should be made. Similarly, the sampling from weathered and altered zones also are avoided as these processes alter the direction of primary magnetism due to the oxidation of magnetite or formation of hydroxides of iron. The dykes of high altitude are prone to effects of lighting. This can be usually detected by the anomalous behaviour in magnetic compass. Dyke sites without the above features were chosen for palaeomagnetic study.

The dykes usually take much time than basalts to cool. Thus, there is a possibility of single dyke (or individual dykes in a swarm) showing variations in direction due to secular variation. Each sample or dyke may represent a particular instant of time. Many samples widely separated in space within a dyke constitute a site and many such sites (dykes) were sampled across the swarm in order to average out the palaeosecular variation.

In the present study, oriented block samples were taken from fourteen sites covering the entire geographic distribution of Tiruvannamalai dykes. The palaeomagnetic site location are shown in figure 5.1. Seven samples each were collected from the sites. The magnetic north was marked using a magnetic compass held at the top of a rectangular plane board at 40 cm height from the surface, to reduce the effects of dyke's magnetism on the compass. Two horizontals were marked on two adjacent sides using precision spirit level. After marking the north and horizontals, the samples were cut and removed from the *in situ* block.

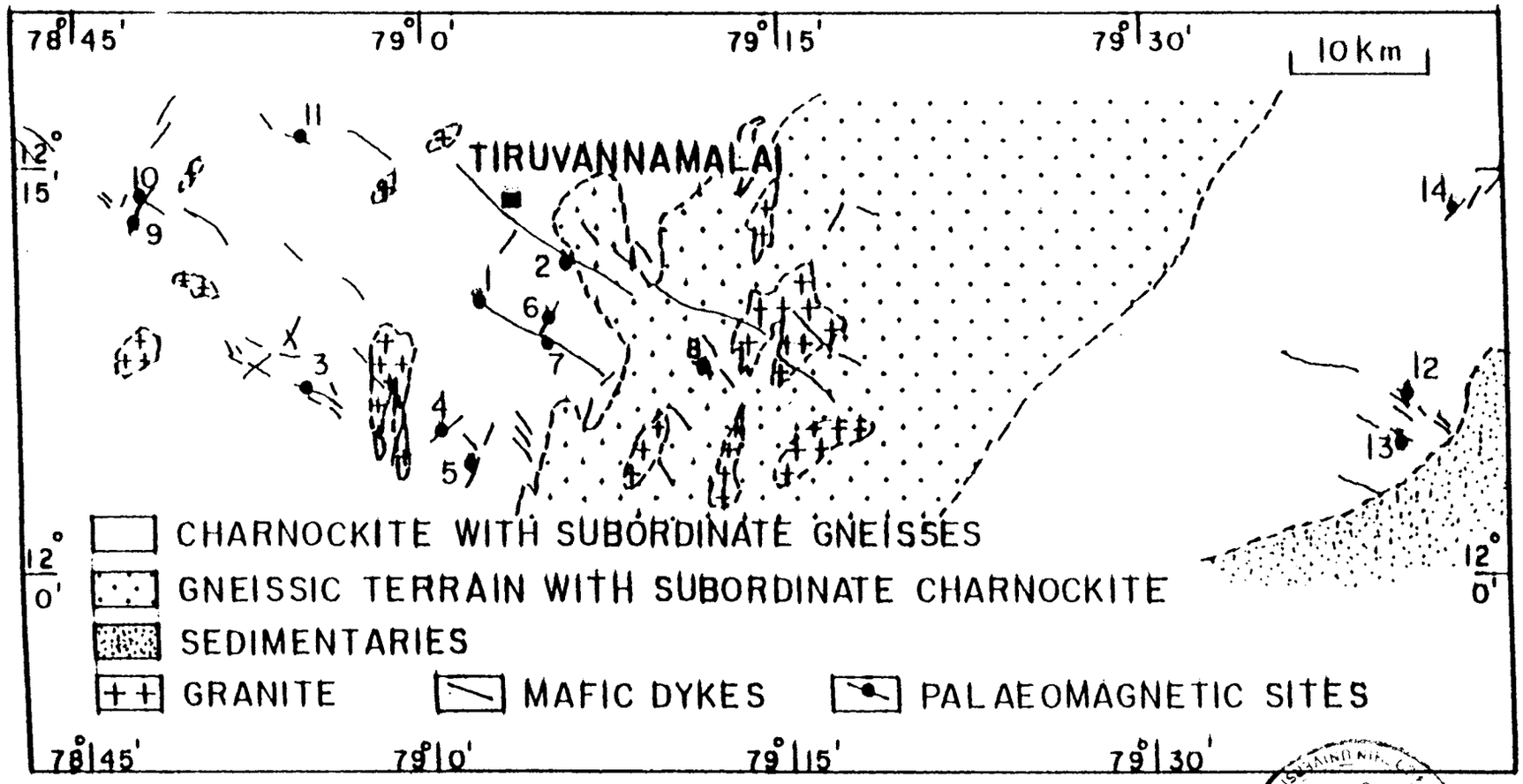

Figure 5.1: Geological map of Tiruvannamalai area showing the palaeomagnetic sites.

The samples were reoriented on a stage in the Laboratory Drilling Unit (Bharat Diamond Industries Ltd., India) using spirit level before drilling. The north was transferred to the top of the vertical core and removed from the sample. The cored samples were cut to cylindrical specimens of 2.54 cm diameter and 2.54 cm height.

5.5.2 LABORATORY SET-UP AND METHODOLOGY

The Palaeomagnetic Laboratory at the Centre for Earth Science Studies, Trivandrum is well equipped with the modern facilities like Minispin Spinner Fluxgate Magnetometer (MOLSPIN Ltd., UK), AF Shielded Demagnetiser (MOLSPIN Ltd., UK) and MMTD-1 Thermal Demagnetiser (Magnetic Measurements, UK).

5.5.2.1 Minispin spinner fluxgate magnetometer

The Minispin is a highly sensitive fluxgate spinner magnetometer. The instrument is designed and constructed with a view to use it as a laboratory as well as field instrument (more details in Molyneux, 1971). The rock specimen is rotated at 6 Hz about a vertical axis within an annulus-shaped fluxgate. This will improve the signal to noise ratio. The sensitivity is better than $10^{-4}Am^{-1}$. The unit is surrounded by a three layer mumetal shield to shield the ambient earth's magnetic field from influencing the measurement. The Minispin is interfaced with a computer (Epson HX-20) and is run by a software package.

The instrument is calibrated using the standard provided with the instrument. The standard has an intensity of 973 Am^{-1}. The declination of the standard is 360°. The

declination calibration is done by rotating the fluxgate and shield assembly slightly relative to the body of the instrument and remeasuring. The North component and the East component are indicated at the LCD. If East is positive the fluxgate is rotated clockwise and if it is negative the fluxgate is rotated anticlockwise. This is repeated until the East component is less than 1% of the North and the declination is 360° ±2.

The specimens are measured for their X, Y, Z components of magnetic moment in mutually perpendicular directions from which declination, inclination and intensity of magnetisation can be computed. The specimen is spun inside the fluxgate in four perpendicular positions. From each position, two orthogonal components of magnetisation are obtained. Thus two of each sign of X, Y and Z components are measured. Spinning in four directions, while facilitating the measurement of magnetic components in mutually perpendicular directions, will average out any random noise on the signal or inhomogeneity in NRM.

The NRM of a sample is always a combination of a primary magnetic component acquired during the formation of the rock and a secondary magnetic component acquired after the formation. Generally, the secondary component has a lower stability than the primary component. In order to randomise the secondary components, proper thermal and alternating field cleaning techniques have been employed.

5.5.2.2 AF shielded demagnetiser

The AF Shielded Demagnetiser (Molspin Ltd; UK) has an electronically controlled field with peak value of up to 1000 Oe. The alternating magnetic field is created along the axis of a coil through which very pure alternating current is passed. The frequency of the sinusoidal waveform is 200 Hz. The coil is shielded by a double-walled mumetal bucket shield to cancel the effects of earth's field. The samples are spun inside the coil while demagnetising. This is done to randomise the direction while demagnetising.

The basic principle is that the magnetic moment of grains with coercivity less than or equal to the field applied will be randomised. The samples are subjected to incremental demagnetisation from lower fields to higher fields. After each increment the sample is measured for the declination, inclination and intensity. The demagnetisation is continued till the secondary magnetic component is removed and the stable directions are isolated.

One specimen from each of the samples was subjected to AF demagnetisation. The demagnetisation fields were chosen at 25, 50, 75, 100, 125, 150, 175, 200, 225, 250, 275, 300, 325, 350, 375, 400, 450, 500, 550, 600 Oe. Some of the samples were demagnetised up to 800 Oe. Most of the samples responded to the demagnetisation and characteristic magnetisation vectors were derived. However, some samples failed to give stable vectors.

5.5.2.3 MMTD 1 thermal demagnetiser

The MMTD 1 Thermal Demagnetiser facilitates heating up to 800°C. The heating chamber is covered by a four layer active mumetal shield to cancel the influence of earth's magnetic field. The oven controller is programmable. The increase in temperature can be achieved in two ramps with a hold time in between. The rate of heating can be 25°C/minute for targets below 300°C. The heating ramps are linear to minimise thermal shock. The temperature shown on the control panel is the oven wall temperature while the sample will be at a lower temperature. At the maximum temperature a hold-time of 15 minutes is selected for heating, so that the samples reach the target temperature. The temperature overshoot would be ±1°C or less even at higher temperatures.

The samples are heated to a target temperature and cooled in a field-free environment. This process randomises magnetisation of all grains with blocking temperature less than the target temperature and thereby erases the NRM carried by these grains. After each increment, the samples are measured for the declination, inclination and intensity. If the secondary components are erased by thermal demagnetisation then the subsequent magnetic vectors will remain the same and the characteristic magnetic vectors can be determined. Above the Curie temperature the complete magnetisation will be erased.

Seventeen samples representative of all NRM in the total sites of Tiruvannamalai were selected for the thermal demagnetisation from the area. After NRM measurements the samples were demagnetised at 150, 250, 350, 450, 500, 525, 550, 580, 610, 640/650 and 680°C.

5.6 RESULTS OF TIRUVANNAMALAI DYKES

The NRM results obtained on all samples are plotted site-wise in figure 5.2. The AF and thermal demagnetisations carried out on the samples showed that almost all of them contained superposed magnetic components. The AF demagnetisations were found effective in removing the viscous remanence. Usually these were removed at lower increments of demagnetistion (< 150 Oe). Orthogonal projections of remanent magnetic vectors (Zijderveld, 1967) and the standard stereographic projections have aided to delineate the characteristic vectors. The orthogonal projections for the responses of AF and thermal demagnetisations on one sample from each site are shown in figure 5.3 and 5.4 respectively. The characteristic magnetisation vectors from each site are shown as stereographic projection in figure 5.5. The progressive demagnetisation details of each site are presented below and the site-wise data are given in table 5.1 at the end.

Site Tp 1

The NRM directions of this site are scattered. Three samples have a northeast declination with negative and positive medium inclinations. Two samples have moderate negative inclination with northwesterly and southwesterly declination. The NRM intensities range between 109.6 A/m and 6 A/m. During AF demagnetisation, the sample (Tp1A) with highest intensity (109.6 A/m) retained the NRM declination even after the removal of 90% of the original remanence. But the NRM inclination was changed at 50 Oe to very shallow negative inclination. Sample Tp1B from its southwesterly NRM declination and negative inclination attained a declination of 320° with positive shallow inclination at 200 Oe. Sample Tp1C, after 150 Oe increment, gave a stable direction with D = 81° and I = -40°. In samples

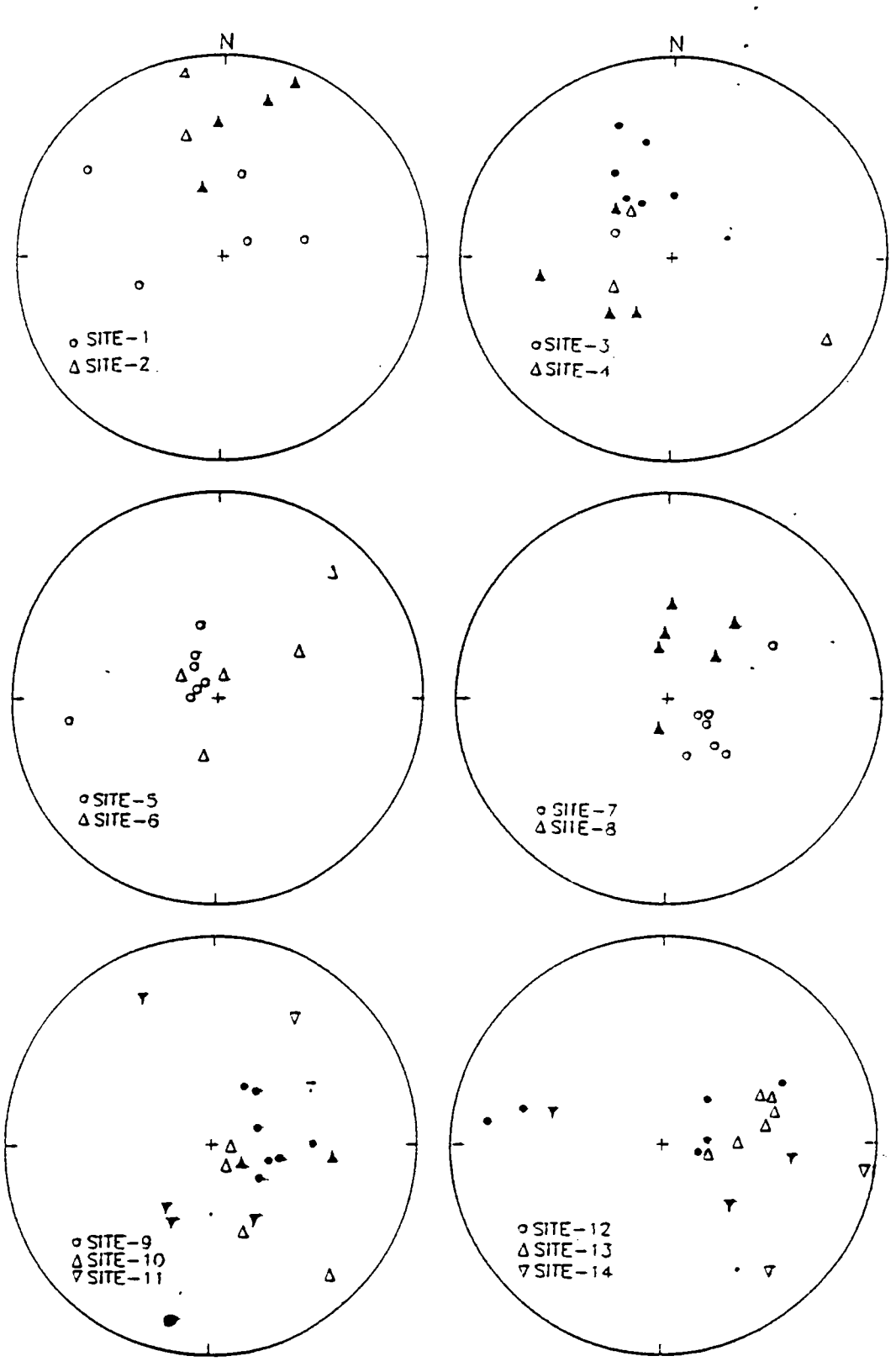

Figure 5.2: Distribution of natural remanent magnetisation in Tiruvannamalai dyke sites. The negative and positive inclinations are shown in open and closed symbols.

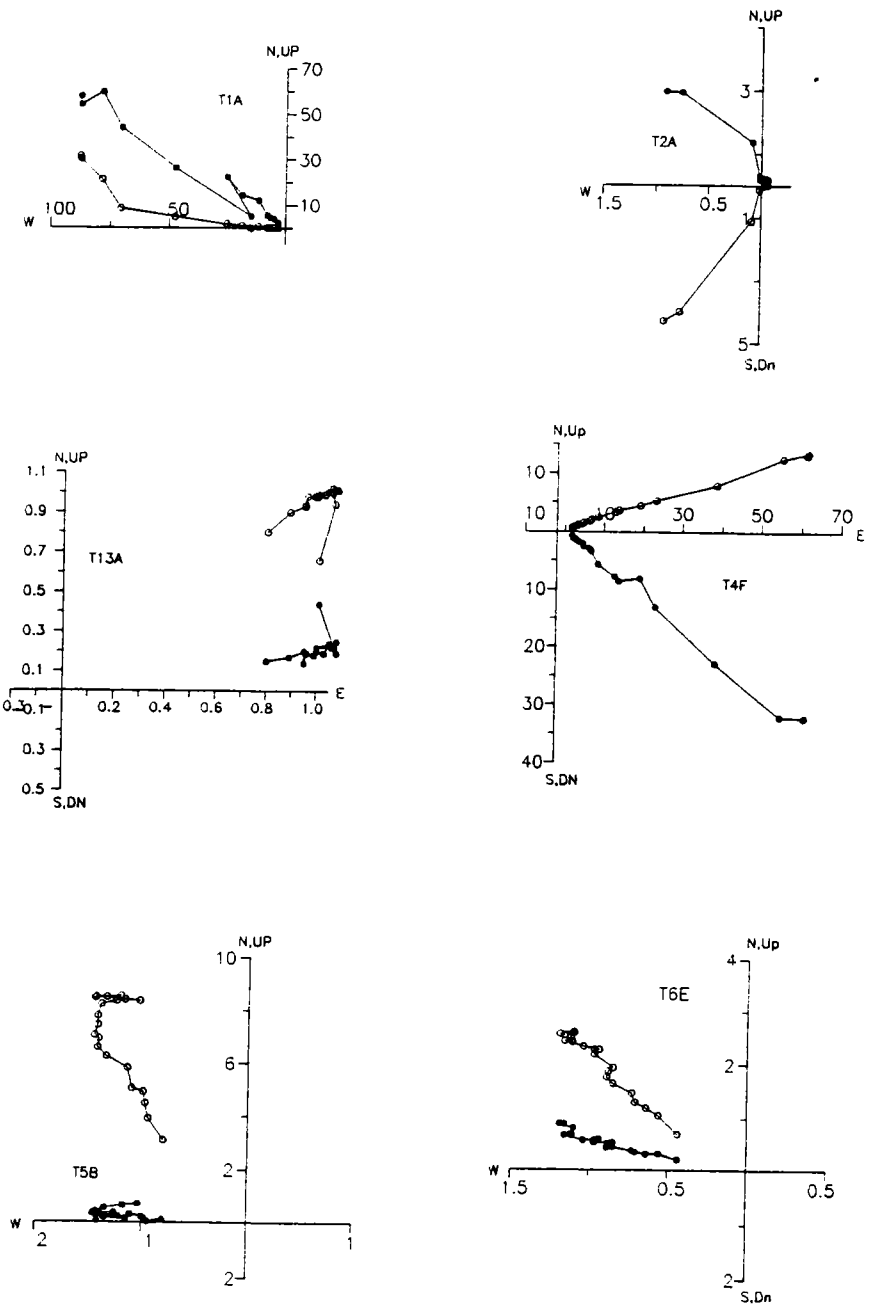

Figure 5.3: Orthogonal vector plots of alternating field (AF) demagnetisations of representative Tiruvannamalai dyke samples. Vertical projection and horizontal projection are shown in open and closed symbols respectively. Scale in A/m.

Successive demagnetisations are at 25 Oe interval up to 400 Oe and then at 50 Oe steps up to 600 Oe.

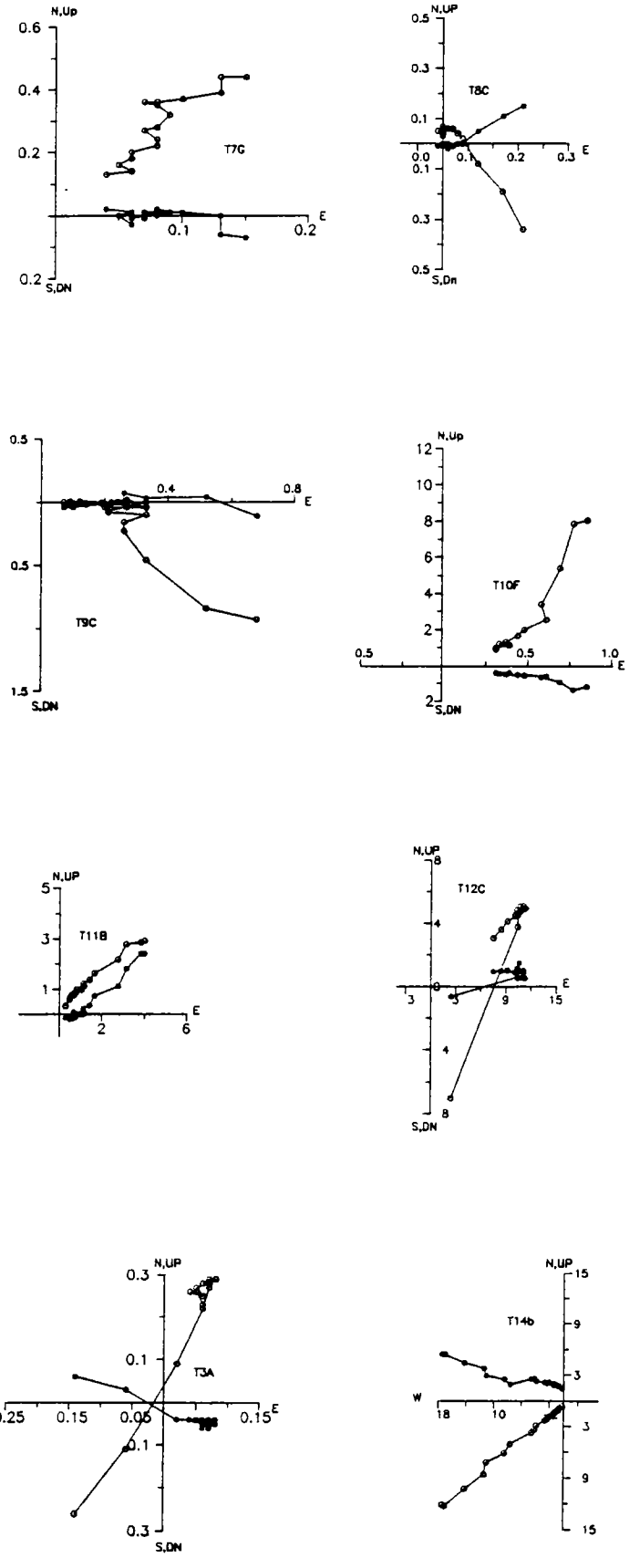

Figure 5.3 continued

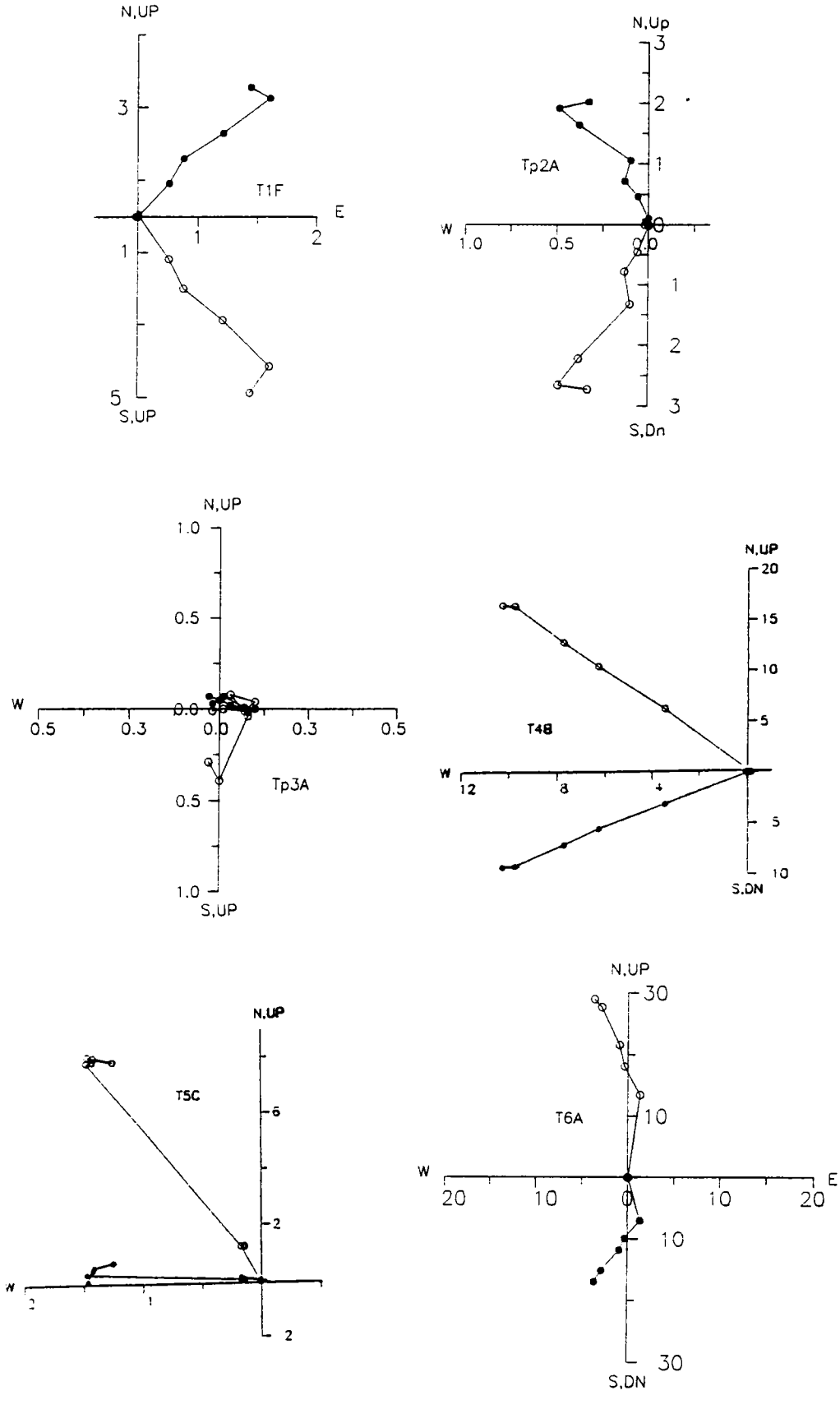

Figure 5.4: Orthogonal vector plots of thermal demagnetisations of representative Tiruvannamalai dyke samples. Vertical projection and horizontal projection are shown in open and closed symbols respectively. Scale in A/m.

Successive demagnetisations are in steps at 150, 250, 350, 450, 500, 525, 550, 580, 610, 640/650 and 680°C.

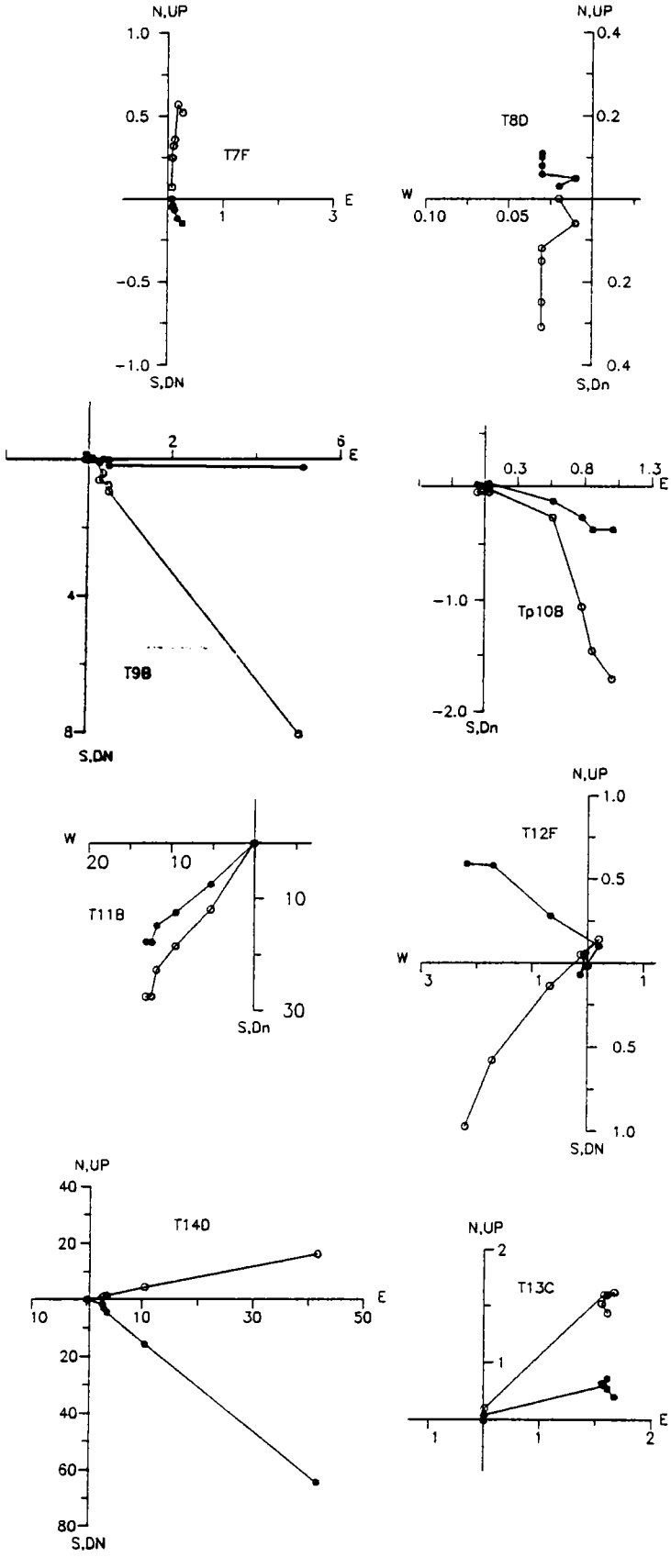

Figure 5.4 continued

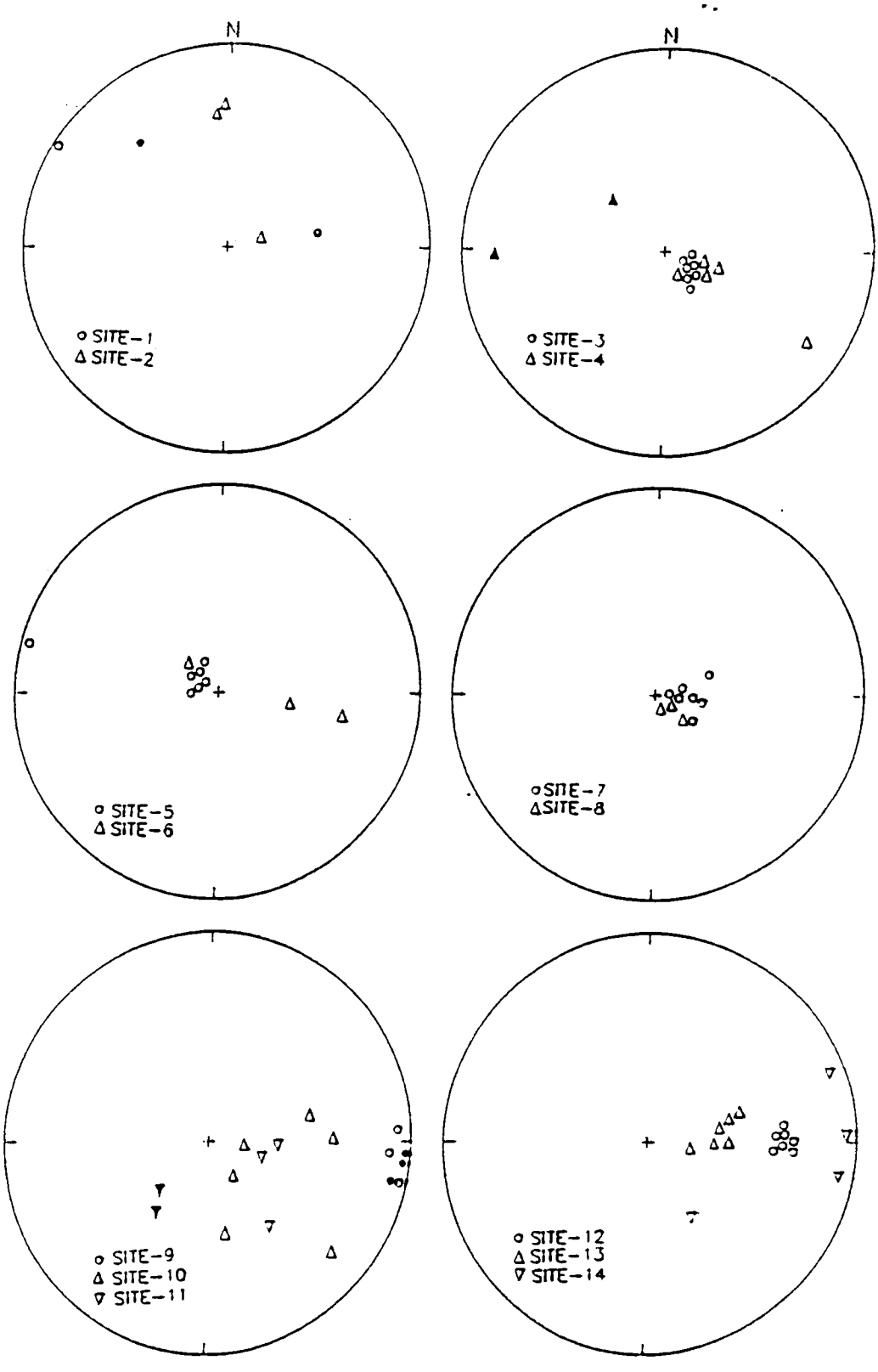

Figure 5.5: Distribution of characteristic magnetisation in Tiruvannamalai dyke sites. The negative and positive inclinations are shown in open and closed symbols.

Tp1E and Tp1F more than 95 % of the remanence was removed at lower increments (75 Oe), but these did not yield stable vectors. The sample Tp1F, which did not yield a stable vector through AF demagnetisation, was subjected to thermal demagnetisation. The NRM was stable up to 450°C retaining ~25% of the total remanence. 550°C onwards, the directions were not consistent and the remanence was reduced to less than 10% of the original. Magnetite seems to be the main carrier of magnetisation.

Site Tp 2

Six samples have given north-northeasterly or northwesterly NRM declination with two negative and four positive inclinations with shallow to medium values. The NRM intensities are relatively low, varying between 0.4 and 5 A/m. The sample Tp2A, after the removal of initial NRM directions (D = 343°; I = 54°), attained a characteristic vector (D = 79°; I = -74°) after 250 Oe increment. Samples Tp2C and Tp2D have yielded stable vectors with northerly declinations and shallow positive inclinations. Two samples (Tp2A, Tp2B) were subjected to thermal demagnetisation. The NRM directions of Tp2A were nearly intact up to 550°C and then inclination suddenly became very shallow and intensity dropped to 3% of the original. In the case of Tp2B, directions show wide scatter during thermal demagnetisation.

Site Tp 3

All seven samples collected from the site have low intensities (<1 A/m). All the samples have yielded characteristic stable vectors through AF demagnetisation. Six samples have northwesterly NRM declinations and medium positive inclinations (D = 292-359°; I = 59-18°) while one has a negative inclination. The characteristic vector was achieved by 100

Oe for each sample. All the rock samples have yielded characteristic remanent magnetism with nearly easterly and steep negative inclination. The characteristic remanent magnetisation is calculated at D = 129.7° and I = -73.5° with a very high precision κ (481) and very low α_{95} (2.8)The thermal demagnetisation was performed on Tp3A. The NRM (D = 339°; I = 74°) was changed and show easterly steep negative directions close to the characteristic remanent magnetism, at 350 and 450°C and then became shallow.

Site Tp 4

The NRM intensities in six samples vary between 10 and 27 A/m while one sample (Tp4F) has a very high intensity of 75 A/m. The initial NRM directions have declinations towards northwest and southwest, with moderate to medium positive and negative inclinations. One sample has southeasterly shallow negative NRM inclination. Generally, the initial NRM directions were changed at lower increments (< 75 Oe). In Tp4A, (NRM: D = 316°; I = 52.42°) the response to the AF demagnetisation is not conspicuous and the characteristic vectors are almost similar to the NRM. In sample Tp4F also the NRM directions (D = 117°; I = -10°) and the characteristic magnetic directions are not much different. In sample Tp4E, the declination was consistent while the inclination was decreasing. The four samples Tp4B, Tp4C, Tp4D and Tp4G gave a grouping with D = 114.4° and I = -67.9° (κ = 92; α_{95}= 9.6). Three samples (Tp4A, Tp4B and Tp4F) were subjected to thermal demagnetisation. The declination of Tp4A, did not change while there was a little change in inclination. In the case of Tp4B the declination and inclination did not change up to 450°C, but there was a sudden change at 550°C with a drop of intensity to about 1% of the original. Magnetite appears to be the main carrier of magnetism. Tp4F retained the NRM vectors up to 450°C and at 525°C the remanence was less than 1% of the original and the directions were inconsistent thereafter.

Site Tp5

The initial NRM intensities range between 2-8 A/m. Six out of seven samples, except Tp5G, show west to northwesterly NRM declination with medium to steep negative inclination. The sample Tp5G has a westerly shallow negative NRM direction. This sample (Tp5G), after the removal of NRM (D = 262.48°; I = -20.11°), has yielded stable vector by 100 Oe with D = 286° and I = 12°. Other samples showed a good grouping of characteristic magnetisation with D = 306.5° and I = -76° (κ = 275 and α_{95}= 4.1). Thermal demagnetisation was performed on two samples, one belonging to the site group (Tp5C) and Tp5G which did not fall into the group. In sample Tp5C, the NRM intensity was retained up to 525°C and the declination is nearly constant around 280°. After the 610°C increment, the remanent magnetisation dropped to zero and the directions were disturbed. In Tp5G, the declination was around 285° and even at 640°C the declination was not changed but the inclination changed, from shallow negative to positive.

Site Tp6

The NRM intensities in three specimens vary between 1-2 A/m, while two other samples Tp6A and Tp6B have very high intensity (32 and 115 A/m respectively). The NRM declinations are scattered in northeasterly, southerly and northwesterly directions with shallow to steep negative inclinations. Only three samples have responded to AF demagnetisation and yielded characteristic vectors. After AF demagnetisation, the samples Tp6A and Tp6B have given characteristic magnetisation with easterly declinations and medium negative inclinations. Tp6E gave a characteristic magnetism with D = 313.8° and I = -72.4°. Tp6A was subjected to thermal demagnetisation. The declination shows a gradual decrease from the NRM while

the inclinations are consistent up to 450°C. At 550°C, the remanent magnetism suddenly dropped to less than 1% of the original value and the directions are scattered thereafter.

Site Tp7

Six samples have the NRM declination in southeasterly direction with moderate negative inclinations. One sample has a northeasterly declination and moderate negative inclination. The NRM intensities are always low (<1 A/m). During AF demagnetisation, the viscous remanence were removed below 75 Oe in all samples. The characteristic magnetisation shows good within-site grouping with easterly declination and negative steep inclinations. The site mean characteristic magnetisation vectors are calculated as D = 92.1° and I = -70.7° (κ = 69; α_{95} = 7.3). During thermal demagnetisation, the sample (Tp7F) retained the initial NRM directions up to 580°C retaining about 44% of the original NRM intensity. After the 610°C increment, the intensity dropped to 18% and the directions changed.

Site Tp8

A total of six specimens were subjected to measurements. Five samples have north-northeasterly NRM declinations with positive medium inclinations. One sample (Tp8G) recorded southerly declination with steep positive inclination. The NRM intensities are always <0.5 A/m. Tp8A, Tp8B and Tp8D did not yield characteristic vector. The other three samples (Tp8C, Tp8E and Tp8G) have obtained characteristic magnetisation and grouped with a mean D = 121° and I = -78.1° (κ = 109, α_{95} = 11.9). The sample Tp8D was subjected to thermal demagnetisation. The NRM declination was not disturbed up to 350°C, above

which declinations show continuous change. The inclinations also do not show consistency between the increments.

Site Tp9

Seven specimens were subjected to AF demagnetisation. The NRM declination range from northeast to southwest. The inclinations are positive and moderate to steep. The intensities vary between 1-1.6 A/m. In all the samples, initial NRM component was removed by 75 Oe. Six samples, except Tp9A, yielded stable characteristic vectors which can be grouped together. The site mean characteristic magnetisation is calculated at D = 96.6°; I = -0.8° (κ = 111; α_{95} = 6.4). Two samples (Tp9A and Tp9B) were subjected to thermal demagnetisation. The declinations are between 92° an 115° and inclinations are between 55° and 64° up to 350°C, beyond which the directions because inconsistent.

Site Tp10

The NRM intensities of all the six samples from this site vary between 0.5 and 16 A/m. The NRM declinations vary between northeast and southwest. The inclinations, except in Tp10C, are negative and ranges from moderate to steep values. Five samples have yielded characteristic magnetisation vectors. The vectors of only two samples (Tp10F and Tp10G) show grouping with a mean D = 120.9° and I = -72° (κ = 57 and α_{95} = 33). Characteristic vectors of other three samples are scattered. Sample Tp10B was subjected to thermal demagnetisation. The NRM was retained up to only 250°C and thereafter it gave scattered directions. At 525°C remanent magnetism was about 2% of the original.

Site Tp11

The NRM declinations of all the seven samples are widely scattered. Except in two samples (Tp11C and Tp11G), the inclinations are positive with medium values . In Tp11C and Tp11G the inclinations are negative with medium values having northeasterly declination. The intensities vary between 1-41 A/m. Samples Tp11A and Tp11B did not show any drifting while AF demagnetisation. These two samples have higher intensities of 31 and 41 A/m. In the case of Tp11D, the stable vectors were not reached even after demagnetisation at 800 Oe. Four samples achieved characteristic magnetisation at higher increments of 300-375 Oe. The mean characteristic direction is calculated at D = 109.6° and I = -55.8° (κ = 45 and α_{95} = 18.5). Sample Tp11B was subjected to thermal demagnetisation and the NRM directions were intact up to 450°C retaining about 43% of the original remanence. At 550°C the remanence dropped to less than 1% and the directions got scattered.

Site Tp12

Seven samples were taken up for demagnetisation. The NRM intensities vary between 0.7-1.7 A/m. The NRM declinations of Tp12A, Tp12C, Tp12D and Tp12E range from E to NE. They have moderate to steep positive inclination. Tp12F and Tp12G have shallow positive inclinations and westerly declinations. Tp12B has a southerly declination and shallow positive inclination. During AF demagnatisation, all the samples have yielded characteristic remanent magnetism.. The samples have shown a strong grouping with mean declination of 90.1° and inclination of -23.1° (κ = 550 and α_{95} = 2.8). Tp12F was subjected to thermal demagnetisation. There was a drastic change in declination at 350°C with a drop in intensity, to 11% of the original, and thereafter the direction changes were random.

Site Tp13

Six samples of this site have NRM declinations ranging from northeast to east (63-96°). The inclinations are negative with moderate to steep values. The NRM intensities vary in the range of 1.2-3.9 A/m. All samples have yielded characteristic remanent magnetism through AF demagnetisations. Generally, the declinations and inclinations of characteristic vectors vary between 77-96° and 44-65° respectively. The mean characteristic direction was calculated at D = 84.3° and I = -51° (κ = 74 and α_{95} = 7.9). Sample Tp13C was subjected to thermal treatment. The directions remain nearly constant up to 450°C and became scattered in the later increments.

Site Tp14

The intensities in four of the five samples of this site range between 2-6 A/m. The NRM declinations are between 96° and 140°. Sample Tp14B has a higher intensity (21 A/m) with westerly declination. All other samples have yielded stable vectors. Tp14B has yielded northwest declination with moderate positive inclination. In others, the characteristic remanent magnetism has easterly declinations and inclinations, varying between shallow to moderate values, without showing a cluster. The thermal demagnetisations (Tp14D) did not show any response up to 450°C, and at 550°C, the intensity was reduced to far less than 1% and the directions were scattered thereafter.

Table 6.1: Palaeomagnetic results of Tiruvannamalai dykes.

Site No.	Trend	Lat	Long	N	Ns	D	I	κ	α_{95}	λ	ϕ	K-Ar Age (Ma)	Width (Appr.) in m.
@T1	NW-SE	12.15	79.03	5	3		no grouping						50
*T2	NW-SE	12.20	79.08	6	2(1)	79.7	-74.7	-	-	-5.8	230.7	1630±30	60
*T3	NW-SE	12.09	78.92	7	7	129.7	-73.5	481	2.8	-29.9	232.0		75
*T4	NE-SW	12.06	79.01	7	7(4)	114.4	-67.9	92	9.6	-24.6	219.8	1650±30	65
*T5	NE-SW	12.05	79.03	7	7(6)	306.5	-76.7	275	4.1	3.4	279.2	1650±30	55
@T6	NE-SW	12.05	79.08	5	3		no grouping					1660±30	40
*T7	NW-SE	12.05	79.08	7	7	92.1	-70.7	69	7.3	-11.0	223.3	2550±30	55
*T8	NW-SE	12.11	79.10	6	3	121.0	-78.1	109	11.9	-29.9	232.0		80
+T9	NE-SW	12.22	78.80	7	6	96.6	-0.8	111	6.4	-6.5	167.8	2210±20	68
*T10	NW-SE	12.22	78.80	6	5(2)	120.7	-72.1	57	33.7	-26.7	227.3	2270±40	78
+T11	NW-SE	12.27	78.91	7	5(3)	109.6	-55.8	45	18.5	-22.9	203.4		75
+T12	NW-SE	12.08	79.66	7	7	90.1	-23.1	550	2.8	-2.6	181.4	1670±20	65
+T13	NW-SE	12.06	79.66	6	6	84.3	-51.1	74	7.9	-1.6	201.9		80
@T14	NE-SW	12.22	79.72	5	4		no grouping					1640±20	65
mean swarm ,vector				7		106.9	-77.6	42	9.4				

N = number of samples studied from the site; Ns=number of samples yielded stable vectors; D and I are the declination and inclination (in degrees) respectively of the characteristic remanent magnetic vectors; κ=precision parameter; α_{95} =radius of the 95% confidence cone about the mean direction; λ and ϕ are respectively the latitude and longitude of VGP. *site mean values included to calculate mean swarm vectors and @site not considered for mean calculation either because it failed to yield stable end point or grouping. + is an anomalous or a distinct direction that is not considered for mean swarm vectors. All samples of the study are from the central part of the dykes.

INTERPRETATION OF RESULTS

6.1 INTRODUCTION

The geochemical and palaeomagnetic results presented in the previous sections are interpreted and their implications are worked out in this chapter. The geochemical data is mainly used to discuss and probe into the petrogenetic aspects such as crystal fractionation, crustal contamination and the mantle source characteristics. The geochemical data of the NW-SE and NE-SW dykes are compared to probe whether they can be related to a single magmatic suite. A geochemical comparison of the Tiruvannamalai dykes with other well studied Proterozoic mafic rocks was made to bring out common characteristics among the Proterozoic continental magmas in general. The palaeomagnetic data is evaluated to isolate primary directions for the Tiruvannamalai dykes. An attempt is made to compare and correlate the data with the available similar palaeomagnetic record from south India and the neighbouring continental blocks of Gondwana. Finally, the implications of the present geochemical and palaeomagnetic data set for the development and the movement of the Proterozoic south Indian continental lithosphere are discussed.

6.2 GEOCHEMISTRY

6.2.1 PETROGENETIC CONSIDERATIONS

Continental tholeiitic magmas are generated in extensional tectonic setting. Earlier they were thought to be chemically uniform Fe-rich basalts (Kuno, 1969). However, latter studies (Cox, 1980; BVSP, 1981; Mahoney et al 1985 etc) have revealed significant chemical

diversity within individual provinces which indicate the petrogenesis of these rocks is more complicated. Wilkinson and Binns (1977) considered that they are unusual primary magmas derived by partial melting of Fe-rich mantle sources, while Cox (1980) considered them as products of fractional crystallisation from Picritic basalts, near the base of the crust. The low Mg number of basalts means that they cannot have equilibrated with normal mantle lherzolite mineralogies and water undersaturated conditions (Cox, 1980). The most simple explanation for this is that the primary magmas were not basaltic but were high MgO picrites, which subsequently underwent low-pressure fractionation to produce the basalt. If CFBs are products of extensive low pressure crystal fractionation, then extensive piles of complementary cumulates must exist within the crust. Cox (1980) suggested that these occur in sill like bodies near the crust/mantle boundary which acted as feeder system for the surface eruptions. Such sills provide an ideal environment for the fractionation of large volumes of magmas. Extrusion/intrusion of these magmas through thick continental crust undoubtedly provides great potential for contamination. Therefore, it is petrogenetically essential to assess judiciously the nature of magma, fractional crystallisation and the extent to which the magmas have interacted with the rocks of the continental crust en route to the surface. Upon careful evaluation of the data, especially in terms of incompatible element chemistry, the compositional characteristics of primary magmas could be used to understand the nature of mantle characteristics and the process involved in its development. In view of these, the data on Tiruvannamalai dykes are evaluated here to understand the influence of fractional crystallisation, crustal contamination and then to deduce the mantle characters/processes.

6.2.1.1 Crystal fractionation

The ascend of magma from the mantle to the crustal levels exposes the magma to varying P-T conditions. The early stages of the ascent may be adiabatic up to the crustal depths. But as it approaches shallow depths the magma is forced to cool and respond to the changed environment by crystallisation. The temperature at which the crystals start appearing is the liquidus and the temperature at which the crystallisation is completed is the solidus. The magma may accumulate in temporary magma chambers within the low density crustal rocks where the conditions are conducive for crystal formation.

All the dyke samples of Tiruvannamalai have some aspect of their chemistry which identifies them as more evolved compared to the primary basalt compositions. It is therefore pertinent to evaluate the mechanism of differentiation. A vast account of petrological research has documented crystallisation as a means of producing variation within the magmatic suites, and the constraints that major and trace element data place upon fractionation models of basaltic magma are fairly well established. The evaluation of crystal fractionation models using major oxides and least square mixing techniques have become a standard practice in igneous petrology. However, the pertaining mineral chemistry data to use in the mixing calculations are not available for the Tiruvannamalai dykes. Therefore a more general approach is followed here using several binary variation diagrams to assess the fractional crystallisation in these dykes. Olivine, pyroxene, plagioclase and magnetite have been considered to be the most common low pressure fractional crystallisation phases. It may be important to assess whether the more evolved nature of these rocks is controlled by high pressure fractional crystallisation. However, assessment of high pressure fractional

crystallisation is constrained by the lack of high pressure megacryst in the dykes and thus no clue in petrography on medium to high pressure phase relations. The pressure dependents of most trace element Kds are not known and the trace element modelling at high pressure can be less precise than at low pressures. Despite these problems, dyke chemistry can be more judiciously used for testing high P fractionation. The more primitive dyke rocks (Mg number > 0.60) are olivine normative and contain olivine phenocrysts. Because any partial melt of peridotite is in equilibrium with olivine, a fractionated tholeiitic basalt crystallising olivine at low pressure is likely to have olivine at all pressures. Thus, olivine is probably an important component of any fractionating assemblage at moderate and high pressures. Plagioclase in tholeiitic liquids is stable only in moderate pressures (9-13 kbs), more over, its upper temperature stability limit is inhibited by pressure. Plagioclase is therefore unlikely to be an important liquidus or near liquidus phase above 5 kb. Both clinopyroxene and orthopyroxene can occur as liquidus phases with increasing pressure, especially clinopyroxene at high pressures. Garnet is another important phase that can fractionate at high pressures along with clinopyroxenes. The partition coefficients of many trace elements for garnet are less precisely known than for the olivine,clinopyroxene and orthopyroxenes. The high pressure experimental studies have suggested that tholeiitic character of basalts, especially with low normative olivine or quartz, is generally established at pressures lower than those where garnet is stable as liquidus phase and in many tholeiitic rocks garnet does not figure in fractionation schemes. In the dolerite samples of present study REE offers the best means to identifying whether garnet was fractionated in the evolution of magmas. Garnet fractionation would produce rapid increase in $(Tb/Yb)_N$ with marked decrease of Yb_N in residual liquids. On the other hand, the other silicate phases produce little change in $(Tb/Yb)_N$ with steady increase of Yb_N

The dolerites of Tiruvannamalai have Mg numbers ranging from <0.60 to 0.30 (only rocks with cumulus olivine have higher values) indicating that they are much evolved than primary basalts (Bence et al., 1979; Sun et al., 1979). The major element and Cr and Ni contents of both sets of dykes have been plotted against Mg number (figure 6.1) while the trace elements have been plotted against Zr values (figure 6.2) to assess the role of fractionation. These plots reasonably explain the compositional variation within the suite by fractional crystallisation.

The average content of compatible elements like Ni and Cr in the noncumulus samples of both sets are low (150 to 55 ppm and 200 to 60 ppm respectively in NW-SE and NE-SW dolerites of Tiruvannamalai) when compared with the Ni and Cr content of primary melts (250-350 ppm and 500-600 ppm respectively; Green, 1980). These are easily incorporated into early crystallising mafic minerals like olivine and clinopyroxene. The fractionation of olivine is indicated by a steep decrease of Ni as Mg number decreases. The amount of olivine fractionation necessary to decrease the Ni content from high concentration of primary basalt would be 5 to 10%. However clinopyroxene is a likely mineral phase in the liquidus rather than olivine between 11 and 30 kb (Takahashi, 1980). According to general estimates, clinopyroxene can remove Ni from the melt and for $D^{cpx\text{-}liq} = 4$ or more, the concentration of Ni is decreased to half or less if 15% of clinopyroxene is fractionated. The variation of Fe_2O_3 and TiO_2 (also V) against Mg number indicates that titanomagnetites were not an early fractionating phase.

In figure 6.3, Sr/Ce has a decreasing trend against the Mg number indicating plagioclase control in fractionation. This feature may have resulted marked depletion of Sr

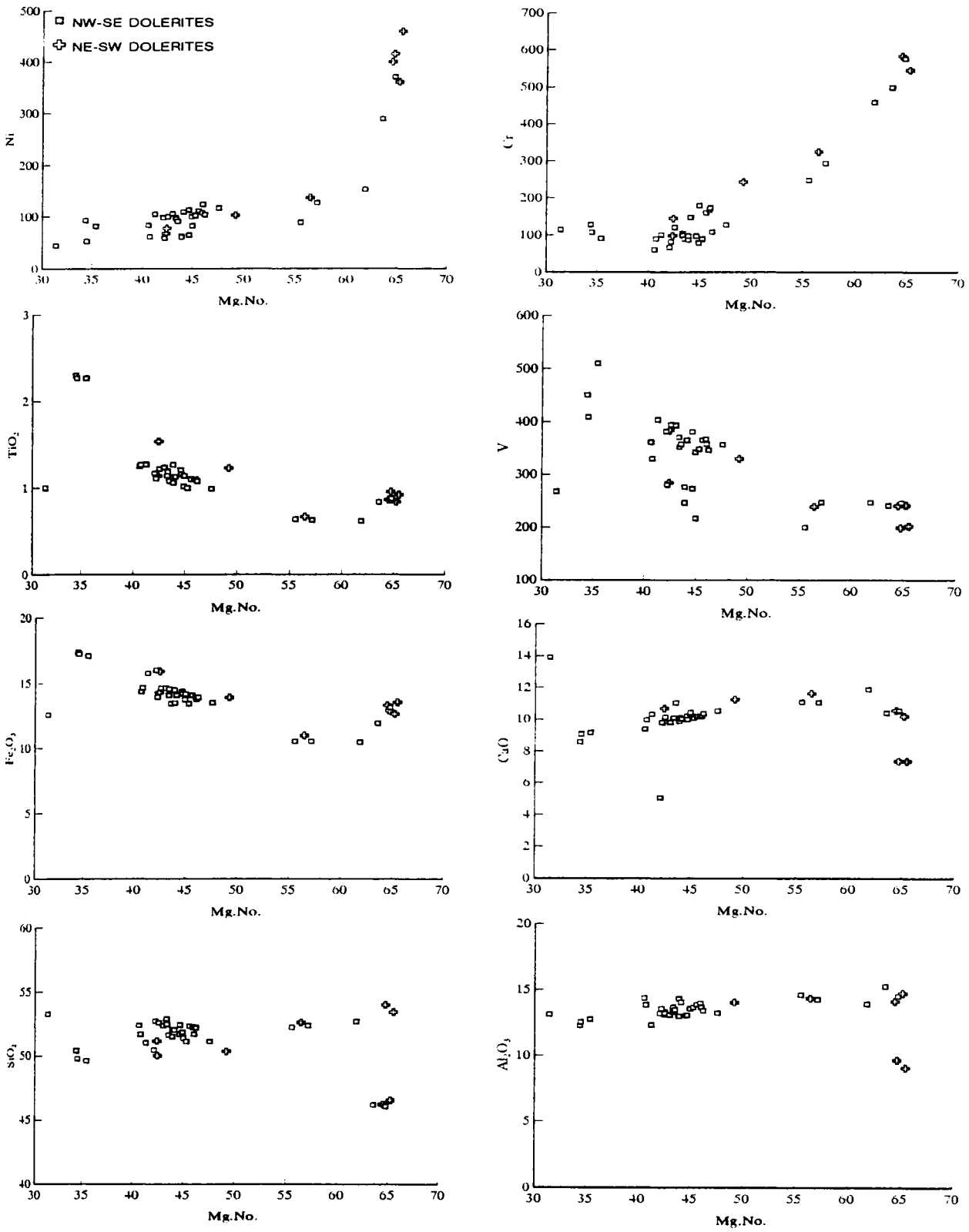

Figure 6.1: Variation plots of 100.Mg/Mg+Fe versus major and compalitible. trace elements.

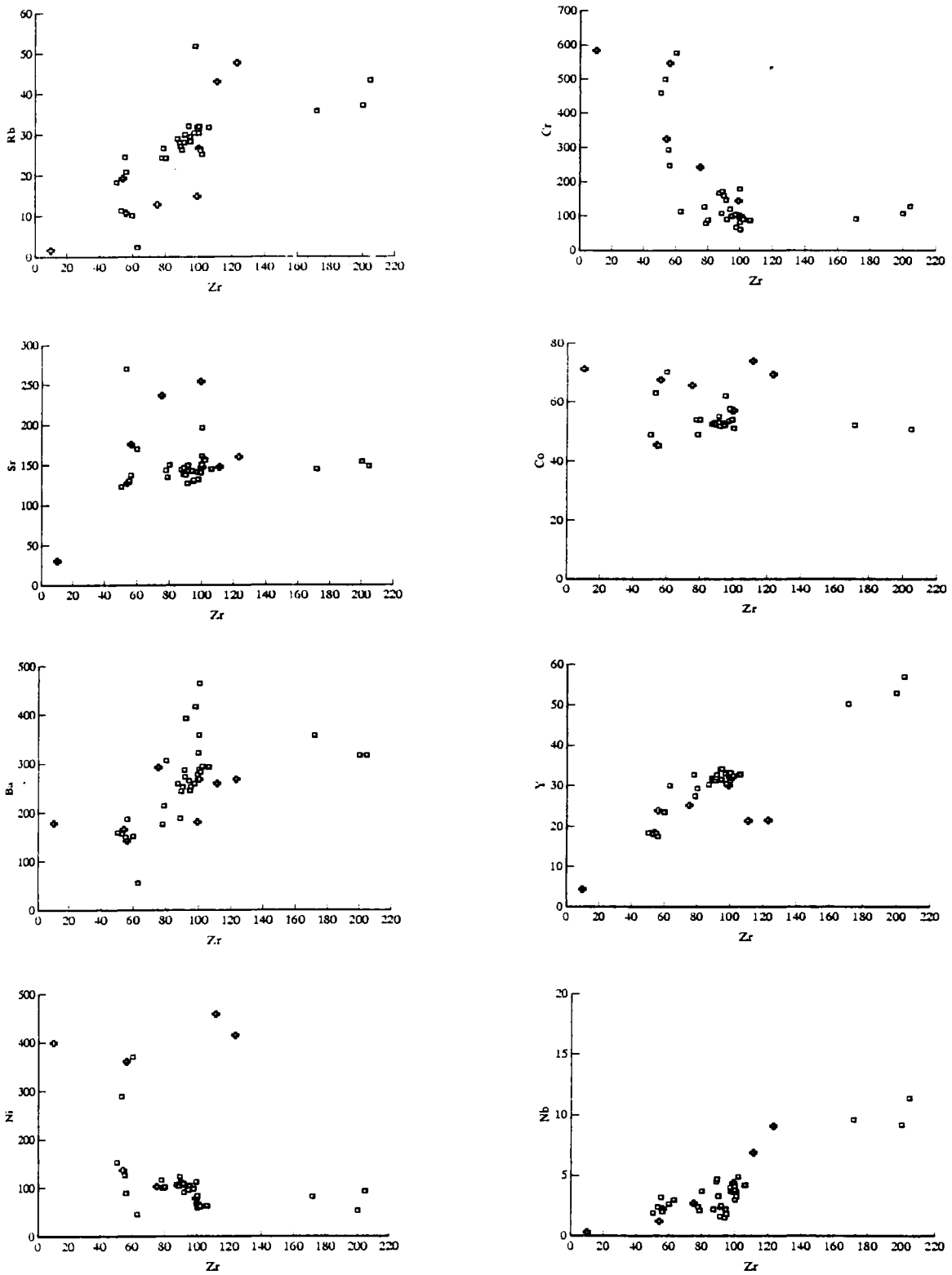

Figure 6.2: Variation of Zr vs trace elements of Tiruvannamalai.

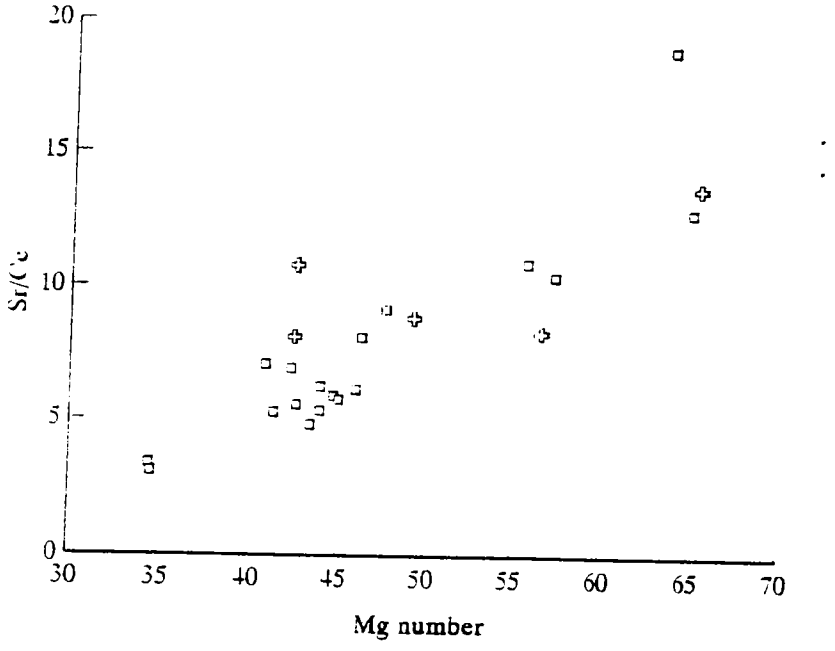

Figure 6.3: Variation of Mg number vs Sr/Ce in Tiruvannamalai dykes. Symbols are as in figure 6.1.

relative to La and Ce in more fractionated samples in a multielement mantle normalised plot (figure 6.4). Further, three samples which have highest Zr do not have high Sr (figure 6.2). But they are rich in K, Rb, Ba and Nb and the Sr/Zr display decrease as Zr increases. These features can be attributed to plagioclase dominated fractionation in more evolved samples. In samples reflecting plagioclase dominated fractionation marked Eu anomaly is expected. Eu effects are predicted because D_{Eu} for plagioclase related to basaltic liquids are high (0.3; McKay, 1989). However, lack of Eu anomalies in total population of Tiruvannamalai dykes require further comment. In high oxidation (fO_2) condition, during which high Fe^t magmas crystallises, plagioclase will have much reduced D_{Eu} (Williams, 1989). Also the proportion of plagioclase and pyroxene have important implication for Eu anomaly. The D values of Eu have a dip compared to that of other REE. Apatite also has a minor dip in its D value related to the other REE. As the Tiruvannamalai dykes show mild increase of P with decrease of Mg number (figure 6.1) apatite may not have any role in the fractionation history. Thus

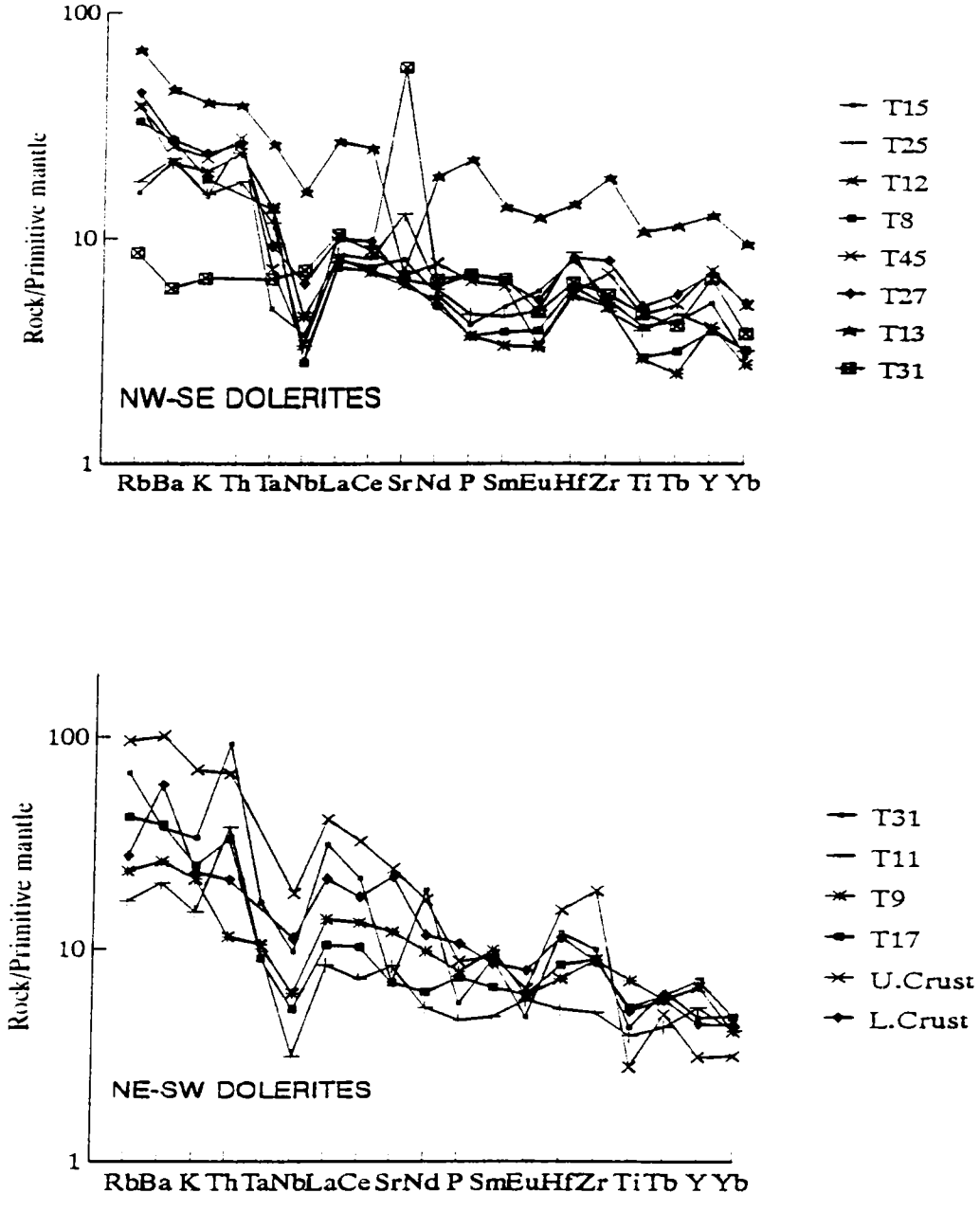

Figure 6.4: Mantle normalised plots of incompatible element abundances in the representative samples of Tiruvannamalai dykes. For comparisons plotted are the upper crust (Weaver and Tarney, 1984) and lower crust (Kempton et al., 1991).

clinopyroxene crystallisation earlier in the frame work of plagioclase may explain lack of Eu anomaly in the Tiruvannamalai dykes. The Tiruvannamalai dykes have parallel REE patterns with out marked correlation between Yb_N and $[Tb/Yb]_N$. These features do not indicate garnet to have any significant role in fractionation.

In summary, the NW-SE and NE-SW dykes have similar behavior in their elemental distribution; the distribution patterns which show considerable overlap, are explained by fractionation of olivine, clinopyroxene and plagioclase, the latter is dominant in more evolved samples. It is unlikely that these mineral phases inferred in fractionation would affect considerably the relative incompatible element chemistry. Therefore, it is important to evaluate whether crustal contamination has had any significant role in controlling the incompatible element chemistry of Tiruvannamalai dolerites.

6.2.1.2 Crustal contamination

When magma ascends through continental crust, heat transfer can be rapid and the wall rock of the conduit can melt and be assimilated into the magma. A few geochemists argued that mantle-derived magmas have been subjected to some degree of contamination during ascent and/or temporary residence in crustal magma chambers (Mohr, 1987). The chances for chemical exchange with wall rock is more in intrusive rocks. There are several mechanisms for the interaction of mantle derived magmas with crustal rocks involving both mixing of crustal and mantle partial melts and bulk assimilation (Wilson, 1989). Magmas stored in sheet-like bodies (dykes or sills) clearly have a greater contact area with their wall rocks and therefore should be the most susceptible to contamination. The magnitude of contamination

will vary with the size and surface area of the intrusion, thermal gradients in the wall rock, tectonic setting and the pore water content and lithology of the country rock through which the mantle derived magma passes. Mohr (1987) argued that the degree and to some extent the nature of contamination is mostly influenced by melting point of the wall-rock, temperature difference between magma and wall-rock and the bulk of magma available to heat the adjoining country rock per unit area of the wall-rock. The rate of flow of the magma will also have a role in the contamination process. Huppert and Sparks (1985) suggested that if the flow in a dyke feeder is turbulent, the assimilation and thermal erosion of the wall rock will be maximum leading to active contamination. These remarks show that for Tiruvannamalai dykes or other dyke swarms/ CFB emplaced through continental crust, there exist a great potential for addition of lower-melting crustal components to the basaltic magmas. Therefore, crustal contamination has become the most discussed topic in geochemistry of continental basalts and dyke rocks. Thus it is essential to answer the questions whether uncontaminated magmas can be identified, whether crustal effects can be striped off to deduce the mantle source characteristics and to what extent the magmas have been affected by crustal contamination. The view points on these aspects for the continental flood basalts are generally equivocal. For example, some authors rule out major crustal effects and appeal for mantle heterogeneity (Weaver and Tarney, 1981; Condie, et al., 1987; Tarney, 1993 etc) while some others argue for crustal contamination (Patchett, 1980; Cambell, 1985; Mohr, 1987).

Enrichment of LREE and LILE and quartz normative compositions of the Tiruvannamalai dykes are superficially suggestive of crustal contamination. Geochemical study across the dykes of Greenland have indicated contamination only in the dyke margins (increase of K, Rb, Ba) while the dyke centres are unmodified (Gill and Bridgwater, 1979;

Kalsbeek and Taylor, 1985). Distribution of elemental data across one Tiruvannamalai dyke (figure 4.8) shows that, although the completely altered contact sample (T31) is depleted in K, Rb, Ba and LREE, the other fresh contact sample (T30) is rich in LILE, Rb, Ba, K indicating minor contamination. All other samples of geochemical study taken from dykes centres have a good internal consistency and the residual contamination may be minimal. However, assimilation of crust by hotter and more primitive melts before fractionation or assimilation fractional crystallisation (AFC) remains to be the possible contamination processes. In the former, least fractionated dolerites will be the most contaminated (for example, Deccan; Mahoney, 1988). In the AFC process, fractionation invokes the main source of energy for assimilation of crustal wall rocks (for example, Parana; Carlson and Hart, 1988). In the Tiruvannamalai dykes, assimilation before fractionation is readily recognisable only in two samples (T37 and T39) which have high Mg number (~0.65) and at the same time have distinctly high SiO_2 (>53%), K_2O (>1.0%), Rb (>40 ppm) and Th (7-9 ppm) compared to the whole range of other samples.

To evaluate the possible role of combined wall rock assimilation and crystal fractionation (AFC) processes in the evolution of the Tiruvannamalai dolerites the ratios of the highly incompatible elements K_2O/P_2O_5 and TiO_2/P_2O_5 against Mg number have been plotted (figure 6.5). Most mantle derived magmas have K_2O/P_2O_5 ratios of 2 or less (BVSP, 1981). Carlson and Hart (1988) have used K_2O/P_2O_5 and TiO_2/P_2O_5 ratios against Mg number to evaluate crustal contamination. Crustal assimilation would result elevated K_2O/P_2O_5 ratios. The crustal assimilation causes a gradual decrease of TiO_2/P_2O_5 ratio as Mg number decreases. However, in Tiruvannamalai dolerites, both K_2O/P_2O_5 and TiO2/P2O5 ratios are within the

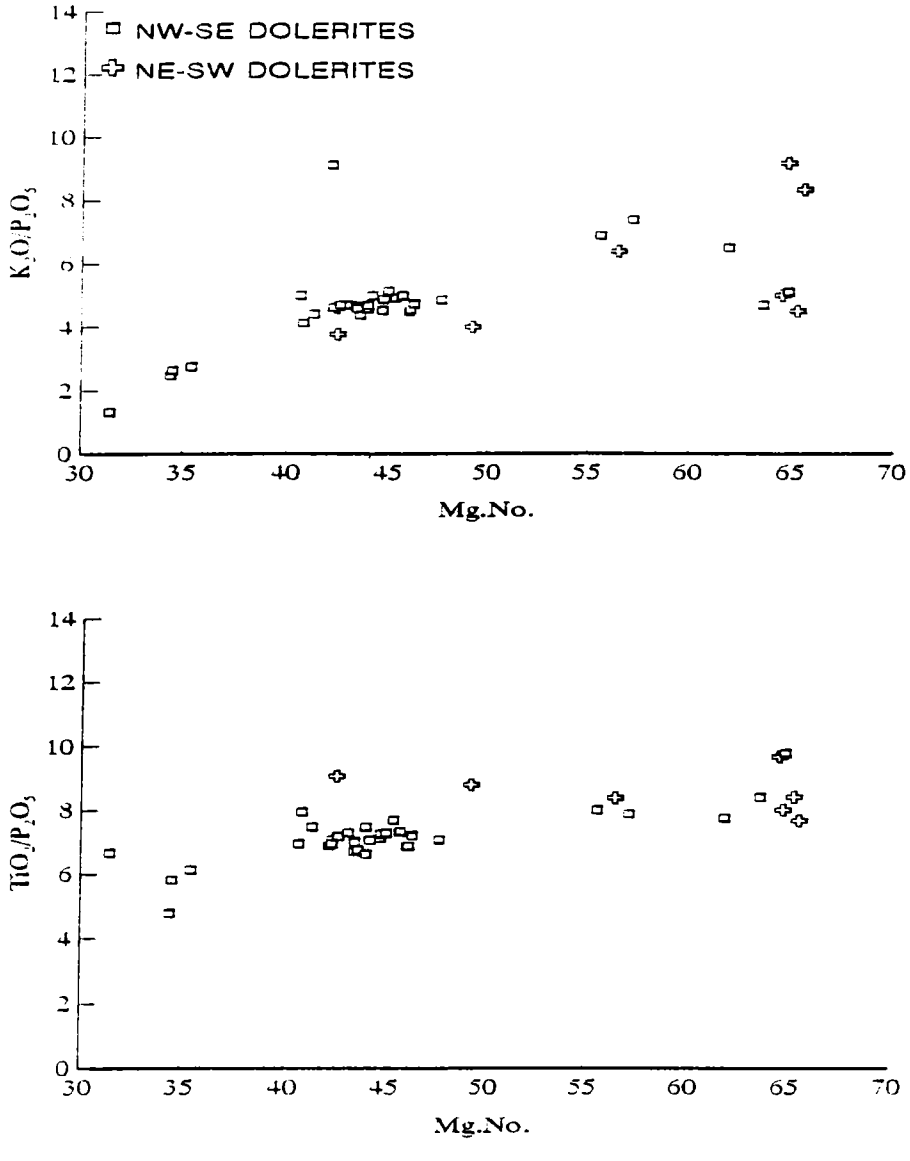

igure 6.5: Distribution of Mg number vs K_2O/P_2O_5 and TiO_2/P_2O_5 of Tiruvannamalai dykes. Symbols are as in figure 6.1.

OIB and MORB range showing close tight patterns with the decrease of Mg number and these variations do not indicate crustal contamination.

The majority of the Tiruvannamalai dyke samples have Ti/V, Sr/Nd Ti/Zr, Zr/Nb, Zr/Y, Y/Nb, La/Ta, Ce/Y, Sr/Y, Sm/Hf, Zr/Sm, Ti/Eu ratios range within the NMORB and EMORB values (table 4.10). Some of the ratios like Nb/La and Nb/Th are lower than MORB and also lower than the values of lower and upper crustal averages, but the ratios K/Zr, Ba/Nb, La/Nb are higher than the values of MORB and the Lower and upper crustal averages. Similarly some other ratios like K/Rb, Rb/Sr, Ti/Zr, La/Ta etc., are either too high or too low than the granulite country rocks (table 4.10) and do not imply contamination. The ratio-ratio plots in figure 6.6 do not support assimilation of crust.

Multielemental spidergrams would readily display relative abundances of many incompatible elements. The Tiruvannamalai dykes display enrichment of LILE and LREE while Nb and Ta are depleted (figure 6.5). As a first approximation, crustal contamination appears to be responsible to these characteristics. Considering bulk assimilation of the lower crust or upper crust, the Tiruvannamalai dolerites do not show positive Ba spike and their negative Nb spikes are quite large (figure 6.4). The low Nb/La or Nb/Th ratios in the dykes would require a contaminant with a large negative anomaly. The country rocks which have negative Nb anomaly are more silicic and possess strong positive or negative Eu anomalies while the SiO_2 content in the Tiruvannamalai dykes are within the basic range and the samples do not show Eu anomalies. From the calculated contaminants of NMORB with

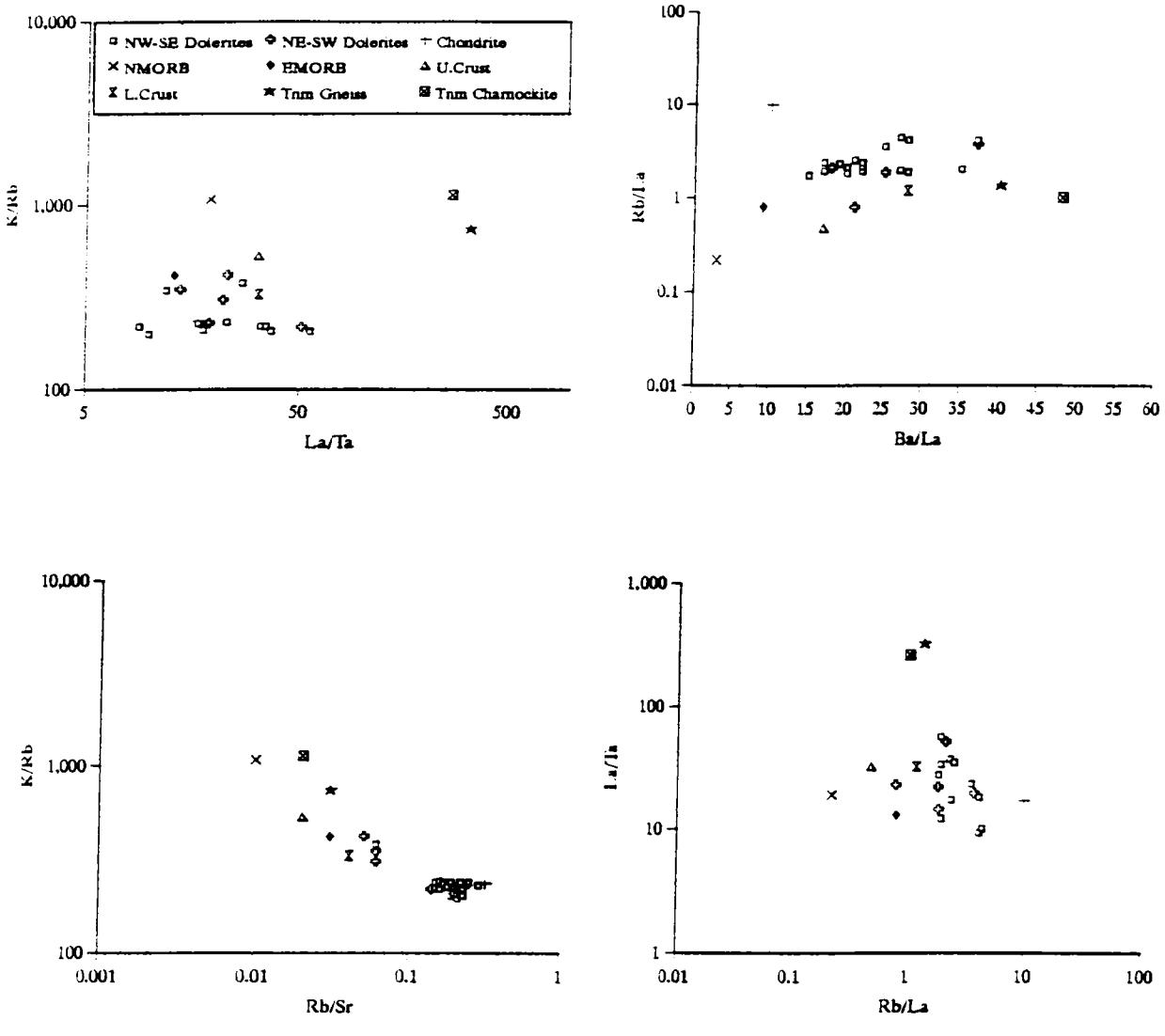

Figure 6.6: Ratio-ratio plots of Tiruvannamalai dykes.

varying amounts of upper crust (incidentally the Tiruvannamalai dyke country rocks are nearly similar to upper crustal average) and lower crust, it is clear that assimilation of even 25% of upper/lower crustal units cannot produce the patterns shown by Tiruvannamalai dolerites.

Crustal rocks are highly enriched in $\delta^{18}O$ when compared to mantle derived magmas. Most silicate rocks have $\delta^{18}O$ values between +5 to +15 ‰. Usually the $\delta^{18}O$ values of uncontaminated basalts and gabbros range between +5.5 to +7.4 ‰ (cf: Kyser, 1990). All analysed samples from the Tiruvannamalai dykes have $\delta^{18}O$ values (+5 to +6 ‰) within the mantle values.

6.2.1.3 Nature of mantle sources

The chemistry of Tiruvannamalai dyke samples can be constrained by fractional crystallisation of mafic phases. However, it would be curious that in the complete selection of samples over the total geographic area, there are none with higher Mg number, Ni and Cr content which can be considered to be primary liquids. Further, these samples are Fe- rich quartz tholeiites. A possible means of explaining these features is to consider primary melts with low Mg number. Studies of mantle nodules with high Fe rich ferromagnesian minerals compared to traditional mantle source (Wilkinson and Binns, 1977; Bergman et al.,1981; Wilkinson and Le Maitre, 1987) and mantle sources which contain amphibole have shown that primary melts with lower Mg number can be produced. Existence of such mantle sources for Fe rich CFB has been explored using [Mg] and [Fe] mole percent based on the approach of Hanson and Langmuir (1978). Rajamani et al. (1985) have defined [Mg] and [Fe] as compositonally corrected Mg and Fe abundances in cation mole percent adopting the corrections in accordance with Ford et al. (1983) equation. Horan et al. (1987) have calculated the solidii of melt fields at 1 atm and 25 kb for Fe-rich non-pyrolite source for which Fe/Mg ratio is 0.25 as against the ratio of 0.12 in pyrolite. Most of continental flood basalts like Tiruvannamalai dykes fall between the solidii of 1 atm and 25 kb of non-pyrolite

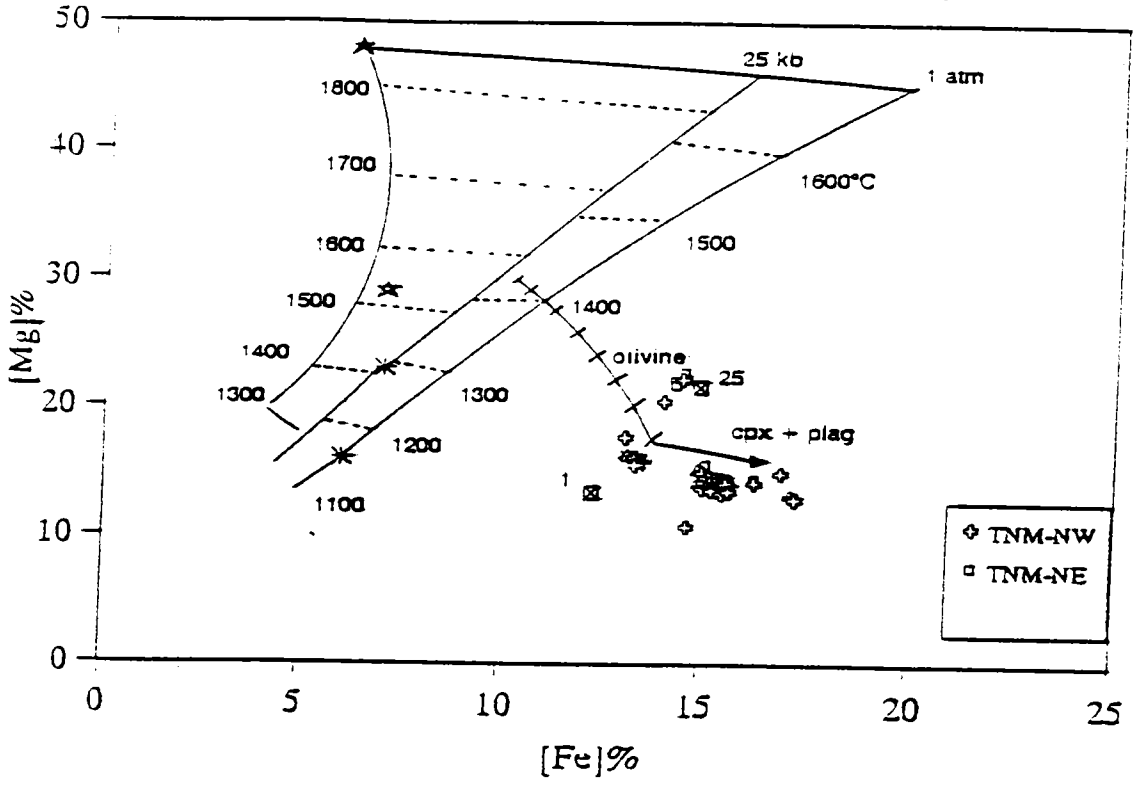

Figure 6.7: [Fe]-[Mg] mole % variation in Tiruvannamalai dykes. Marked are the pyrolite mantle source (Fe/Mg = 0.12; closed star) and non-pyrolite mantle source (Fe/Mg = 0.25; open star). Isotherms of olivine crystallisation for 1 atm and 25 kb pressure, solidii for pyrolite (*) and non-pyrolite (□) sources and fractionation trends marking 5% increment for olivine and clinopyroxene+plagioclase (cf: Ahmad and Tarney, 1991).

Fe rich source (figure 6.7). These results suggest that the Tiruvannamalai dykes were derived from an Fe rich non-pyrolite mantle source.

Distribution coefficient values of many trace elements (REE, Rb, Ba, Ta, Zr, Nb) are very low for mineral phases (olivine, clinopyroxene, orthopyroxene, spinel) expected to crystallise in the Tiruvannamalai dykes. As these minerals are the likely phases of residual as well as the crystallising phases, the ratios of these elements may be used to constrain the

mantle ratios and mineral constituents. There is a systematic variation in REE abundances (figure 4.6) with high $[Ce/Yb]_N$ (range 1.4-3.7). It would require involvement of mineral phases such as clinopyroxene or garnet in the petrogenesis, which mildly fractionate LREE from HREE. The $[Tb/Yb]_N$ in all the Tiruvannamalai dykes are only about unity and do not show any correlation with Yb_N distribution. Therefore, involvement of garnet either as residual or as crystallising phase in the petrogenesis of the Tiruvannamalai dykes is ruled out. The high $[Ce/Yb]_N$ ratios can therefore be attributed to large proportion of clinopyroxene in the mantle sources. Lack of large Eu anomalies in the Tiruvannamalai dykes (figure 4.6), combined with the experimental data that plagioclase is stable only at very shallow depths (Jaques and Green, 1980), preclude plagioclase bearing mantle source for Tiruvannamalai dykes. Alternatively, it may be suggested that the Tiruvannamalai dolerite magmas have originated in the depths corresponding to spinel peridotite mantle.

In the preceding discussion (section 6.2.1.2) it has been argued that crustal contamination has had no significant role in the compositional character of Tiruvannamalai dykes. Further it has also been shown that the mineral phases fractionated had insignificant role in many trace element relative abundances. Therefore, it follows that the LILE and LREE enrichment and negative Nb and Ta anomalies have been the characteristic of the mantle source. The importance of mantle metasomatism and the role of accessory phases such as amphibole, phlogopite and apatite to explain these characteristics have been advocated by various workers (cf. Hammond et al. 1986; Hawkesworth et al., 1990; Gallagher and Hawkesworth, 1992). However the amount of apatite required to produce all the phosphorous in the melt is very negligible and its effect is not observed in the REE content. Similarly, phlogopite produces much higher K rich melts than that encountered in the Tiruvannamalai

dykes. Therefore, amphibole could be the most probable metasomatic phase in the mantle source of the Tiruvannamalai dyke magmas.

The Ti/Zr ratios (avg: 74 and 82 for NW-SE and NE-SW dykes respectively) in the Tiruvannamalai dykes are always lower than the chondrite values (115; Sun and McDonough, 1989). Since the fractionation of titanomagnetite is discounted in the Tiruvannamalai dykes, the low Ti/Zr ratios in these dykes would be a feature of mantle source. It may be constrained that mantle has minor amphibole as an accessory phase because amphibole would retain more Ti than Zr, suppressing Ti/Zr ratios. Presence of hornblende in the mantle is also supported by low K/Rb ratios (av: 230 for NW-SE and 290 for NE-SW dykes) in all Tiruvannamalai dolerites. Experimental results of Ringwood (1975) showed that amphibole is stable up to the depths of about 75 km and is capable of holding many of the LREE and LILE which show enrichment in the Tiruvannamalai dykes. Thus, the metasomatism is relatively a shallow level enrichment process in the lithospheric mantle (Hawkesworth et al 1990). The hydrated lithospheric mantle would produce significant melts having compositions controlled by amphibole (Gallagher and Hawkesworth, 1992).

6.3 GEOCHEMICAL COMPARISON

6.3.1 COMPARISONS BETWEEN NW-SE AND NE-SW DYKES

The occurrence of dykes in two different (NW-SE and NE-SW) strike trends may readily give an impression of two different episodes of magmatic activity. Venkatesh et al (1987) have also advocated that these dykes belong to two geochemically distinct suites. However, their geochemical distinctions are based on only major elements and a few trace

elements of limited samples. Therefore, a comparison between the dyke suites is attempted here based on the large data set, including the more incompatible elements and REE, presented in the earlier chapter.

The major element chemistry (table 4.4 and 4.5) indicates that both sets of dykes are iron rich tholeiites. The range of the Mg number in both the sets are similar. The variation of major elements and trace elements against Mg number and Zr are similar with considerable overlap indicating that they have followed the same fractionation history. The absolute concentrations of major and trace elements in all non-cumulus samples are also similar. The REE contents of both NW-SE and NE-SW dykes (see fiigure 4.6) have similar and parallel patterns, and overlap. The incompatible trace element ratios of NW-SE and NE-SW dykes presented in table 4.10 do not show marked differences.

The absolute concentration and range of major and trace elements, the similarity in evolutionary trends and REE patterns, strong overlap of both sets of samples on a variety of variation plots etc strongly suggest that all Tiruvannamalai dykes irrespective of their strike trends belong to a single magmatic suite. The similar isotope ages and palaeomagnetic directions (sections 6.4.1) also support the suggestion that they belong to a single magmatic episode.

6.3.2 COMPARISONS WITH OTHER PROTEROZOIC DYKES

Multielemental plots are particularly useful to compare geochemistry of the dykes with other known Proterozoic magmatic suites. Figure 6.8 displays mantle normalised spidergrams

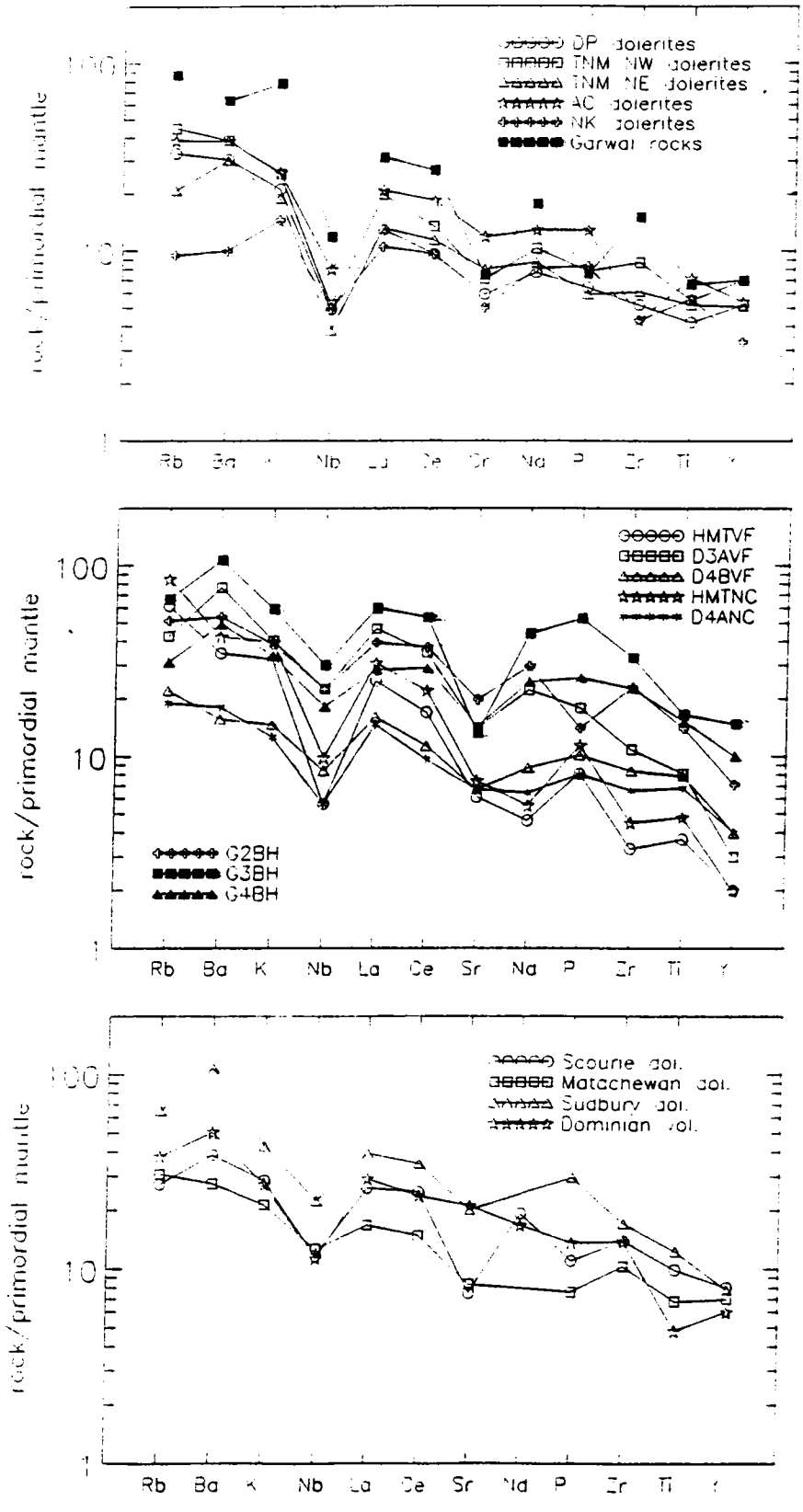

Figure 6.8: Multi-elemental patterns of average Tiruvannamalai dykes and other Proterozoic mafic suites. HMTVF = High Mg-tholeiites, Vestfold Hills (2400 Ma); D3AVF = Vestfold Hills group 3a dolerites (1800 Ma); D4BVF = Vestfold Hills group 4b dolerites (1400 Ma); HMTNC = High Mg-tholeiites, Napier Complex (2400 Ma); D4ANC = Napier Complex group 4 a dolerites (1400 Ma).

ıor average Tiruvannamalai dykes along with averages of other Proterozoic rocks. Agali-Coimbatore dykes to the south of Nilgiri Massif (figure 2.1) constitute an early mid-Proterozoic (ca. 2000 Ma; K-Ar and Rb-Sr age; Radhakrishna et al., 1994b) dyke swarm, whereas a few dykes in north Kerala are of mid-Proterozoic age (ca. 1650-1700 Ma; K-Ar age, Radhakrishna et al, 1986; 1991a). The Agali-Coimbatore dykes show some differences such as minor depletion in Zr with high Ti/Zr ratios and contain high Ce/Y ratios which may be explained by the clinopyroxene ± garnet residual mineralogy in the sources. Otherwise, these rocks display a general Nb depleted and LIL and LREE enriched pattern. North Kerala dykes show a depletion of Ta which follows Nb on the spidergrams, and enrichment of LIL and also LREE in some samples. A similar pattern has been found in the Proterozoic Garwal flows and dykes in the Himalayan region (Ahmad and Tarney, 1991; figure 5). Ahmad and Tarney (1991) showed a good correlation of Garwal rocks, in terms of these characteristics, with the middle Proterozoic Mandi - Darla volcanics of the Himachal Himalaya (Ahmad and Bhat, 1987) and early Proterozoic basal Aravali volcanics of Rajasthan, northwest India (Ahmad and Rajamani, 1991). Interestingly these chemical characteristics (enrichment of LILE and LREE and depletion of Nb and Ta) are conspicuously seen in the ca. 2400 Ma high Mg-dykes of Napier Complex and Vestfold Hills, in the ca. 1200 Ma Group 1 and Group 2 Amundsen dykes in Antarctica (Sheraton and Black, 1981) and in the c.1080 Ma Stuart and Kulgera dyke swarms in Australia (Zhao and McCulloch, 1993). However, among the late Proterozoic (ca. 1.1 Ga) dyke systems from Bunger Hills, in east Antarctica, except the Group 1 dykes, which have small positive Nb and Sr anomalies characteristic of certain OIB, the dykes of other three different groups have large Nb anomalies and enriched LIL and LREE (Sheraton and Black, 1981; Collerson and Sheraton, 1986). Volcanic rocks of the Dominion Group in south Africa represent the oldest cover sequences of 2.72 Ga overlying the basement

rocks in Kaapvaal craton in south Africa. These rocks also display a striking geochemical similarity (Marsh et al., 1990) with the Tiruvannamalai dykes in terms of Nb, LIL and LREE (figure 6.8).

About 2.0 Ga old Scourie dolerites of NW Scotland (Weaver and Tarney, 1981) and the 2.45 Ga old Matachewan dykes and 1.25 Ga old Sudburry dykes from the Superior province in Canada (Condie et al., 1987) include other important Proterozoic dyke swarms of detailed study. These dykes also share the common geochemical features of Nb, LIL and LREE found in the Proterozoic dykes of south India. Although partial melting and crystal fractionation may have important role in controlling various dyke rock geochemistry, the remarkably uniform Nb depletion and enrichment of LIL and LREE would point prevalence of a dominant mantle source with these characteristics on a large regional scale.

6.4 PALAEOMAGNETISM

6.4.1 PRIMARY MAGNETISATION OF TIRUVANNAMALAI DYKES

The characteristic magnetisations of Tiruvannamalai dykes have provided a complex picture. Among the fourteen sites of palaeomagnetic study, few sites (dykes) have obtained between-site grouping with easterly declination and steep negative inclination. One site has an easterly declination and shallow inclination. While in some site samples, data spread between the two directions (figure 5.5). The following discussion evaluates the characteristic remanence magnetism data to deduce the primary magnetisation of Tiruvannamalai dykes.

The sites Tp3 and Tp7 have steep negative inclination with southeast and easterly declination (D = 129.7°, I = -73.5° and D = 92.1°, I = -70.7° respectively). These two site vectors show a good within site as well as between-site grouping. The Tp9 samples have a strong within site grouping with Mean D = 99.6° and I = -0.8° (α_{95} = 6.4, κ = 111). The mean site vectors of Tp12 (D = 90.1°; I = -23.1°, α_{95} = 2.8, κ = 550) and that of Tp13 (D = 84.3°, I = -51.1°, α_{95} = 7.9, κ = 74) fall between the clusters of the site Tp9 and site Tp3 (or Tp7) vectors. The stable vectors of Tp5 have grouped with a mean D = 306.5° and I = -76° (α_{95} = 4.1, κ = 275). The site Tp1 yielded stable vector in three samples which did not group. Among these, the direction of one sample falls into the site Tp3 group while the other two have a moderate inclination and northerly declination. Four samples of site Tp4 has yielded characteristic remanence with mean D = 114.4° and I = -67.9° (α_{95} = 9.6; κ = 92) which falls into the cluster of Tp3 site vectors. Site Tp6 failed to yield grouping while two site vectors fall between Tp3 and Tp9 clusters. The site Tp10 has two samples with characteristic vectors falling into Tp3 cluster, while rest of the characteristic vectors fall away towards the site Tp9 directions. That is, most of the vectors cluster around Tp3 (and Tp7) or Tp9 while others are scattered specially between Tp3 and Tp9 clusters (figure 5.5). This scatter suggests that one of the directions is primary while the other direction would be an overprint. The intermediate data points then indicate streaking of primary direction toward the secondary overprint.

The palaeomagnetic directions of Tp9, when compared to the other available palaeomagnetic directions, show a grouping with the Group 1 dykes of Hargraves and Bhalla (1983) which were assigned an age of c.1100-1000 Ma (cf: Radhakrishna and Joseph, 1993). The other rocks which yield similar direction include the Cuddapah sandstone and shale

metamorphosed by sills of 950±110 Ma (cf: Hargraves and Bhalla, 1983), Wajrakarur kimberlites dated at 1090 Ma based on concordant Rb-Sr isotope data of phlogopite megacrysts from different pipes (Anil Kumar et al., 1993) and the NRM of charnockite site from Visakhapatnam on the east coast of India. The recent Pb-Pb ages place the granulite metamorphism in the Eastern Ghat belt at 1000 Ma. Thus, it can be regarded as an indication of overprint of c.1000 Ma magnetism. The site Tp9 has clouded feldspar, yielded a distinctly higher K-Ar age (~2300 Ma) and a low temperature (~450°C) thermal disturbance during thermal demagnetisation. Thus, the directions within the site Tp9 can be regarded as due to magnetic overprinting. The magnetic overprinting may have disturbed the characteristic vectors in some samples resulting in a streaking between primary and overprint directions. The site vectors of Tp12 and Tp13 along with the sample vectors which fall between Tp3 and Tp9 fields are considered as due to streaking.

The mean directions of Tp5 (D = 305°, I = -76°) is comparable to a late Phanerozoic (100-105 Ma) Rajamahal traps for which D =~314° and I = ~-65° (cf. Klootwijk, 1979). This gives readily an impression that these dykes could be late Phanerozoic. However, Tp5 has given a 1650±30 Ma K-Ar age like other dykes and its geochemistry is indistinguishable from the rest of the dykes. Therefore, the direction in Tp5 can be alternatively explained as due to the palaeosecular variation which can produce drastic longitudinal shift. Consequently, the site Tp5 is grouped along with the Tp3 and other similar Tiruvannamalai sites (dykes). It is interesting to find that the palaeomagnetic directions within the NW-SE and NE-SW dykes of Tiruvannamalai are indistinguishable. Thus the palaeomagnetic studies prove that both the NW-SE and NE-SW dykes of Tiruvannamalai area are penecontemporaneous. Among the three directions reported by Venkatesh et al (1987), only the direction of group C dykes (D

= 133°; I = -75°) can be regarded as primary and the other two directions can be attributed to streaking or complete resetting of magnetisation. The primary palaeomagnetic direction delineated within each site of the present study along with the similar directions obtained by Venkatesh et al (1987) have been used to calculate a mean direction for primary magnetisation of Tiruvannamalai dykes. The mean direction calculated for the Tiruvannamalai dykes (D = 110.74°; I = -77.44°; κ = 46; α_{95} = 8) represents the 1650 Ma palaeomagnetic pole of this terrain. All the primary magnetisations of Tiruvannamalai dykes are plotted with α_{95} ellipses in figure 6.9.

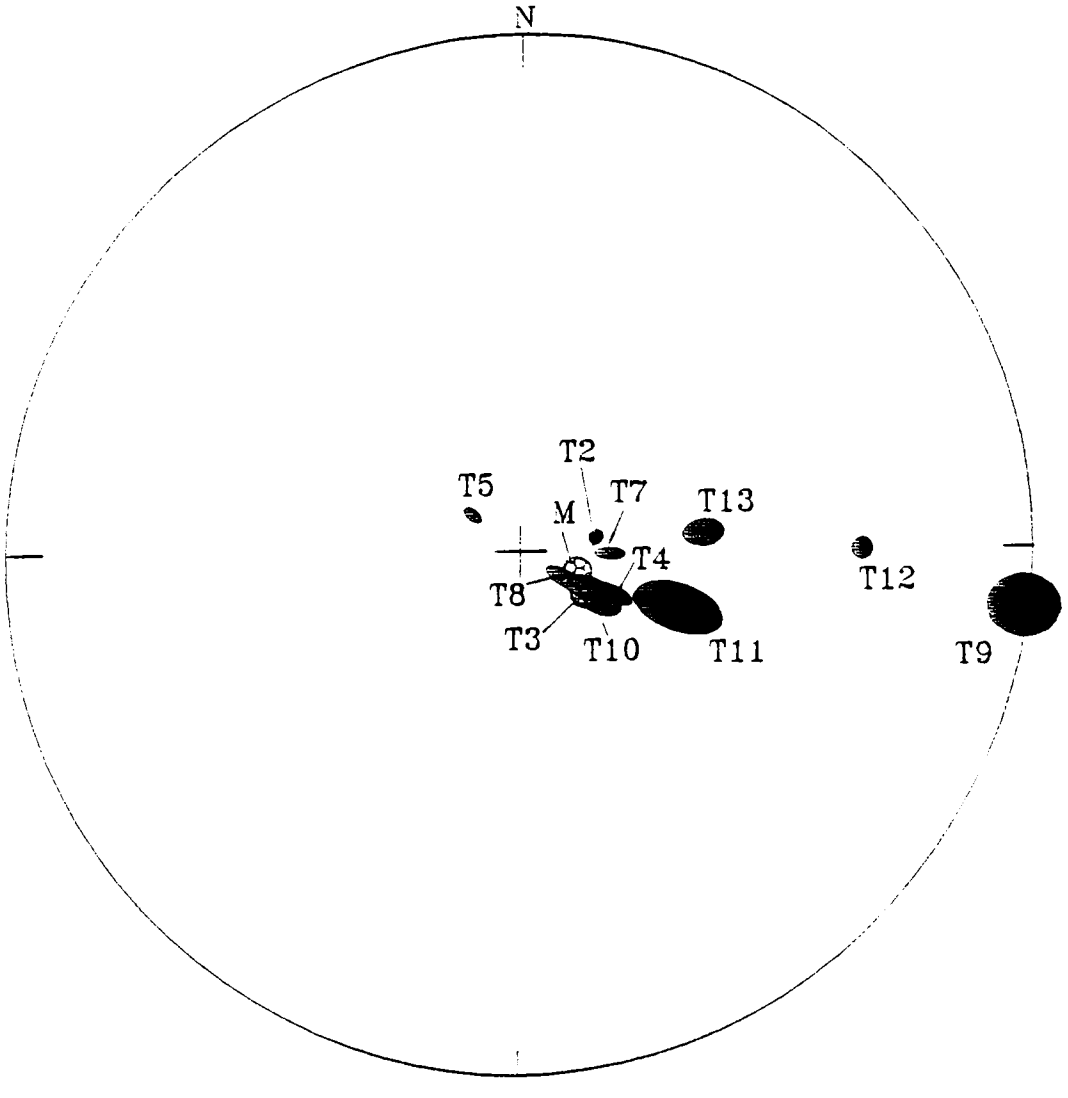

Figure 6.9: Equal area projections of characteristic magnetic vectors (as α_{95}ellipses) of Tiruvannamalai dykes. M indicates mean vector.

6.4.2 CORRELATION OF TIRUVANNAMALAI PALAEOMAGNETIC DIRECTIONS

The Tiruvannamalai dolerites constitute the dyke emplacement of about 1650 Ma. The present palaeomagnetic study could isolate primary characteristic magnetic directions. The calculated palaeopole (20.4°S : 234.66°) and the palaeo-latitude (60°S) of Tiruvannamalai dykes represent the same for the South Indian Granulitic terrain during 1650 Ma.

Similar high quality palaeomagnetic data in terms of number of sites, samples, demagnetisation and isotopic age data are not available for the Proterozoic period from India. However, an attempt is made here to review the available palaeomagnetic data across the Indian shield in order to draw comparisons with the data of Tiruvannamalai dykes. The Tiruvannamalai and other palaeomagnetic directions from the Indian shield was recalculated to the centrally located reference place, Nagpur (21.09°N : 79.09°E).

In the whole of SGT, palaeomagnetic directions comparable to those of Tiruvannamalai dykes are found only in one dyke (D7) in the neighbouring Dharmapuri swarm (Radhakrishna and Joseph, 1994). The Dharmapuri dykes were assigned an age of c.1800-1750 Ma (Radhakrishna et al., 1994c). Therefore, the direction in D7 is either an isolated Tiuvannamalai equivalent dyke emplacement in Dharmapuri area or a magnetic overprint. At the moment, it may be speculated that the direction is an overprint considering the assigned older ages to the Dharmapuri dykes compared to Tiruvannamalai dykes. However, isotopic dating is required to confirm this view.

Palaeomagnetic directions similar to Tiruvannamalai dykes have also been noticed in the neighbouring GGT (table 6.1). These directions were obtained from dykes of Bangarpet, Sargur and Harohalli. Bhalla et al. (1980) reported a comparable steep negative inclination with easterly declination for three Bangarpet dykes and for a Sargur dyke. The direction of Sargur dyke (D = 302° and I = 79°) may constitute a normal vector of Tiruvannamalai. If correct, it implies a polarity reversal during the emplacement of Tiruvannamalai and Sargur dykes. Anil Kumar and Bhalla (1983) reported palaeomagnetic results for two Anantapur dykes, to the south of Cuddapah Basin, comparable to Tiruvannamalai directions. One of the ten Dharwar dykes (Harohalli area) of Hasnain and Quereshy (1971) has also yielded palaeomagnetic vectors (D = 141°; I = -75°) similar to Tiruvannamalai vectors. These data from Dharwar craton were earlier classified into a separate group (Group V) by Hargraves and Bhalla (1983).

Table 6.1: Palaeomagnetic data from south Indian shield comparable to the Tiruvannamalai dykes.

Rock Type	Location Lat.(N).	Lon.(E)	D	I	λ'	Φ'	RD	RI
1. Ananthapur dykes	14.4	77.4	57.00	-69.00	-7.1	226.4	52.1	-65
2. Bangarpet Dykes	12.9	78.2	129.00	-88.00	-24.5	241.7	104.9	-82
3. Sagur Dykes	12.0	76.4	302.00	+79.00	23.00	57.0	305.77	77
4. Harohalli Dykes	12.7	77.5	117.90	-83.30	-18.3	246.1	102.7	-79

RD, RI = Nagpur equivalent declination and inclination

1= Anil Kumar and Bhalla, (1983); 2 = Bhalla et al. (1980); 3 = Bhalla et al. (1980); 4 = Dawson and Hargraves, (1993)

Recently, Dawson and Hargraves (1994) reported additional palaeomagnetic data from Harohalli tholeiitic dykes. Their data confirm easterly declination (D = 79°) and steep negative inclination (I = -82°) for these dykes. These tholeiites were dated at 2420±246 Ma by Rb-Sr whole rock method (Ikramuddin and Stueber, 1976). However, three samples of east west trending dykes alone obtain a regression line corresponding to 2.1 Ga. The palaeomagnetic similarity between the Tiruvannamalai and Harohalli tholeiitic dykes warrant some comments on the assigned older age for latter. The possible scenario could be either the Harohalli tholeiitic dykes are older and their magnetisation dominated an younger 1650 Ma overprint or the Harohalli dykes emplaced at 1650 Ma. In the latter case, the whole-rock Rb-Sr correlation may indicate a mixing phenomenon. Since the age has come from composite samples and the samples from dykes of a single direction have yielded lower age, we suspect that the Tiruvannamalai and Harohalli tholeiitic dykes could be synchronous in emplacement. However, more precise dating of Harohalli tholeiites is required to resolve their age.

From the Aravalli craton, the lower Gwalior traps have yielded a pole position (5°S: 237°) and palaeo-latitude (64°S) comparable to Tiruvannamalai dykes. However, the age of the lower Gwalior traps is uncertain. The Rb-Sr whole-rock isotope age are reported only for the upper Gwalior traps (1830±200 Ma; McElhinny et al., 1978). On the other hand, in Singhbhum craton, Newer dolerites are reported to range in age from 1600-980 Ma (Sarkar, 1980) and none of the dykes have palaeomagnetic results comparable with the data of Tiruvannamalai dykes. In view of the meagre data in terms of their palaeomagnetic record or isotope dating it would not be possible to make meaningful correlations.

Africa, Australia and Antarctica were once contiguous parts of India in the Gondwana reconstruction. Therefore an attempt is made here to compare the ~1650 Ma Tiruvannamalai pole with the pole data of similar ages from these continents. The available pole position from all these continents which fall between 1700 and 1500 Ma are listed in table 6.2.

The Precambrian palaeomagnetic data from east Antarctica was reported for the 1500 Ma dykes of Vestfold Hills (Embleton and Arriens, 1973). On the other hand, in Africa, palaeomagnetic data of Tiruvannamalai age are available for the Van dyke Mine dolerites, the Premire Mine kimberlites, etc. In Australia, the data are available on a few dykes of Gwaler craton and Mount Isa province which are equivalents to Tiruvannamalai dykes in age. The pole data of these Australian/African rocks fall away from the Tiruvannamalai pole and distinctly differ from that of the south Indian shield.

Table 6.2 : Palaeomagnetic pole data from Antarctica, Australia and Africa on rocks of comparable age of Tiruvannamalai dykes.

Rock Unit	Pole Lat:Long	Rotated pole	A_{95} (d_p, d_m)	Age (Ma)	Reference
(Tiruvannamalai Pole 20;235)					
I. ANTARCTICA					
1. Dykes Vestfold Hills	17S:13	6;26	(9,14)	1500	Embleton and Arriens (1973)
II. AUSTRALIA					
A. Gawler Craton					
1. Dykes, Group GB	23N:266	-37;257	11	1700±100	Giddings and Embleton (1976)
2. Dykes, Group BA	61N:231	9;245	9	1500±200	Giddings and Embleton (1976)
B. Mt. Isa Province					
1. Dykes, Group IB	53N: 282	-8;268	11	<1700	Duff and Embleton (1976)
2. Lunch Creek Gabbro	63N: 21	31;298	9	~1500	Duff and Embleton (1976)
III. AFRICA					
1. Van Dyke Mine Dolerite	12N: 14	3;37	-	1650	Jones and McElhinny (1966)
2. Premier Mine Kimberlite	51N: 38	40;13	-	1750	Jones (1968)

The pole coordinates are rotated into the common frame of Indian coordinates for comparisons made in the text.

6.5 IMPLICATIONS FOR GEODYNAMICS OF SOUTH INDIAN LITHOSPHERE

6.5.1 DEVELOPMENT AND MELTING OF LITHOSPHERE

It was evident that the Proterozoic Tiruvannamalai dykes have enriched geochemical features (LILE and LREE) characteristic CFB chemistry; crustal contamination and assimilation have not contributed to achieve these characteristics. The enriched nature of sources has to be explained by some kind of mantle processes. The Tiruvannamalai dykes also have large negative Ta and Nb anomalies. Subduction related magma produces the enrichment of LILE and LREE along with depletion of Nb and Ta (Saunders et al.,1980; Arculus, 1987). In a plot of Nb/La vs Ba/La (figure 6.10), the Tiruvannamalai dolerites spread towards the field of island arc basalts. In the Hf-Th-Ta plot (figure 4.5), these samples fall in the field of subduction related basalts. However, the conspicuous Fe-rich trend in the dyke rocks is in sharp contrast to the typical calc alkaline magmas of island arc setting. Further, there are not obvious evidences for subduction process to have been operational at the time of Tiruvannamalai dyke intrusion. Alternatively, enrichment of sub-continental lithosphere through metasomatism by subduction related processes have been suggested to explain similar characteristics. The petrogenetic model for the Tasmanian dolerites by Hergt et al. (1989) is one of the best recent examples suggesting the process. Such enrichment characteristics in the mantle lithosphere may have been controlled by one or more mineral phases stabilised during the development of subcontinental mantle (cf: Tarney, 1993). Amphibole has been suggested (section 6.2.3.3) to be the main mineral phase for the Tiruvannamalai dolerite magma sources while phlogopite is also considered in some other continental flood basalt sources. These minerals are stable only up to a limited depth (>75 km) and therefore the hydrous metasomatism is relatively shallow level enrichment process in the upper mantle (Hawkesworth et al., 1990). It is more critical that these enriched LILE and LREE and the

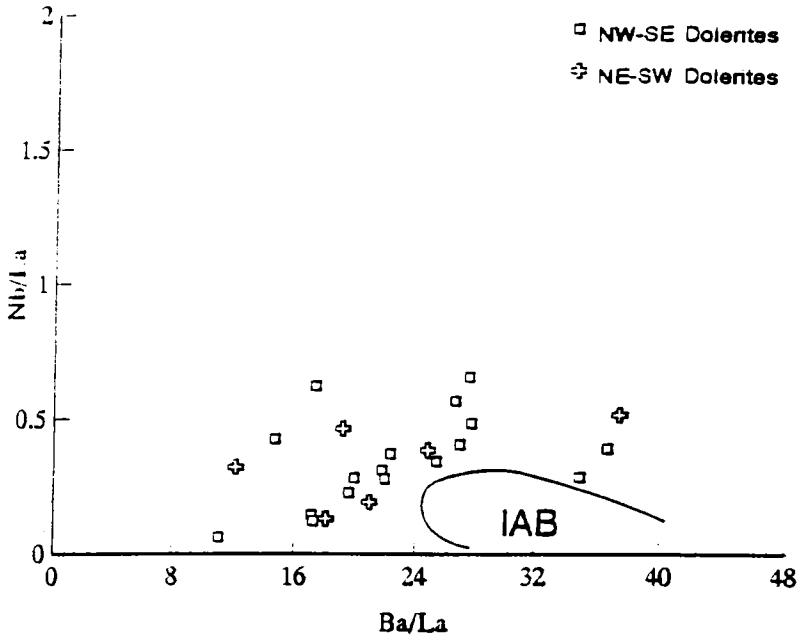

Figure 6.10: Ba/La vs Nb/La diagram for Tiruvannamalai dykes.

depleted Nb and Ta characteristics are spread geographically over large areas in the Gondwanaland and span for over 1.5 Ga. at least since 2.72 Ga. (age of Dominian group volcanics). That is, the lithosphere under the Indian shield together with that of many parts of Gondwanaland may have developed much earlier than the dyke emplacement.

From the foregoing discussion it is critical to know when the south Indian lithosphere has developed. Although the Nd isotope data are particularly informative in this regard, the data are not available for Tiruvannamalai dykes. However, the data are available on the geochemically similar Agali-Anaikatti dykes, where the data yielded 2.87±0.08 Ga crustal residence age (T^{DM} model ages) and 3.15±0.53 Ga (2σ error) Sm/Nd isochron (Radhakrishna et al. 1994b) reflecting it to be the age of lithosphere development. This age interestingly

coincides with the major crustal general process in south India (cf: Radhakrishna and Ramakrishnan, 1993). Similarly the volcanic sequences of Dominian Group also obtained Nd model age of 3.0 Ga coinciding with major crustal formation in Kaapvaal craton in South Africa which was adjacent to south India in the Gondwana configuration (Marsh et al.,1990).

It follows from the preceding arguement that the lithosphere of the south Indian shield has had enriched by subducting-slab-derived incompatible elements about 3.0 Ga and interestingly this is the period of major crustal building in the craton. Such subduction related mantle characteristics were recently inferred in mantle xenoliths from a present day mantle wedge (Maury et al., 1992) and employed as explanation for crustal geochemical signature in dolerite magmas (for example, Tasmanian dolerites: Hergt et al.,1989; Scourie dykes: Weaver and Tarney, 1981 and Waters et al., 1990; Stuart and Kulgera dykes: Zhao and McCullaoch, 1993). There are strong views which argue for lithosphere melting (Gallaghar and Hawkesworth, 1992) while there are also arguements which do not allow large melting of lithosphere and consider only asthenosphere melting to dominate in continental flood basalts (for example: Arndt and Christensen, 1992). However, there is unanimity that the enriched characters of magmas are derived from the metasomatic lithosphere. Therefore, thermal perturbation, probably by plume impinging at the base of enriched south Indian lithosphere has resulted either lithosphere melting or interaction of asthenospheric melts with lithosphere and intruded as dyke magmas in Tiruvannamalai area.

6.5.2 LITHOSPHERIC PLATE MOVEMENT

In the south Indian shield, the SGT is distinct from the GGT in terms of metamorphic grade, structural style and lithologies associated with metasedimentary units (detailed in

chapter 2). The GGT grades into high grade (charnockitic) rocks along a narrow transitional zone bordering the craton. These two terrains were suggested to have come into contact involving subduction/collision tectonics (Peucat et al. 1989; Radhakrishna, 1989). Some workers (for example; Peucat et al., 1989) suggested the southern granulite (charnockites) bordering the GGT has developed as a result of crustal shortening processes. Bhaskararao et al (1988) indicated major anticlockwise rotation of a dyke swarm to the west of Chitradurga Schist belt in the Dharwar craton. Drury et al. (1984) argued that the high grade Granulite terrain is traversed by shear zones dividing it into several distinct blocks with substantial displacements. According to them, the shearing and related tectonic activity post dates the Cuddapah sedimentation and may have occurred during late Proterozoic. Detailed geological and geochronological data can be used to infer the nature of plate interactions and their timing. Palaeomagnetism is the only tool in favourable circumstances which can provide information on whether relative displacement between cratonic blocks have occurred (McWilliams, 1981). Therefore, the present palaeomagnetic direction/pole of the Tiruvannamalai dykes, their ages and their similarity with some of the directions in the GGT have important tectonic implications. Although the isotopic dating for the palaeomagnetic directions for the GGT are still awaited, a close comparison of the palaeomagnetic data of the Tiruvannamalai dykes with that of the dykes in GGT suggests no major rotational movement/displacement to have occurred within or between the GGT and the SGT. That is, the movement along the major shear zones should have occurred prior to 1650 Ma. The reported 2000 Ma age for the unsheared dykes in the western Bhavani shear zone (Radhakrishna et al. 1989; 1994b) also support that the displacements along shear zones could be much earlier (early Proterozoic).

In the light of above results, it is curios to know the timing of shearing/relative displacements within the south Indian shield. The granulite event in the Tiruvannamalai immediately to the south of Dharwar craton, is associated with the 2.5-2.6 Ga tectonics, i.e., the closure of Archaean period. The major displacements, if any, along the shear zones must have occurred during or immediately after the main granulite event but prior to the emplacement of Tiruvannamalai dykes or other similar unshared dykes. These tectonic deductions and the correlation of the Tiruvannamalai palaeomagnetic data with that in the GGT, suggest that the combined data from the SGT and the GGT can be used to compile the APW curve of Indian shield at least since early mid-Proterozoic. Also the poles from the GGT and the SGT can be used together to probe whether the South Indian shield was a contiguous unit with adjoining cratons of the Gondwanaland. The attempted correlation (section 6.3.3) of the Tiruvannamalai poles with the poles of similar age range in the African and Australian shields indicate that the south Indian lithospheric block was an independent crustal unit at 1650 Ma. It may have joined the African and Australian shields, leading to the formation of the Gondwanaland, during the late Precambrian-early Cambrian age (McWilliams,1981).

CONCLUSIONS

The present work on Tiruvannamalai dolerite dykes, one of the Proterozoic magmatic suites of south India, constitutes a comprehensive integrated multidisciplinary study encompassing geochemistry, petrology, palaeomagnetism and isotope dating. The study is significant, as no other comparable data are available on the Proterozoic magmatic suites in the south Indian shield. The study helped in drawing the following conclusions.

* In Tiruvannamalai, dolerite dykes occur in NW-SE and NE-SW directions and they have been geochemically characterised using large data set including many incompatible and rare earth elements. The dykes of both NW-SE and NE-SW trends are sub-alkaline, iron rich continental tholeiites. Both NW -SE and NE-SW dykes show similar evolution trends with remarkable overlap of major, trace and rare earth elements.

* The Tiruvannamalai dykes possess evolved chemistry that can be explained through fractionation of olivine, clinopyroxene and plagioclase, the latter being more dominant in the more evolved samples.

* The Tiruvannamalai dykes show enriched LIL and LRE elements with depleted Nb and Ta patterns. In this respect, these dykes show many geochemical characteristics common to the Proterozoic and other continental basalts. Although crustal contamination is one explanation, it is argued that the chemistry is derived from subcontinental lithosphere of the south Indian shield and the crustal effect are minimal.

The geochemistry indicates that the subcontinental mantle lithospheric source could have developed by hydrous metasomatism (forming amphibole) of non-pyrolite Fe-rich mantle. The lithosphere could have developed by interaction with subduction related fluids much earlier to the formation of Tiruvannamalai dyke magmas, probably around 3.0 Ga, a period during which a major crustal building activity has taken place in the south Indian shield.

The palaeomagnetic data of Tiruvannamalai dykes are more complex because of magnetic overprinting. However, detailed stepwise demagnetisations have successfully delineated the primary characteristic remanent magnetism at D = 110.7°; I = -77.4° (κ = 46; α_{95} = 8). The palaeomagnetic directions of NW-SE and NE-SW dykes are indistinguishable and paleomagnetic pole for the entire Tiruvannamalai dyke suite was calculated at λ =20°S; Φ = 235°.

The K-Ar isotope results of both NW-SE and NE-SW dolerites of Tiruvannamalai have yielded similar age indicating that both sets of dykes intruded about 1650 Ma ago. The isotope age data combined with palaeomagnetic results could establish the palaeomagnetic pole for the Tiruvannamalai dykes as well as the SGT at 1650 Ma.

The combined geochemical, petrological, palaeomagnetic results and the isotope age of the present study unequivocally argue that all dykes in Tiruvannamalai area, irrespective of their strike direction, were derived from a single penecontemporaneous magmatic episode, revising the earlier concept that these dykes constitute distinct magmatic events.

* The palaeomagnetic data of Tiruvannamalai dykes are comparable with some of the available data from Dharwar craton and based on these comparisons and review, it can be suggested that the GGT and the SGT remained to be a single tectonic block at least since early- mid Proterozoic. Large scale displacements, if any, along the shear zones are suggested to have occurred prior to these dyke intrusions. Thus, combined palaeomagnetic data from both the GGT and the SGT can be used to draw an apparent polar wander path of south Indian shield at least since mid Proterozoic.

* The Palaeomagnetic pole of the Tiruvannamalai dykes is not consistent with the limited pole data of comparable age available from Africa, Australia and Antarctica. Although these preliminary comparisons indicate that these tectonic blocks were apart during that time, more detailed work is needed to evaluate the tectonic configurations.

References

Afnasseyev, G.D., Bayouk, E.I., Belikova, B.P., Volarovich, M.P. and Zalesskii, V.V., 1964. On the physical properties of some minerals and rocks of India and Ceylon and their absolute ages. IZV Acad. Nauk. USSR Sci. Geol., 3: 22-24.

Aftalion, M., Bowes, D.R., Dash, B. and Dempster, T.J., 1988. Late Proterozoic charnockites in Orissa, India: a U-Pb and Rb-Sr isotopic study. Jour. Geology, 96: 663-676.

Ahmad, T. and Rajamani, V., 1991. Geochemistry and petrogenesis of the Aravalli volcanics near Nathdwara, Rajasthan, India. Precamb. Res., 49: 185-204.

Ahmad, T. and Tarney, J., 1991. Geochemistry and petrogenesis of Garwal volcanics: implications for evolution of the north Indian lithosphere. Precamb. Res., 50: 69-88.

Ahmad, T. and Bhat, M.I., 1987. Geochemistry and petrogenesis of the Mandi - Darla volcanics, northwestern Himalayas, Precamb. Res., 37: 231-256.

Allen, P., Condie, K.C. and Narayana, B.L., 1985. The geochemistry of prograde and retrograde charnockite - gneiss reactions in southern India. Geochim. Cosmochim. Acta, 49: 323-336.

Anil Kumar, Bhaskararao, Y.J., Padmakumari, V.M., Dayal, A.M. and Gopalan, K., 1988. Late Cretaceous mafic dykes in the Dharwar Craton, Proc. Indian. Acad. Sci. (Earth and Planet. Sci.) 97: 107-114.

Anil Kumar and Bhalla, M.S., 1983. Palaeomagnetic and igneous activity of the area adoining the southwestern margin of the Cuddapah basin, India. Geophys. Jour. Roy. Astron. Soc., 73: 27-37.

Anil Kumar and Prasada Rao, N.T.V., 1979. Palaeomagnetic studies of the Precambrian dyke near Hyderabad. Proc. 3rd workshop status, problems and programmes in Indian peninsular shield. Inst. Indian Penin. Geol., Hyderabad, 146-152.

Anil kumar, Padmakumari, V.M., Dayal, A.M., Murty, D.S.N. and Gopalan, K., 1993. Rb-Sr ages of Proterozoic kimberlites of India: evidence for contemporaneous emplacement. Precamb. Res., 62: 227-237.

Anil kumar, Sivaraman, T.V., Bhaskararao, Y.J. and Gopalan, K., 1989. Rb-Sr ages of two dyke swarms from the Dharwar craton, Karnataka. (abstract), International Symposium, Structure and Dynamics of the Indian Lithosphere. NGRI, 3-4.

Anjanappa, K., 1975. Palaeomagnetism and age of the dolerite dykes of the Tirupathi area, Chittoor district, Andhra Pradesh. In: Recent Researches in Geology, Hindustan Publishers Co., 2: 162-169.

Arculus, R.J., 1987. The significance of source versus process in the tectonic controls of magma genesis. Jour. Volcanol. Geotherm. Res., 32: 1-12.

Armstrong, R.L., 1988. Dating mafic dyke swarms (contribution to IGCP-257). unpublished report of IGCP-257, 7p.

Arndt, N.T. and Christensen, U., 1992. The role of lithospheric mantle in continental flood volcanism: thermal and geochemical constraints. Jour. Geophys. Res., 97: 10967-'81.

Balaram, V, Manikyamba, C., Ramesh, S.L. and Saxena, V.K., 1990. Determination of rare earth elements in Inductively coupled plasma - Mass Spectrometry. Atomic Spectroscopy, 11: 19-23.

Balasubrahmanyan, M. N., 1975. The age of the dykes of south Kanara, Mysore State Geol. Surv. India Misc. Publ., 23: 303-316.

Bence, A.E., Baylia, D.M., Sender, J.F. and Grove, T.L., 1979. Control on the major and minor element chemistry of mid-oceanic ridge basalts and glasses. In: Deep Drilling Results in the Atlantic Ocean: Oceanic crust (Eds: Talwani, M., Harrison, C.G and Hayes, D.E.), Am. Geophys. Union, Washington, D.C, 331-341.

Bergman, S.C., Foland, K.A. and Sera, S.J., 1981. On the origin of an amphibole rich vein in a peridotite inclusion from the lunar crator volcanic field, Nevada, USA. Earth Planet. Sci. Lett., 56: 343-361.

Bhalla, M.S. Hansraj, A. and Prasad Rao, N.T.V., 1980. Paleomagnetic studies of Bangarpet and Sargur dykes of Pre-Cambrian age from Karnataka. Geoviews, 8: 181-192.

Bhaskar Rao, Y.J., Anilkumar, and Gopalan, K., 1988. Metadolerite dykes in the Dharwar craton and their tectonic significance (Abst.) Int. Symp. on Mafic Dykes and related magmatism in rifting and intraplate environments. CP-257-Tech. Rep., 1: 40.

Butler, R., 1992. Palaeomagnetism. Blackwell scientific publications, Boston, USA, 319p.

BVSP., 1981. Basaltic volcanism on the terrestrial planets. Pergamon press, NewYork, 1286p.

Campbell, I.H., 1985. The difference between oceanic and continental tholeiites: a fluid dynamic explanation. Contrib. Mineral. Petrol., 91: 37-43.

Carlson, R.W. and Hart, W.K., 1988. Flood basalt volcanism in the northwestern United States. In. Continental flood basalts (Ed: Macdougall, J.D.), Dordrecht: Kluwer Acad., 35-61.

Collerson, K.D. and Sheraton, J.W., 1986. Age and geochemical characteristics of a mafic dyke swarm in the Archaean Vestfold Block, Antarctica: inferences about Proterozoic dyke emplacement in Gondwana. Jour. Petrol., 27: 858-886.

Condie, K.C., Bobrow, D.J. and Card, K.D., 1987. Geochemistry of Precambrian mafic dykes from the southern Superior province of the Canadian shield. In: (Eds: H.C. Halls and W.F Fahrig), Mafic Dyke Swarms, Geol. Asso. Canada, Spl. Publ., 34: 95-108.

Condie, K.C., 1987. Plate tectonics and crustal evolution. Pergamon, New York,

Cox, K.G., 1980. A model for flood basalt volcanism. Jour. Petrol., 21: 629 -650.

Cox, K.G., Bell, J.D. and Pankhurst, R.J., 1981. The interpretation of igneous rocks. George Allen & Unwin, London, 450p.

Cox, A.V., Doell, R.R. and Dalrymple, G.B., 1965. Quaternary palaeomagnetic stratigraphy in the Quaternary of the United States (Eds: Wright, H.E. and Frey, D.G.), Princeton University Press, Princeton, New Jersey, 817-830.

Crawford, A.R. and Compston, W., 1973. The age of Cuddapah and Kurnool systems, South India. Jour. Geol. Soc. Australia, 19: 453-464.

Creer, K.M., Irving, E. and Runcorn, S.K., 1954. The direction of the geomagnetic field in remote epochs in Great Britain. Jour. Geomagn. Geoelect., 6: 163-168.

Dalrymple, G.B. and Lanphere, M.A., 1969. Potassium-Argon dating. Freeman and Co., San Francisco, 258p.

Damodara Reddy, V. and Prasad, C.V.R.K., 1979. Palaeomagnetism of the dykes from Kolar Gold Mines, India. Jour. Geol. Soc. India, 20: 498-500.

Dawson, E.M. and Hargraves, R.B., 1994. Palaeomagnetism of Precambrian dyke swarms in the Harohalli area, south of Bangalore, India. Precambrian Res., Spl. issue on palaeomagnetism, palaeogeography and palaeoclimates (preprint).

Devaraju, T.C. and Sadashivaiah, M.S., 1966. Dolerite dykes of Satnur-Halaguru area, Mysore state, Karnataka Univ. Jour. Sci., 11: 89-127.

Devaraju, T.C. and Sadasivaiah, M.S., 1965. Spessartite dykes from Halaguru, Mysore state. The Indian Mineralogist, 6: 27-36.

Drury, S.A., 1983. A regional toctonic study of the Archaean Chitradurga greenstone belt, Karnatakaka, based on Landsat interpretation: Jour. Geol. Soc. India, 24: 167-184.

Drury, S.A., 1984. A Proterozoic intracratanic basin, dyke swarms and thermal evlution in South India. Jour. Geol. Soc. India, 25: 436-444.

Drury, S.A., Harris, N.B.W., Holt, R.W., Reeves-Smith, G.J and Wightman, R.T., 1984. Precambrian tectonics and crustal evolution in south india. Jour. Geol., 92: 3-20.

Drury, S.A. and Holt, R.W., 1980. The tectonic framework of the South Indian Craton: A reconnaissance involving Landsat imagery. Tectonophys. 65: 1-15.

Duff, B.A. and Embleton, B.J.J., 1976. Palaeomagnetic directions in Precambrian basic intrusives from the Mount Isa Province, Australia. Earth Planet. Sci. Lett., 28: 418-426.

Embleton, B.J.J. and Arriens, P.A., 1973. A pilot study of the palaeomagnetism of some Precambrian dykes from East Antartica. Geophys. Jour., 33: 239-245.

Epstein, S. and Taylor, Jr., H.P., 1967. Variation of $^{18}O/^{16}O$ in minerals and rocks. In: Researches in Geochemistry (Ed: Abelson, P.H.), John Wiley, New York, 2: 29-62.

Fahrig, W.F., 1987. The tectonic settings of continental mafic swarms: failed arm and early passive margin, In: Mafic dyke Swarms, (Eds. Halls, H.C. and Fahrig, W.F.), Geol. Asso. Canada, special paper, 34: 331-348.

Faure, G., 1986. Principles of isotope geology. 2nd Edition, John Wiley, NewYork,

Fermor, L.L., 1936. An attempt at the correlation of the ancient schistose formations of Peninsular India. Geol. Surv. India Mem., 70: pt 1, 1-52.

Fisher, R.A., 1953. Dispersion on a sphere. Proc. Roy. Soc., A., 217: 295-305.

Ford, C.E., Russel, D.G. and Frisk, M.R., 1983. Olivine-liquid equilibria: temperature, pressure and composition dependence of the crystal /liquid partition coefficients for Mg. Fe^{2+}, Ca and Mn. Jour. Petrol. 24: 256-265.

Friend, C.R.L. and Nutman, A.P., 1992. Response of zircon U-Pb isotopes and whole rock geochemistry to CO_2- fluid induced granulite facies metamorphism, Karnataka, south India. Contrib. Mineral. Petrol., 111: 299-310.

Furnes, H., Hertogen, J., Mitchell, J.G., Austraheim, H. and Sinha-Roy, S., 1983. Trace element geochemistry and age of mafic dykes from the Kerala region, India. Neues. Jahrb. Miner. Abh., 146: 82-100.

Gallagher, K. and Hawkesworth, C.J., 1992. Dehydration melting and generation of continental flood basalt. Nature, 358: 57-59.

Geological Survey of India, 1975. Geological and mineral map of Andhra Pradesh, Geological Survey of India.

Gibson, I.L., Sinha, M.N. and Fahrig W.F., 1987. The geochemistry of the Mackenzie dyke swarm, Canada. In: Mafic dyke swarms (Eds: Halls. H.C. and Fahrig W.F.), Geol. Assoc. of Canada Spl. Paper. 34: 109-123.

Giddings, J.W. and Embleton, B.J.J., 1976. Precambrian palaeomagnetism in Australia, II: basic dykes from Gawler Block. Tectonophysics, 30: 109-118.

Gill, R.C.D. and Bridgwater, D., 1979. Early Archaean basic magmatism in west Greenland: the geochemistry of Ameralik dykes. Jour. Petrol., 20: 695-726.

Gopalakrishnan, K., Sugavanam, E.B. and Venkata Rao, V., 1975. Are there rocks older than Dhawars? A reference to rocks in Tamil Nadu. Indian Mineralogist., 16: 26-34.

Grew, E. and Manton, W.I., 1986. A new correlation of sapphirine granulites in the Indo-Antarctic metamorphic terrain: late Proterozoic dates from the eastern ghat province of India. Precamb. Res., 33: 123-137.

Gubbins, D., 1987. Mechanism for geomagnetic polarity reversals. Nature, 326: 167-169.

Halls H.C. and Fahrig, W.F., 1987. Mafic Dyke Swarms, Geol. Assoc. Can. Spl. Publ., 34: 503pp.

Hammond J.G., 1986. Geochemistry and petrogenesis of Proterozoic diabase in the southern Death Valley region of California. Contrib. Mineral. Petrol., 93: 312-321.

Hanes, J., 1988. Potassium-Argon (K-Ar) geochronology of diabase dykes. unpublished report of IGCP-257, 20p.

Hanes, J.A. and York, D., 1979. A detailed $^{40}Ar/^{39}Ar$ age study of an Abitibi dyke from the Canadian Superior Province. Can. Jour. Earth Sci., 16, 1060-1070.

Hansen, H.C., Hickman, M.H., Grant, N.K. and Newton, R.C., 1985. Pan-African age of peninsular gneissnear madurai, south India. EOS, 65: 419-420.

Hansen, E.C., Newton, R.C. and Janardhan, A.S., 1984. Geochemistry, geobarometry and fluid inclusions of a continuous prograde amphibolite-facies gneiss to a charnockite succession in southern Karnataka. In: Archean Geochemistry: the origin and evolution of Archaen continental crust (Eds: Kroner, A., Hanson, G.N. and Goodwin, A.M.), Springer-Verlag, Berlin, 161-181.

Hanson, G.N. and Langmuir, C.H., 1978. Modelling of major elements: in mantle-melt system using trace element approaches. Geochim. Cosmochim. Acta., 42: 725-741.

Hargraves, H.B. and Bhalla, M.S., 1983. Precambrian palaeomagnetism in India through 1982: a review. In: Precambrians of south India (Eds: S.M. Naqvi and J.J.W. Rogers), Geol. Soc. India Mem., 4: 491-524.

Hari Narian and Subrahmanyam, C., 1986. Precambriam tectonics of the south Indian shield inferred from geophysical data. Jour. Geol., 94: 187-198.

Haskin, L.A., Wildeman, T.R. and Haskin, M.A. 1968. An accurate procedure for the determination of the rare earths by neutron activation. Jour. Radioanal. Chem., 1, 337-348.

Hasnain, I. and Qureshy, M.N., 1971. Palaeomagnetism and geochemistry of some dykes in Mysore state, India. Jour. Geophys. Res. 76: 4786-4795.

Hawkesworth CJ., Kempton P.D., Rogers, N.W., Ellam, R.M., van Calsteren P.W., 1990. Continental mantle lithosphere, and shallow level enrichment processes in the earth's mantle. Earth Planet. Sci. Lett., 96: 256-268.

Heaman, L.M., Corfu, F. and Krough, T.E., 1988. Dating of mafic dyke swarms (contribution to IGCP-257) part 1. Unpublished report of IGCP-257, 12p.

Hergt, J.M., Chappell, B.W., McCulloch, M.T., McDougall, I. and Chivas, A.R., 1989. Geochemistry add isotopic constraints on the origin of the Jurassic dolerites of Tasmania, Jour. Petrol., 30: 841-883.

Horan, M.F., Hanson, G.N. and Spencer, K.J., 1987. Pb and Nd isotope and trace element constraints on the origin of basic rocks in an early Proterozoic igneous complex, Minnesota. Precamb. Res., 37: 323-342.

Hunziker, J.C., 1979. Potassium Argon dating. In: Lectures in Isotope Geology (Eds: Jager, E. and Hunziker, J.C.), Springer-Verlag, Berlin, 52-76.

Huppert, H.C. and Sparks, R.S.J., 1985. Cooling and contamination of maffic and ultramafic magmas during ascend through continental crust. Earth Planet. Sci. Lett., 74: 371-386.

Ikramuddin, M., 1968. Geochemistry and geochronology of Precambrian dykes from Mysore State, India. Ph.D. thesis submitted to Miami University, USA, 170p.

Ikramuddin, M. and Stueber, A.M., 1976. Rb-Sr ages of Precambrian dolerite and alkaline dykes, south-east Mysore State, India. Lithos, 9: 235-241.

Irvine, T.N. and Baragar, W.R.A., 1971. A guide to the chemical classification of the common volcanic rocks. Can. Jour. Earth. Sci., 8: 523-523.

James, D.E., 1981. The combined use of oxygen and radiogenic isotopes as indicators of crustal contamination. Ann. Rev. Earth Planet. Sci., 9: 311-344.

Janardhan, A.S., Newton, R.C. and Hansen, E.C., 1982. The transformation of amphibolite- facies gneiss to charnockite in southern Karnataka and northern Tamilnadu, India. Contrib. Mineral. Petrol., 79: 130-149.

Jaques, A.L. and Green, D.H., 1980. Anhydrous melting of peridotite at 0-15 kb pressure and the genesis of tholeiitic basalts. Contrib. Mineral. Petrol., 73: 287-310.

Jones, D.L, 1968. Palaeomagnetism of the Premier Mine kimberlite. Jour. Geophys. Res., 73: 6937-6944.

Jones, D.L. and McElhinny, M.W., 1966. Palaeomagnetic correlation of basic intrusions in the Precambrian of southern Africa. Jour. Geophys. Res., 71: 543-552.

Kaila, K.L., Chowdhury, K.R., Reddy, P.R., Krishna, V.G., Harinarain, Subbotin, S.I., Sollogub, V.B., Chekunov, A.V., Kharetchko, G.E., Lazarenko, M.A. and Ilchenko, T.V., 1979. Crustal structure along Kavali-Udipi profile in the Indian peninsular shield from deep seismic sounding. Jour. Geol. Soc. India, 20: 307-333.

Kaila, K.L. and Bhatia, S.C., 1981. Gravity study along the Kavali-Udipi deep seismic sounding profile in the Indian peninsular shield: some inferences about the origin of anorthosites and the Eastern Ghats orogeny. Tectonophysics, 79: 129-143.

Kalsbeek, F. and Taylor, P.N., 1985. Age and origin of early Proterozoic dolerite dykes in south-west Greenland. Contrib. Mineral. Petrol., 89: 307-316.

Kalsbeek, F. and Taylor, P.N., 1986. Chemical and isotopic homogeneity of a 400 km long basic dyke in central West Greenland. Contrib. Mineral. Petrol., 93: 439-448.

Kempton, P.D., Harmon, R.S., Hawkesworth, C.J. and Moorbath, S., 1991. Petrology and geochemistry of lower crustal granulites from the Geronimo volcanic field, southestern Arizona, Geochim. Cosmochim. Acta, 54: 3401-3426.

Klootwijk, 1979. A review of palaeomagnetic data from the Indo-Pakistani fragment of Gondwanaland. In: Geodynamics of Pakistan (Eds: A.Fara and K.A. Dejong), Geol. Surv. Pakistan, Quetta, 41-80.

Kovacheva, M., 1980. Summarised results of the archaeomagnetic investigation of the geomagnetic field variation for the last 8000 yr in southeastern Europe. Geophys. Jour. Roy. Astron. Soc., 61: 57-64.

Krogstad, E.J., Hanson, G.N. and Rajamani, V., 1991. U-Pb ages of zircon and sphene for gneiss terrains adjacent to the Kolar schist belt, south India: evidence for separate crustal evolution histories. Jour. Geol., 99: 801-816.

Kroner, A., 1991. African linkage of Precambrian Sri Lanka. Geol. Rundschau, 80: 429-440.

Kuno, H., 1969. Plateau basalts. In: The Earth's crust and upper mantle, (Ed: Hart, P.), Am. Geophys. Union, Geophys. Monogr., 13: 495-501.

Kyser, T.K., O'Neil, J.R. and Carmichael, I.S.E., 1982. Genetic relations among basic lavas and ultramafic nodules: Evidence from oxygen isotope compositions. Contrib. Mineral. Petrol., 81: 88-102.

Kyser, K.T., 1990. Stable isotopes in the continental lithospheric mantle. In: Continental Mantle (Ed: M.A. Menzies), Larendon press, Oxford, 67-86.

Lanyon, R. Black, L.P., Seitz, H.M., 1993. U-Pb zircon dating of mafic dykes and its application to the Proterozoic geological history of the Vestfold Hills, East Antartica. Contrib. Minerol. Petrol., 115: 184-203.

Le Bas, M.J., Maitre, R.W. and Woolley, A.R., 1992. The construction of the total alkali-silica chemical classification of volcanic rocks. Mineral. Petrol., 46: 1-22.

Le Maitre, R.W. and eleven others, 1989. A classification of igneous rocks and glossary of terms: recommendations of the International Union of Geological Sciences Subcommission on the systematics of igneous rocks. Blackwell Scientific Publications, Oxford, 193p.

Leelanandam, C., 1990. The Kandra volcanics in Andhra Pradesh: possible ophiolite? Curr. Sci., 59: 785-788.

Levy, E.H., 1972. Kinematic reversal schemes for the geomagnetic dipole. Astrophys. Jour., 171: 635-642.

Macdonald, G.A. and Katsura, T., 1964. Chemical composition of Hawaiian lavas. Jour. Petrol., 5: 82-133.

MacGregor, I.D and Manton, W.I., 1986. Robert Victors eclogites: ancient oceanic crust: Jour. Geophy. Res., 91: 14063-14079.

Mahadevan, M.S., 1964. The origin of charnockite suite of rocks forming parts of the Western Ghats in Kerala , India. Rep. 22nd Intl. Geol. Cong., New Delhi, 13: 88-96.

Mahoney, J.J., 1988. Deccan Traps. In: Continental flood basalts (Ed: J.D. Macdougall), Kluwer Academic, Hingham, Mass., 151-194.

Mahoney, J.J. , Macdougall, J.D., Lugmair,G.W., Gopalan, K. and Krishnamurthy P., 1985. Origin of contemporaneous tholeiitic and K-rich alkalic lavas: A case study from the northern Deccan plateau, India. Earth. Planet. Sci. Lett. , 73: 39-53.

Manikyamba, C., Balaram, V. and Naqvi, S.M., 1993. Geochemical signatures of polygenetic origin of a banded iron formation (BIF) of the Archaean Sandur greenstone belt (schist belt)Karnataka nucleus, India. Precamb. Res., 61: 137-164.

Marsh, J.S., Bowen, M.P., Rogers, N.W and Bowen, T.B., 1990. Volcanic rocks of the Wittwatersrand Triad, South Africa. II: Petrogenesis of mafic and felsic rocks of the Dominion Group. Precamb. Res.,

Marzocchi, W. and Mulargia, 1992. The periodicity of geomagnetic reversals. Phys. Earth Planet. Inter., 73: 222-228.

Matsuhisa, Y., Bhattacharya, S.K., Gopalan, K., Mahoney, J and MacDougall, J.D., 1986. Oxygen isotope evidence for crustal contamination in Deccan basalts. Terra Cognita, 6:181.

Maury, R.C., Defant, M.J. and Joron, J.L., 1992. Metasomatism of the sub-arc mantle inferred from trace elements in Philippine xenoliths. Nature, 360: 661-663.

McElhinny, M.W., Cowley, J.A. and Edwards, D.J., 1978. Palaeomagnetism of some rocks from Peninsular India and Kashmir. Tectonophysics, 50: 41-54.

McFadden, P.L. and Merrill, R.T., 1984. Lower mantle convection and geomagnetism. Jour. Geophys. Res., 89: 3354-3362.

McKay, G.A., 1989. Partitioning of rare earth elements between major silicate minerals and basaltic melts. In: Geochemistry and mineralogy of rare earth elements (Eds: Lipin, B.R and McKay, G.A.), Mineral. Soc. Am. Rev. Mineral., 21: 45-77.

McWilliams, M.O., 1981. Palaeomagnetism and Precambrianm tectonic evolution of Gondwana. In: Precambrian plate tectonics (Ed: A. Kroner), Elsevier, 649-687.

Meschede, M., 1986. A method of descriminating between different types of mid ocean ridge basalts and continental tholeiites with the Nb-Zr-Y diagram. Chem. Geol., 56: 207-218.

Middlemost, E.A.K., 1980. A contribution to the nomenclature and classification of volcanic rocks. Geol. Mag., 117, 51-57.

Mohr, P.A., 1987. Crustal contamination in maffic sheets: a summary. In: Mafic dyke swarms (Eds: Halls, H.C. and Fahrig, W.F.), Geol. Ass. Canada Spl. paper, 34: 75-80.

Molyneux, L., 1971. A complete result magnetometer for measuring the remanent magnetisation of rocks. Geophys. Jour. Roy. Astron. Soc., 24: 429-433.

Murty, Y.G.K., Baburao, V., Guptasarma, D., Rao, J.M., Rao, M.N. and Bhattacharji, S., 1987. Tectonic, petrochemical and geophysical studies of mafic dyke swarms around the Proterozoic Cuddapah basin, south India. In: Mafic Dyke Swarms (Eds: Halls, H.C. and Fahrig, W.F.), Geol. Ass. Canada Spl. paper, 34: 303-316.

Nagata, T., 1961. Rock magnetism. 2nd edition, Maruzan, Tokyo,350p.

Nair, M.M and Vidhyadaran, K.T., 1982. Rapakivi granite of Ezhimala complex and its significance. Jour. Geol. Soc.India, 23: 46-51.

Nair, M.M., Vidyadharan,K.T., Pawar, S.D., Sukumar, P.V. and Murty, Y.G.K., 1975. The structural and stratigraphic relationships of the schistose rocks and associated igneous rocks of the Tallichery - Mananthody area, Cannanore district, Kerala, Indian Mineral. 16: 89-100.

Naqvi, S.M. and Rogers, J.J.W., 1987. Precambrian geology of India. Oxford University press, Oxford, 223p.

Naqvi, S.M. and Rogers, J.J.W. (Eds.), 1983. Precambrian of South India, Geol. Soc. India, Mem., 4: 573p.

Neel, L., 1951. L'invrsion de l'aimantion permanente des roches. Ann. Geophys., 7: 90-102.

Norrish, K. and Chappell., 1967. X-ray fluorescence spetrography.In: Physical methods in determinative mineralogy (Ed: Zussman, J.), Academic press, London, 514p.

Opdyke, N.D., Glass, B., Hays, J.D. and Foster, J., 1966. Palaeomagnetic study of Antarctic deep sea cores. Science, 154: 349-357.

Opdyke, N.D. and Henry, K.W., 1969. A test of the dipole hypothesis. Earth Planet. Sci. Lett., 6: 139-151.

Padmakumari, V.M. and Dayal A.M., 1987. Geochemical studies of some mafic dykes around the Cuddapah Basin, south India. Geol. Soc. India Mem. 6: 369-373.

Parker, E.N., 1969. The occasional reversal of the geomagnetic field. Astrophys. Jour., 158: 815-827.

Pascoe, E.H., 1950. A manual of the geology of India and Burma. Calcutta, 485p

Patchett, P.J., 1980. Thermal effects of basalt on continental crust and crustal contamination of magmas. Nature, 283: 559-561.

Paul, D.K., Ray Barman, T., McNaughton, N.J., Fletcher, R., Potts, P.J. and Augustine, P.F., 1990. Archaean - Proterozoic evolution of Indian charnockites: isotopic and geochemical evidence for granulites of the Eastern ghat belt. Jour. Geol., 98: 253-263.

Pearce, J.A., and Cann J.R., 1973. Tectonic setting of basic volcanic rocks determined using trace element analyses. Earth. Planet. Sci. Lett. 19: 290-300.

Peucat, J.J., Vidal, P., Griffiths, J.B. and Condie, K.C., 1989. Sr, Nd and Pb isotopic systematics in the Archaean low- to high-grade Transition Zone of Southern India: syn- accretion vs post accretion granulites. Jour. Geol., 97: 537-550.

Pitchamuthu, C.S., 1959. The significance of clouded plagioclase in the basic dykes of Mysore State, India. Jour. Geol. Soc. India, 1: 68-79.

Radhakrishna, B.P., 1967. The result status of geological, geophysical and geochemical studies in the Dharwar region. Paper presented at the Upper Mantle Project, Hyderabad.

Radhakrishna, B.P., 1989. Suspect Tectono-Stratigraphic Terrane elements in the Indian Sub-continent. Jour. Geol. Soc. India, 34: 1-24.

Radhakrishna, T., Dallmeyer,R.D. and Joseph, M., 1994a. Palaeomagnetism and $^{36}Ar/^{40}Ar$ vs $^{39}Ar/^{40}Ar$ isotope correlation ages of dyke swarms in central Kerala, India: tectonic implications. Earth Planet. Sci. Lett., 121: 213-226.

Radhakrishna, T., Gopakumar, K., Murali, A.V.and Mitchell, J.G. 1991. Geochemistry and petrogenesis of Proterozoic mafic dykes in north Kerala, southwestern Indian shield-primary results. Precamb. Res. 49: 235-244.

Radhakrishna, T., John Mathai and Yoshida, M., 1991b. Geology and structure of the high-grade rocks from Punalur - Achankovil sector, south India. Jour. Geol. Soc. India, 35: 263-272.

Radhakrishna, T. and Joseph, M., 1992a. Geochemistry of basic dykes of Kerala and Tamil Nadu region. Project Report, Submitted to Indian. Natn. Sci. Academy, New Delhi. 115p.

Radhakrishna, T. and Joseph, M., 1992b. Palaeomagnetism of basic dykes of Kerala and Tamil Nadu region. Project Report, Dept. Sci. & Tech., New Delhi, 79p.

Radhakrishna, T. and Joseph, M., 1993. Proterozoic Palaeomagnetism of South Indian shield and tectonic constraints. Mem. Geol. Soc. India, 25: 321-336.

Radhakrishna, T. and Joseph, M., 1994. Proterozoic palaeomagnetism of the mafic dyke swarms in the high grade region of south India. Precamb. Res., (press).

Radhakrishna, T., Joseph, M., Thampi, P.K. and Mitchell, J.G.,1990. Phanerozoic mafic dyke intrusions from the high grade terrain from southwestern India: K-Ar isotope and geochemical implications. In: A.J.Parker, P.C.Rickwood and D.H.Tucker, (Eds), Mafic

dykes and emplacement mechanisms, A.A. Balkema, Rotterdam, 363-372.

Radhakrishna, T., Mathai, J. and Mitchell, J.G., 1989. Mafic dykes of Agali -Coimbatore region, India: geochronology, geochemistry and petrogenetic implications for Proterozoic subcontinental mantle. Abstract in proceedings of 28th International Geological Congress, Washington, 2: 657-658.

Radhakrishna, T., Mitchell, J.G. and Joseph, M., 1994. K-Ar geochronology of dyke swarms in the south Indian granulite terrain (communicated).

Radhakrishna, T., Panchanathan, P.V. and Joseph, M., 1993. Mafic dyke intrusions in relation to flood volcanism in western India and ocean floor formation in the Arabian Sea. SERC Research Highlights, Dept. Sci. & Tech., New Delhi, 16-18.

Radhakrishna, T., Pearson, D.G. and John Mathai, 1994b. Evolution of Archaean southern Indian lithospheric mantle: a geochemical study of Proterozoic Agali-Coimbatore dykes. Contrib. Mineral. Petrol. (submitted).

Radhakrishna, T., Poornachandrarao, G.V.S., Mitchell, J.G. and Venkatesh, A.S., 1986. Proterozoic basic dyke activity in Kerala along the western continental margin of India. Jour. Geol. Soc. India, 27: 245-253.

Radhakrishna, T. and Ramakrishnan, M., 1993. Udupi-Kavali transect across south India, Global Geoscience Transect 11. Co-published by Inter-Union Commission on the Lithosphere and Geol. Soc. India. 17p.

Rajamani, V., 1991. Geochemistry of greenstones and granites in the transect. Deep continental crust of India: (Integrated multi-disciplinary study on the sub-transect between Kanyakumari-Raichur), Geol. Soc. India and Dept. Sci. Tech., 111-113.

Rajamani, V., Shivakumar, K., Shirey, S.B. and Hannson,G.N., 1985 Geochemistry and petrogenesis of amphibolites, Kolar Schist belts, South India: evidence for Komaitiitic magma derived by low percentages of melting of the mantle. Jour. Petrol. 26: 92-123.

Ramakrishnan, M., 1993. Tectonic evolution of the granulite terrains of southern India. In: Continental crust of south india (Ed: B.P. Radhakrishna), Mem. Geol. Soc. India, 25: 35-44.

Rao, M.S., Godavari, K.S. and Ganganna, 1993. Whole rock analysis data by X-ray fluorescence spectroscopy. Bull. Geol. Surv. India, Series-C, 2.

Rao, J.M., Rao, G.V.S.P. and Patil, S.K., 1990. Geochemical and palaeomagnetic studies on the middle Proterozoic Karimnagar mafic dyke swarm, India. In: Mafic dykes and emplacement mechanism (Eds: A.J. Parker, P.C. Rickwood and D.H. Tucker), Balkema, Rotterdam, 373-382.

Ringwood, A.E., 1975. Composition and petrology of Earths mantle. McGraw-Hill, New York, 618p.

Sadashivaiah, M.S. and Devaraju, T.C., 1963. Tinguaite porphyry from Satnur, Mysore state. Indian Mineralogist, 4: 5-13.

Sahoo, J. and Balakrishnan, S., 1994. Geochemistry and petrogenesis of doleritic dykes in and around Kolar Schist belt, South India. Jour. Geol. Soc. India, 43, 511-528.

Sarkar, S.N., 1980. Precambrian stratigraphy and geochronology of Peninsular India: a review. Indian Jour. Earth Sci., 7: 12-26.

Satyanarayana, K., Divakara Rao, V., Naqvi, S.M. and Hussain, S.M., 1973. Geochemistry and petrogenesis of dykes from Nuggihalli Schist belt, Mysore. Geophys. Res. Bull. 11: 273-280.

Saunders, A.D., Tarney, J. and Weaver S.D., 1980. Transverse geochemical variations across the Antarctica Peninsula: implications for the generation of calc-alkaline magmas. Earth Planet. Sci. Lett., 46: 344-360.

Sheraton, J.W. and Black, L.P., 1981. Geochemistry and geochronology of Proterozoic tholeiite dykes of east Antarctica: evidence for mantle metasomatism. Contrib. Mineral. Petrol., 78: 305-317.

Singh, J. and Bhalla, M.S., 1972. Preliminary palaeomagnetic studies on igneous rocks of U.P., Andhra Pradesh and Mysore, Curr. Sci., 41: 92-94.

Sinha-Roy, S., 1983. Age of basic magmatism in Kerala. Jour. Geol. Soc. India, 24: 93-95.

Srikantappa, C., Raith, M. and Spiering, B., 1985. Progressive charnockitisation of a leptinite-khondalite suite in south Kerala, India - evidence for formation of charnockite through a decrease in fluid pressure? Jour. Geol. Soc. India, 26: 849-872.

Stacey, F.D. and Loper, D.E., 1983. The thermal boundary - layer interpretation of D" and its role as a plume source. Phys. Earth Planet. Inter., 33, 45-55.

Steiger, R.H and Jager, E., 1977. Subcommission on geochronology: convention on the use of decay constants in geo- and cosmochronology. Earth Planet. Sci. Letts., 36: 359-362.

Subbarao, K.V., 1988. Deccan flood basalts. Mem. Geol. Soc. India, 10: 393p.

Sugavanam, E.B., Venkatarao, V., Simhachalam, J., Nagal, S.C. and Murty, M.V.N., 1978. Structure, tectonics, metamorphism, magmatic activity and metallogeny in parts of northern Tamil Nadu. In: Tectonics and Metallogeny south and east Asia. Geol. Surv. India Misc. Publ., III(34): 95-111.

Sun, S.S., Nesbit, R.W. and Sharaskin, A.Y., 1979. Geochemical characteristics of mid oceanic ridge basalts. Earth Planet. Sci. Lett., 44: 119-138.

Sun, S.S. and McDonough, W.F., 1989. Chemical and isotopic systematics of oceanic basalts: implications for mantle composition and processes. In: A.D. Saunders and M.J. Norry (Editors), Magmatism in Ocean Basins, Geol. Soc. Lond., Spl. Publ., 42: 313-345.

Swami Nath, J. and Ramakrishnan, M. (Eds.), 1981. Early Precambrian supracrustalsof southern Karnataka. Geol. Surv.India Mem. 112, 350p.

Takahashi, E., 1980. Melting relations of an alkali- olivine basalt to 30 kbar, and their bearing on the origin of alkali basalt magmas. Carnegie Inst., Washington Yearb 79: 271-276.

Tarling, D.H., 1983. Palaeomagnetism: principles and applications in geology, geophysics and archaeology. Chapman and Hall, London, 379p.

Tarney, J. 1993. Geochemistry and significance of mafic dyke swarms in: The Proterozoic. In: K.C. Condie (editor), Proterozoic crustal evolution, Elsevier, Amsterdam (preprint)

Topping, J., 1958. Errors of observation and their treatment. Chapman and Hall, London, 119p.

Van Alstine, D.R. and DeBoer, J., 1978, A new technique for constructing apparent polar wander paths and revised Phanerozoic path for North America, Geol., 6, 137-139.

Vandamme, D., Courtillot, V., Besse, J. and Motigny, R., Palaeomagnetism and age deleniations of the Deccan traps (India): Results of a Nagpur-Bombay traverse and review of earlier work, Rev. Geophys. 29: 159-190.

Varadarajan, K and Nair, M.K., 1978. Stratigraphy and structure of Tertiary basin. Jour. Geol. soc. India. 19: 217-220.

Verma, R.K., Pulliah, G. and Hasnain, I., 1968. Paleomagnetic study of a dyke near Hyderabad, India Bull. Natl.Geophys. Res. Inst., 6: 79-86.

Venkatesh, A.S., Poornachandrarao, G.V.S., Prasadarao, N.T.V. and Bhalla, M.S., 1987. Palaeomagnetic and geochemical studies on dolerite dykes from Tamilnadu, India. Precamb. Res., 34: 291-310.

Waters, F.G., Cohen, A.S., O'Nions, R.K. and O'Hara, M.J., 1990. Development of Archaean lithosphere deduced from chronology and isotope chemistry of Scourie dykes. Earth Planet. Sci. Lett., 97: 241-255.

Weaver, B.L. and Tarney, J., 1981. The Scourie dyke suite: petrogenesis and geochemical nature of the Proterozoic sub-Continental mantle. Contrib. Mineral. Petrol., 78: 175-188.

Weaver, B.L. and Tarney, J., 1984. Estimating the composition of the continental crust: an empirical approach. Nature, 310: 575-577.

Wilkinson, J.F.G. and Le Maitre, R.W., 1987. Upper mantle amphiboles and micas and TiO_2, K_2O and P_2O_5 abundances and 100.Mg/(Mg+Fe) ratios of common basalts and andesites:

implications for model mantle metasomatism and undepleted mantle compositions. Jour. Petrol, 28: 37-74.

Wilkinson, J.F.G. and Binns, R.A., 1977. Relatively iron rich lherzolite xenoliths of the Cr-diopside suite: a guide to the primary nature of anorogenic tholeiitic andesite magmas. Contrib. Mineral. Petrol., 65: 199-212.

Wilson, M., 1989. Igneous Petrogenesis - A global tectonic approach. Unwin Hyman Ltd., 466p.

Wood, D.A., 1980. The application of a Th-Hf-Ta diagram to problems of tectonomagmatic classification and establishing the nature of crustal contamination of basaltic lavas of the British Tertiary volcanic province.- Earth Planet. Sci. Lett. 50, 11-30.

Yoshida, M., Funaki, M. and Vitanage, P.W., 1989. A Jurassic dolerite dyke from Sri Lanka and its palaeomagnetic analysis. Jour. Geol. Soc. India, 30, 71-76.

Zhao, J.X. and McCulloch, M.T., 1993. Melting of a subduction modified continental lithospheric mantle: evidence from late Proterozoic mafic dyke swarms in central Australia. Geology, 21, 463-466.

Zijderveld, J.D.A., 1967. A.C.demagnetisation of rocks: analysis of results. In: Methods in Palaeomagnetism (Eds: Collinson, D.W., Creer, K.M. and Runcorn, S.K), Elsevier, New York, 254-286.

Zindler, A. and Hart, S., 1986. Chemical geodynamics. Ann. Rev. Earth Planet. Sci., 14, 493-571.